

5-2011

## Patient Characteristics and Outcomes of Gastrointestinal Stromal Tumor Patients Undergoing Imatinib Plasma Level Testing

Laura Nolden

Follow this and additional works at: [https://digitalcommons.library.tmc.edu/utgsbs\\_dissertations](https://digitalcommons.library.tmc.edu/utgsbs_dissertations)



Part of the [Oncology Commons](#)

---

### Recommended Citation

Nolden, Laura, "Patient Characteristics and Outcomes of Gastrointestinal Stromal Tumor Patients Undergoing Imatinib Plasma Level Testing" (2011). *The University of Texas MD Anderson Cancer Center UTHealth Graduate School of Biomedical Sciences Dissertations and Theses (Open Access)*. 139.  
[https://digitalcommons.library.tmc.edu/utgsbs\\_dissertations/139](https://digitalcommons.library.tmc.edu/utgsbs_dissertations/139)

This Dissertation (PhD) is brought to you for free and open access by the The University of Texas MD Anderson Cancer Center UTHealth Graduate School of Biomedical Sciences at DigitalCommons@TMC. It has been accepted for inclusion in The University of Texas MD Anderson Cancer Center UTHealth Graduate School of Biomedical Sciences Dissertations and Theses (Open Access) by an authorized administrator of DigitalCommons@TMC. For more information, please contact [digitalcommons@library.tmc.edu](mailto:digitalcommons@library.tmc.edu).

PATIENT CHARACTERISTICS AND OUTCOMES OF GASTROINTESTINAL  
STROMAL TUMOR PATIENTS UNDERGOING  
IMATINIB PLASMA LEVEL TESTING

by  
Laura K Nolden, BS, MS

APPROVED:

---

Jonathan Trent, MD, PhD  
Supervisory Professor

---

Haesun Choi, MD

---

Russell Broaddus, MD, PhD

---

Judith A. Smith, PharmD

---

Su Chen, MD, PhD

---

APPROVED:

---

George Stancel, PhD  
Dean, The University of Texas  
Graduate School of Biomedical Sciences at Houston



PATIENT CHARACTERISTICS AND OUTCOMES OF GASTROINTESTINAL  
STROMAL TUMOR PATIENTS UNDERGOING  
IMATINIB PLASMA LEVEL TESTING

A  
DISSERTATION

Presented to the Faculty of  
The University of Texas  
Health Science Center at Houston  
and

The University of Texas  
M. D. Anderson Cancer Center  
Graduate School of Biomedical Sciences  
in Partial Fulfillment  
of the Requirements  
for the Degree of

DOCTOR OF PHILOSOPHY

by  
Laura K Nolden, BS, MS  
Houston, Texas  
May, 2011

## **Shohrae Hajibashi**

November 9, 1979 – January 29, 2011

This work is dedicated to the memory of Shohrae Hajibashi, a vibrant, intelligent young woman who, as part of her MD/PhD training at the University of Texas M.D. Anderson Cancer Center, researched potential prognostic markers and therapeutic targets in desmoid tumor, a type of sarcoma.

Shohrae's desire to become a physician scientist was rooted in her deep empathy and concern for others. She had a tangible impact on those around her and, while her friendships were numerous, Shohrae had a unique ability to remain attuned to each relationship, forming a meaningful and constant connection with those she cared about. As your friend, she divided grief and multiplied joy.

In the final year of her predoctoral research training, and just prior to her thirtieth birthday, Shohrae was diagnosed with sarcoma.

Shohrae remained upbeat and strong as she endured punishing treatment and progressing disease that repeatedly tore her down over the subsequent eighteen months. Her contagious effervescence and wit shone through the increasing weakness, fatigue, and pain.

Shohrae has made sarcoma research deeply personal and ignites the drive for earlier diagnostics, better therapeutics, and a cure. Her death was a devastating loss for all who loved her and she is dearly missed, every day.

## Acknowledgements

Sincere acknowledgements and thanks go out to the following: to Dr. Robert Benjamin, Dr. Shreyaskumar Patel, Dr. Jonathan Trent, Dr. Vinod Ravi, Dr. Dejka Araujo, and Dr. Joseph Ludwig who provided patients to this study; to Patricia Neal, Kavin Hanzik, and Maria Olmedo for clinical assistance; to Dr. Alexander Lazar and Dr. Wei-Lien Wang for genotyping assistance; to Wei Qiao for statistical support; to Dr. Dan Yang and Dr. Amaury Dumont for sample processing assistance. Thanks to Dr. Linyee Shum for advice and collaboration regarding imatinib plasma level testing. Thank you to Dr. Haesun Choi and Dr. Piyaporn Boonsirikamchai for assistance with CT analysis. Thank you to Dr. Saroj Vadhan for providing personnel resources to this study.

I sincerely appreciate the support and guidance I received from my Supervisory Committee Members: Dr. Haesun Choi, Dr. Judith Smith, Dr. Russell Broaddus, and Dr. Su Chen.

Thank you, also, to Dr. Dan Yang and Dr. David Reynoso for tremendous support and camaraderie in the laboratory.

All of this would not have been possible without the excellent support and mentorship I received from Dr. Jonathan Trent. He epitomizes the concept of a well-rounded translational researcher, he never lets one forget that the patient is the ultimate focus, and manages to keep an effective foot in both doors by being such an inspiring clinician and experienced investigator. I am incredibly grateful for his mentorship, his faith in me, and the opportunity he has provided.

PATIENT CHARACTERISTICS AND OUTCOMES OF GASTROINTESTINAL  
STROMAL TUMOR PATIENTS UNDERGOING  
IMATINIB PLASMA LEVEL TESTING

Publication No. \_\_\_\_\_ \*

Laura K Nolden, BS, MS  
Supervisory Professor: Jonathan Trent, MD PhD

Although gastrointestinal stromal tumor (GIST) is effectively treated with imatinib, there are a number of clinical challenges in the optimal treatment of these patients. The plasma steady-state trough level of imatinib has been proposed to correlate with clinical outcome. Plasma imatinib level may be affected by a number of patient characteristics. Additionally, the ideal plasma trough concentration of imatinib is likely to vary based on the *KIT* genotype (genotype determines imatinib binding affinity) of the individual patient. Patients' genotype or plasma imatinib level may influence the type and duration of response that is appreciable by clinical evaluation.

The objectives of this study were to determine effects of genotype on the type of response appreciable by current imaging criteria, to determine the distribution of plasma imatinib levels in patients with GIST, to determine factors that correlate with plasma imatinib level, to determine the incremental effects of imatinib dose escalation; and to explore the median plasma levels and outcomes of patients with various *KIT* mutations.

We therefore obtained *KIT* mutation information and analyzed CT response for size and density measurement of GISTs at baseline and within the first four months of imatinib treatment. In 126 patients with metastatic/unresectable disease, the *KIT* genotype of patients' tumor was significantly associated with unique response characteristics measurable by CT. Furthermore, hepatic and peritoneal metastases differed in their response characteristics. A subgroup of patients with *KIT* exon 9 mutation, who received higher doses of imatinib and experienced higher trough imatinib levels, experienced improved progression-free survival similar to that of *KIT* exon 11 patients.

Therefore, we have found that imatinib plasma levels were higher in patients with elevated Aspartate amino transferase, were women, were older, or were being treated concomitantly with CYP450 substrate drugs. As expected, CYP450 inducers correlated with a lower plasma imatinib levels in GIST patients. Renal metabolism of imatinib accounts for <10%, so it was not included in the analysis but may affect covariates. Interestingly, there was a trend for low imatinib levels and inferior progression-free survival in patients who had undergone complete gastrectomy. Patients with *KIT* exon 9 mutation in our cohort received higher imatinib doses, experienced higher trough imatinib levels, and experienced a PFS similar to that of *KIT* exon 11 patients.

In conclusion, imatinib plasma levels are influenced by a number of patient characteristics. The optimal imatinib plasma level for individual patients is not known but is an area of intense investigation. Our study confirms patients with *KIT* exon 9 mutations benefit from high-dose imatinib and higher trough imatinib levels.

## **Table of Contents**

<b>Signature Page</b> .....	i
<b>Title Page</b> .....	ii
<b>Dedication</b> .....	iii
<b>Acknowledgements</b> .....	iv
<b>Abstract</b> .....	v
<b>List of Figures</b> .....	ix
<b>List of Tables</b> .....	xi
<b>List of Abbreviations</b> .....	xii
<b>Chapter 1. Introduction and Background</b> .....	1
1.1 Overview of GIST .....	1
1.2 KIT and KIT Receptor Activation .....	3
1.3 Molecular Genetic Aberrations of <i>KIT</i> and <i>PDGFRA</i> in GIST .....	7
1.4 Prognostic Value of <i>KIT</i> Mutations in GIST .....	12
1.5 Imatinib Mesylate .....	17
1.6 Imatinib in CML .....	21
1.7 Imatinib in GIST .....	22
1.8 Therapeutic Drug Monitoring of Imatinib in GIST .....	29
1.9 Pharmacokinetics of Imatinib .....	35
1.10 Response Evaluation of GIST by CT .....	40
1.11 Specific Aims of the Study .....	45

<b>Chapter 2. Materials and Methods</b> .....	47
2.1 Plasma Level Testing and Calculation of Adj-C <sub>min</sub> .....	47
2.2 Patient Response Assessment.....	49
2.3 GIST Genotyping.....	50
2.4 Statistical Analysis.....	52
<b>Chapter 3. Specific <i>KIT</i> Mutations Correlate with Clinical Outcomes of GIST Patients Treated with Imatinib</b> .....	55
3.1 Introduction.....	55
3.2 Results.....	56
<b>Chapter 4. Relationship of Imatinib Plasma Level to Outcome</b> .....	75
4.1 Introduction.....	75
4.2 Results.....	75
<b>Chapter 5. Discussion and Conclusions</b> .....	93
<b>Bibliography</b> .....	98
<b>Vita</b> .....	132

## List of Figures

Figure 1. Structure of KIT protein.....	5
Figure 2. Schematic illustration of KIT .....	6
Figure 3. Regions of frequent mutations in <i>KIT</i> and <i>PDGFRA</i> .....	9
Figure 4. <i>KIT</i> exon 11 deletions portend poor outcome.....	16
Figure 5. Timeline of imatinib development .....	20
Figure 6. <i>KIT</i> exon 11 mutation portends better response .....	27
Figure 7. Therapeutic range.....	30
Figure 8. Blood levels of a drug over time .....	31
Figure 9. Concentration time curve at steady-state .....	33
Figure 10. Patients experience diverse trough imatinib levels .....	34
Figure 11. Distribution of trough imatinib levels .....	36
Figure 12. Representative response of GIST metastases .....	42
Figure 13. Frequency of <i>KIT</i> exon 11 mutations in our population.....	58
Figure 14. Unique <i>KIT</i> exon 9 mutations identified .....	61
Figure 15. CT response changes in size and density.....	65
Figure 16. Cumulative response comparison .....	66
Figure 17. Genotype is associated with grade of radiographic response.....	69
Figure 18. Specific codon alterations of <i>KIT</i> exon 11 correlate with response.....	71
Figure 19. Distribution of plasma levels in unresectable patients.....	84
Figure 20. Distribution of Adj-C <sub>min</sub> and Outcome.....	86
Figure 21. Response distribution with <i>KIT</i> mutation .....	87



<b>Figure 22. Improved PFS with higher imatinib exposure.....</b>	<b>90</b>
<b>Figure 23. OS and PFS of patients included in efficacy analyses.....</b>	<b>91</b>
<b>Figure 24. PFS of patients by Adj-C<sub>min</sub> quartile.....</b>	<b>92</b>

## List of Tables

Table 1. Genes Regulated by mutations in <i>KIT</i> and <i>PDGFA</i> .....	8
Table 2. Mutations associated with Familial GIST .....	11
Table 3. GIST clinicopathological features.....	13
Table 4. Targets of imatinib signaling consequences.....	19
Table 5. Key principles in the clinical management of GIST .....	26
Table 6. Modified Choi response criteria of GIST .....	44
Table 7. Mutations identified in 528 GIST patients .....	57
Table 8. Study Characteristics.....	62
Table 9. Factors evaluated for radiographic response correlation.....	68
Table 10. Characteristics that influence response .....	74
Table 11. TDM patient, disease, and treatment characteristics.....	76
Table 12. Range of trough imatinib levels observed .....	78
Table 13. Covariates of trough imatinib level.....	80
Table 14. Concomitant medications.....	82

## **List of Abbreviations**

Adj-C <sub>min</sub>	adjusted trough imatinib concentration	MRI	magnetic resonance imaging
ALT	alanine aminotransferase	OS	overall survival
AST	aspartate aminotransferase	PD	progressive disease
ATP	adenosine triphosphate	PDGFRA	platelet derived growth factor receptor alpha
AUC	area under the curve	PET	positron emission tomography
BCR-ABL	breakpoint cluster region-abelson	PFS	progression-free survival
BSA	body surface area	Ph+	Philadelphia chromosome positive (leukemia)
CCyR	complete cytogenic response	PI3K	phosphatidylinositide-3-OH kinase
C <sub>max</sub>	maximum drug concentration	PK	pharmacokinetics
C <sub>min</sub>	minimum (“trough”) drug concentration	PKC	protein kinase C
CML	Chronic Myelogenous Leukemia	PLC-γ	phosphoinositide phospholipase C, γ isoform
CML-AP	CML Accelerated Phase	PPI	proton-pump inhibitor
CML-BP	CML Blast Phase	PR	partial response
CML-CP	CML Chronic Phase	RECIST	Response Evaluation Criteria in Solid Tumors
CSF-1R	colony stimulating factor 1 receptor	RFS	recurrence-free survival
CT	computed tomography	RTK	receptor tyrosine kinase
CYP450	cytochrome P450	SCF	stem cell factor
FDA	US Food and Drug Administration	SD	stable disease
<sup>18</sup> FDG-PET	2-deoxy-2[F-18]fluoro-D-glucose positron emission tomography	SEER	Surveillance Epidemiology and End Results
GIST	Gastrointestinal Stromal Tumor	SEM	standard error mean
GRB(2/7)	growth factor receptor bound protein	SFK	SRC- Family protein tyrosine kinase
Hmg Co-A	3-Hydroxy-3-Methyl-Glutaryl-CoA	SMA	smooth muscle actin
HU	Hounsfield’s Units	STAT	Signal Transducer and Activator of Transcription
ICC	Interstitial Cells of Cajal	TDM	therapeutic drug monitoring
LOH	loss of heterozygosity	TKI	tyrosine kinase inhibitor
MMR	major molecular response	UTMDACC	University of Texas M. D. Anderson Cancer Center
		WT	wild-type, no mutation

## Chapter 1. Introduction and Background

### 1.1 Overview of GIST

Gastrointestinal stromal tumors (GIST) were first described in 1983 by Mazur and Clark as a group of tumors that were non-epithelial in origin, lacked smooth muscle cell ultrastructural features, and did not express immunohistological characteristics of Schwann cells (1). GISTs were rarely diagnosed at the time, and often diagnosed as gastrointestinal smooth muscles tumors (GI leiomyosarcoma, leiomyoblastoma, or leiomyoma), until research revealed in 1998 that most GISTs experience gain-of-function activating mutations in the *KIT* prot-oncogene (2). This discovery led to increased study of the biology of GIST and provided the first effective therapeutic target for therapy.

The incidence of GIST in the United States is approximately 5,000 new cases annually, or about 6.8 per million people (3). Most GISTs arise from the stomach (60%) or small intestine (25%), but may also arise from the colon and rectum (10%), or the esophagus, omentum, mesentery, and rarely the retroperitoneum. GISTs account for 14% of all tumors of the small intestine, about 2% of all stomach tumors, and 0.1% of all colon tumors diagnosed (4, 5). The median age of GIST diagnosis is 58 years, GIST is rarely diagnosed in children with only ~3% diagnosed before the age of 21 (6, 7). In a US study from 1992-2000, based on Surveillance Epidemiology and End Results (SEER), there was a slight gender bias of GIST in men (55%), whereas several other population-based studies

in Europe and Asia found an equal incidence among men and women (8, 9). No predisposing factors have been identified to date (10).

GISTs are thought to arise from the interstitial cells of Cajal (ICC), pacemaker cells that control gut motility, and this supported by recent genomic research that shows that GISTs display a distinct gene expression profile from that of other soft tissue sarcomas (11). Immunohistochemically, 95% of GISTs stain positively for the KIT protein, irrespective of the site of origin, histologic characteristics, or biology of the individual tumor, making KIT expression a key diagnostic marker of the disease (8, 10, 12, 13). Mast cells, germ cells, hemopoietic stem cells, and melanocytic cells also express KIT, and so immunostaining of CD34, a sialylated transmembrane protein expressed in GISTs, is also used diagnostically (2). Protein kinase C (PKC)-theta, an isoform of PKC, is highly expressed and useful to identify the rare subset of GISTs that do not express KIT (~5%) (14-16). GISTs may also have positive staining for smooth muscle actin (SMA, 30-40%) but are generally negative for desmin, an intermediate filament protein found in muscle, and negative for S-100, a neural cell marker, in ~95% of cases (10, 17). A proper diagnosis of GIST is often only reached through a careful comparison of pathological and clinical findings.

Surgery is the incipient therapy for patients with resectable primary disease and complete resection is achieved in approximately 70% of patients (18). Approximately 54% of completely-resected patients survive for 5 years without further therapy, 40% recur at a median of 2 years post-surgery, and recurrence often involves the peritoneum and liver (18, 19). Outcome of GIST patients upon

recurrence is poor (19). About half of patients are metastatic or unresectable at the time of presentation (20). Patients with advanced or inoperable disease have historically had limited treatment options, prior to 2001. Response to chemotherapy, such as doxorubicin, ifosfamide, temozolomide produced response rates of 5 to 10% (21-23). Radiotherapy has little disease management role in GIST (24). Therefore, more effort was placed into understanding the underlying biology of GIST and the KIT oncogene to develop better therapies. In 2001, imatinib was found to potently inhibit autophosphorylation of the tyrosine kinase receptor KIT (25). The notable impact of imatinib therapy in GIST and its mechanisms are discussed further in subsequent sections, below.

## **1.2 *KIT and KIT Receptor Activation***

Overexpression of the KIT protein, a product of the *KIT* gene, is a defining feature of GIST (26). A receptor tyrosine kinase (type III), KIT is homologous to platelet-derived growth factors  $\alpha/\beta$  (PDGFRA/B) and also shares homology with colony stimulating factor-1 receptor (CSF-1R). Functional investigation of KIT began in the 1920's, and *v-KIT* was cloned from the Hardy-Zuckerman sarcoma virus (HZ4-FeSV), a strain of feline sarcoma viruses isolated from a feline fibrosarcoma tumor in 1986 (6, 27, 28). It was identified as a proto-oncogene, localizing in humans to chromosome 4q11-q12 and encoding a 145 kilodalton transmembrane glycoprotein (28, 29). KIT is critical to the function of interstitial cells of Cajal and to normal gastrointestinal peristalsis, and also plays a role in hematopoiesis, melanogenesis, and gametogenesis (30-32).

The *KIT* gene encodes a 976 and 972 amino acid protein divided into 19 exons, with four extracellular amino acids (GNNK) absent in one isoform (33, 34). The functional difference between the two isoforms is not known, both are expressed in murine and human normal tissues, and both are simultaneously expressed in KIT positive tissues (35). The 19 exons of *KIT* encode an extracellular ligand-binding domain (exons 2-5), a region thought to promote dimerization of the receptor (6-7), an intracellular juxtamembrane region (exon 11), an ATP binding site (exons 12-14), two intracellular catalytic domains (exons 13, 16-19 respectively), and a kinase insert (exon 15), represented in **Figure 1** (33, 36, 37).

KIT activation and signaling occurs through binding of its ligand, stem cell factor (SCF). SCF has two isoforms, SCF<sup>220</sup> and SCF<sup>248</sup>, both are membrane-bound and can be cleaved to release soluble SCF, which exists in human plasma as a monomer (38-45). Both SCF isoforms are capable of kit activation following SCF homodimerization (38). Upon binding SCF, the KIT receptor homodimerizes, autophosphorylates tyrosines 567, 569, 702, 719, 728, 934, which in turn attract SH2 binding partners, signaling through major mediators such as Phosphatidylinositolide-3-OH Kinase (PI-3K, binds Y719), RAS, STATs, PLC- $\gamma$  (binds Y728), and Src family kinases (SFK, bind Y567 and Y569), GRB2 (binds Y702) and GRB7 (binds Y935), as shown in **Figure 2** (46). Kit-mediated cell survival occurs primarily via SFK and PI-3K (27, 46, 47). Both SCF and KIT are expressed by numerous cells in the body, including epithelial cells, smooth muscle cells, stromal cells, endothelial cells, fibroblasts, and ICCs (40, 48, 49). Signaling of KIT through its downstream mediators is important in normal cellular function, yet contributes to

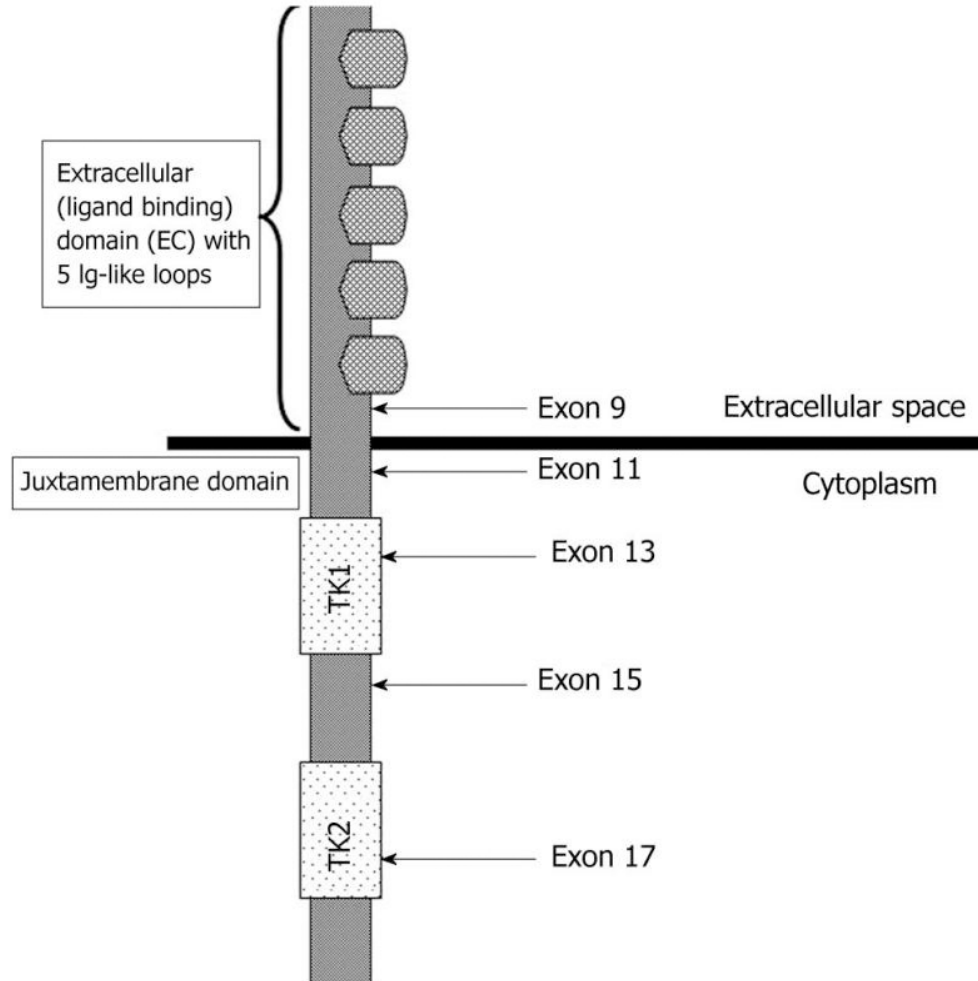


### Figure 1. Structure of KIT protein

KIT structure and localization of common mutations within the highlighted exons 9, 11, 13, 15, and 17. The structure of KIT includes the extracellular ligand-binding domain, which contains 5 immunoglobulin-like loops. This region is thought to promote dimerization of the receptor. Intracellularly, KIT has an ATP-binding site, two catalytic domains and a kinase insert. Ig: Immunoglobulin. TK1/2: tyrosine kinase domains 1/2. Reprinted with permission from Bayraktar, U et al, World J Gastroenterol 16:2726-2734 copyright 2010.



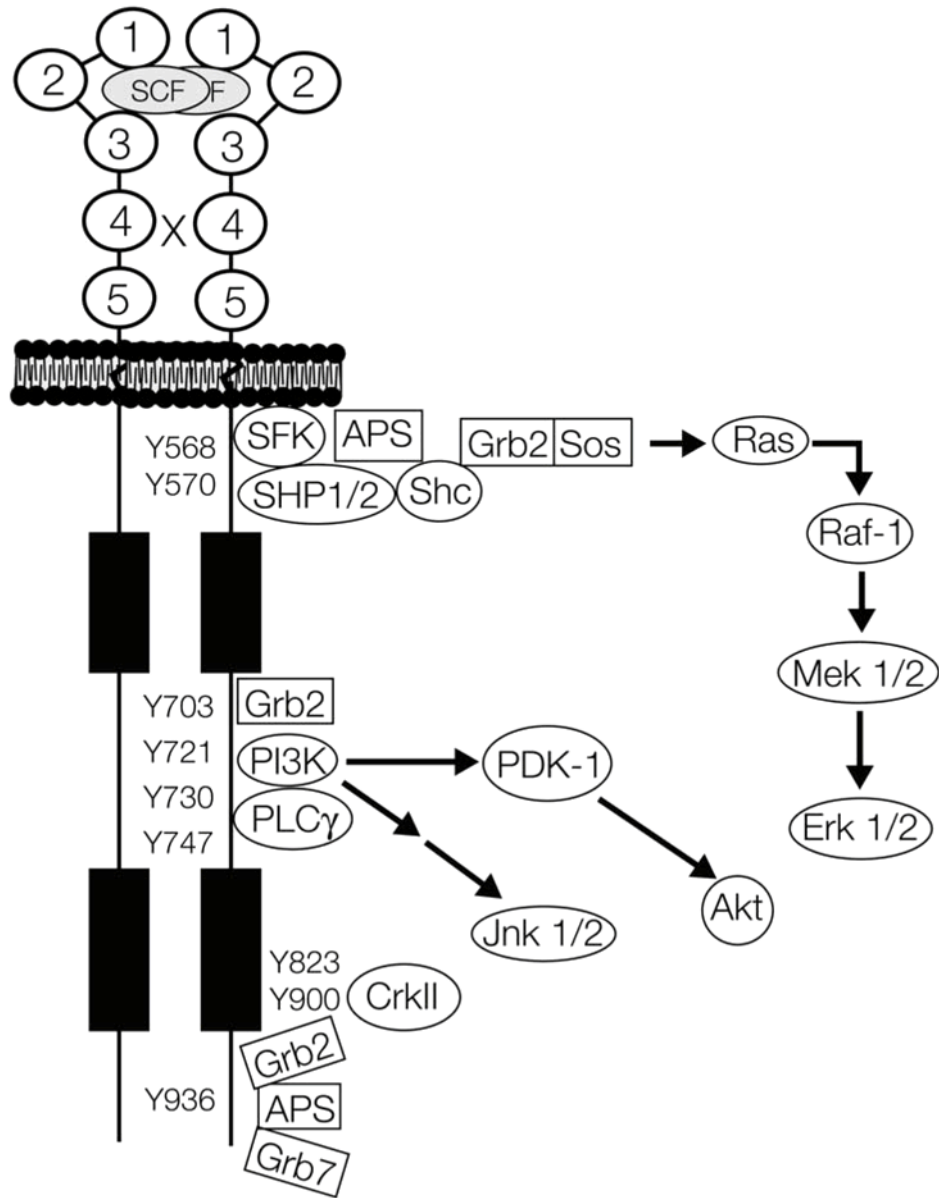


**Figure 2. Schematic illustration of KIT**

This figure summarizes signaling proteins activated by KIT and interaction sites on the receptor. Abbreviations: SCF, stem cell factor; SFK, Src family kinases. Reprinted by permission from John Wiley and Sons: Stem Cells 23:16–43, copyright 2005.

transformation, aberrant proliferation, cell survival, and metastasis when oncogenic mutations are acquired (50). These mutations are discussed in detail, below.

### **1.3 Molecular Genetic Aberrations of *KIT* and *PDGFRA* in *GIST***

A central pathogenic event of most GISTs, sporadic or familial, is activation of the PDGFRA or KIT receptor tyrosine kinase (RTK) whereby the extracellular juxtamembrane domain or cytoplasmic domains of the receptor develop activating, gain-of-function deletions or missense mutations. These oncogenic mutations lead to downstream signal transduction promoting cell survival, proliferation, chemotaxis, and adhesion via KIT phosphorylation of substrate proteins. Docking sites of KIT phosphorylation substrates are represented in **Figure 2**. A broad summary of KIT target genes, their downstream signaling factors, and consequences of this interaction are presented in **Table 1**. Constitutive activation of KIT is observed in more than 80% of GISTs. *KIT* mutations occur in two general regions, some affect regulatory regions of the protein and modulate its enzymatic activity, while other mutations occur in the enzymatic region itself (51). Four coding regions of *KIT* harbor a majority of primary mutations: *KIT* exons 11, 9, 13 and 17 (in order of highest frequency) (52). These mutations are visualized on the KIT protein in **Figure 3**. Intracellular, juxtamembrane exon 11 mutations are most common, accounting for over 65% of all *KIT* mutations in GIST, and a diverse spectrum of changes occur across the region, including more than 80 deletions, missense mutations, and duplications described to date (53-56). Interestingly, these mutations group by type as one examines *KIT* exon 11 from the 5' to the 3' end:

Gene	Target Genes	Downstream	Signaling Factors	Signaling Consequences
<b><i>KIT</i> mutation</b>	<i>MAPK</i>	JAK1/2	STAT	Induce progression through cell cycle; prevent apoptosis
		ERK1/2( P44/22)	P90RSK	Inhibit cell differentiation
			MSK	
			ELK-1, STAT	
		p38	PLA2, MNK1, PRAK, Hsp27, STAT1, ELK-1	Inhibit apoptosis
	<i>GRB2</i>	SOS, RAS, RAF, MEK, ERK	P90RSK, MSK, ELK-1, STAT	Inhibit apoptosis
	<i>PI3K</i>	p70S6K	RPS6, ELF-4	Regulate cell growth
		PKB(AKT) ↓	mTOR signaling (p70S6K, RPS6, ELF4, STAT)	Regulate cell growth
			RAF, ERK, p70S6K ↓	Inhibit apoptosis
			p21, p27	Regulate cell cycle and proliferation
			cyclinD1, p53	
			BAD, FXHR/AFX ↓	Induce cell survival
			p53, NF-KB	Modulate cell death
		BAD ↓	BCL-XL, BCL-2	Inhibit apoptosis
		NF-KB	IKB, IKK, <i>et al</i>	Inhibit cell differentiation
				Negative regulation of KIT signaling pathway
	<i>SHP1/2</i>	—	—	
	<i>CBL</i>	—	—	Unknown
	<i>SHC</i>	—	—	Unknown
	<i>EPHA4</i>	—	—	Unknown
	<i>Paxillin</i>	—	—	Unknown
<b><i>PDGFRA</i> mutation</b>	<i>MAPK</i>	JAK1/2, ERK1/2, p38	STAT, P90RSK, MSK, ELK-1, PLA2, MNK1, PRAK, Hsp27	Inhibit apoptosis; inhibit cell differentiation; induce progression through cell cycle
	<i>AKT (with controversy)</i>	mTOR signaling (p70S6K, RPS6, ELF4, STAT)	—	Regulate cell growth
		RAF, ERK, p70S6K	—	Modulate cell growth
		p21, p27	—	Regulate cell cycle and proliferation
		cyclinD1	—	Modulate cell cycle ( <i>indirectly</i> )
		BAD, FXHR/AFX	—	Induce cell survival
		p53, NF-KB	—	Modulate cell death ( <i>indirectly</i> )
	<i>STAT</i>	—	—	Induce progression through cell

**Table 1. Genes Regulated by mutations in *KIT* and *PDGFRA***

Mutations in *KIT* and *PDGFRA* elicit a number of signaling consequences through downstream mediators. Reprinted by permission from John Wiley and Sons: Cancer 113:1532-1543, copyright 2008.

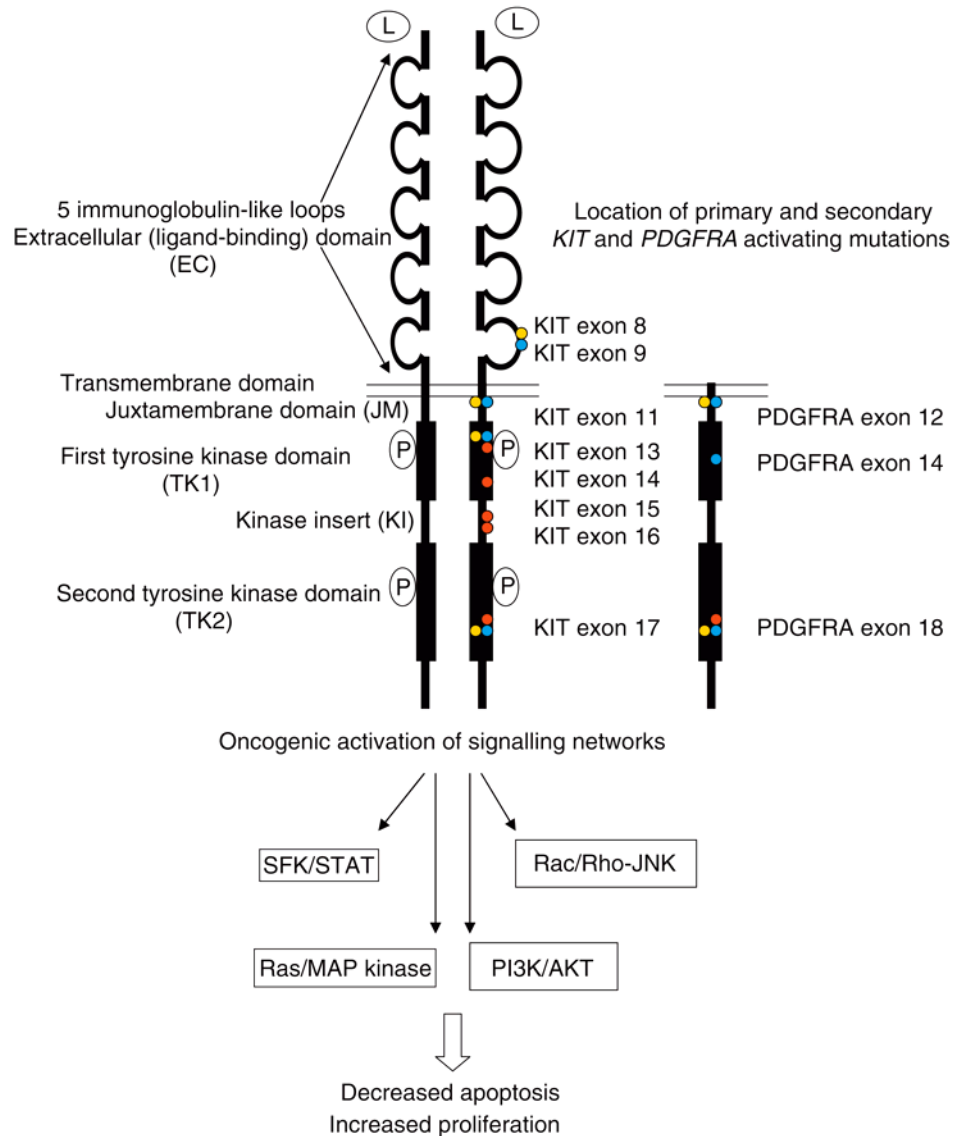


### Figure 3. Regions of frequent mutations in *KIT* and *PDGFRA*

Activation of receptor by gain-of-function mutation (blue, yellow, red dots) independent of ligand (L) binding induces dimerization of the receptor, autophosphorylation of tyrosines and causes activation of downstream signaling pathways. Location of primary (sporadic and hereditary) and secondary (detected during treatment) *KIT* and *PDGFRA* mutations is indicated by blue, yellow and red dots, respectively. Reprinted by permission from John Wiley and Sons: Histopathology 53:245-266, copyright 2008.

while missense mutations occur sporadically across the entire region, deletions tend to cluster toward the 5' terminal region and extend into the mid-region, whereas insertion/duplications cluster almost exclusively at the 3' C-terminus (51). Exon 9 mutations within the extracellular, ligand-binding domain of *KIT*, occur in approximately 18% of cases, are strongly associated with intestinal GISTs, and are almost exclusively a six base pair (bp) insertion resulting in a tandem A502\_Y503 duplication (57). Primary mutations of *KIT* exons 13 and 17 are less frequent; each singularly identified in only one to two percent of cases, and are almost always missense mutations (58). *KIT* exon 13 mutations occur in GISTs from various regions of the gastrointestinal tract and are predominantly a L642G missense mutation, whereas *KIT* exon 17 mutations are twice as prevalent in intestinal GISTs and are often an A822L missense mutation (51, 58). In GIST, *PDGFRA* mutations occur principally as missense mutations in exons 12 and 18, and some substitutions in exon 14 have been reported (59). The most common *PDGFRA* mutation is an A842A missense mutation, which is known to be insensitive to imatinib treatment, and variations of this change, A842Y and A842I have been reported (60-63).

In Familial GIST, heritable germ-line mutations in *KIT* or *PDGFRA* are observed, summarized in **Table 2**. These patients develop hyperplasia of the ICC and multiple GISTs at early ages. It is interesting to note that these hereditary mutations are mostly missense mutations and most, if not all, are observed in sporadic GIST as well, indicating the activating potential of these small changes (64-79).

Location	Mutation at Protein Level	Genetic Syndrome (n)	Reference
<i>KIT</i> -JM (exon 8)	Asp419del	Familial GIST syndrome (1)	(75)
<i>KIT</i> -JM (exon 11)	Trp557Arg	Familial GIST syndrome (2)	(70, 77)
<i>KIT</i> -JM (exon 11)	Val559Ala	Familial GIST syndrome (4)	(67,68,72,78)
<i>KIT</i> -JM (exon 11)	Val560Gly	Familial GIST syndrome (1)	(78)
<i>KIT</i> -JM (exon 11)	Val560del	Familial GIST syndrome (1)	(65)
<i>KIT</i> -JM (exon 11)	Gln575_Leu576dup	Familial GIST syndrome (1)	(71)
<i>KIT</i> -JM (exon 11)	Asp579del	Familial GIST syndrome (2)	(73, 76)
<i>KIT</i> -TK1 (exon 13)	Lys642Glu	Familial GIST syndrome (2)	(66, 79)
<i>KIT</i> -TK2 (exon 17)	Asp820Tyr	Familial GIST syndrome (2)	(64, 74)
<i>PDGFRA</i> -TK1 (exon 12)	Tyr555Cys	Familial GIST syndrome* (1)	(80)
<i>PDGFRA</i> -TK1 (exon 12)	Asp561Val	Multiple small intestinal fibrous polyps, lipomas and GISTs (1)	(81)
<i>PDGFRA</i> -TK2 (exon 18)	Asp846Tyr	Familial GIST syndrome (1)	(69)
<b>Total</b>		<b>( 19 )</b>	

\*Previously diagnosed as intestinal neurofibromatosis.

*PDGFRA*, Platelet-derived growth factor receptor-alpha; GIST, gastrointestinal stromal tumour; JM, juxtamembrane domain; TK1, TK2, cytoplasmic tyrosine kinase domains I and II.

## Table 2. Mutations associated with Familial GIST

Hereditary *KIT* and *PDGFRA* mutations associated with familial GIST syndrome and other related genetic syndromes. Reprinted by permission from John Wiley and Sons: Histopathology 53:245-266, copyright 2008.

Following the advent of imatinib treatment in GIST, resistance to the drug was shown to occur with the acquisition of secondary mutations in *KIT*. These missense mutations occur in *KIT* exons 13 and 17, are observed in addition to continued expression the primary mutation, and significantly decrease the sensitivity of the KIT receptor to inhibition by imatinib, impacting response (58).

#### **1.4 Prognostic Value of *KIT* Mutations in GIST**

Mutation of *KIT* and its subsequent activation is a driving factor in GIST and several investigators have evaluated the prognostic relevance of different types of *KIT* mutations. As a new treatment, imatinib mesylate, was being clinically tested in GIST, it became important to understand the natural history of the disease and the influence of genetic mutation in the absence of this targeted treatment. A summary of the prognostic relevance of *KIT* mutations is presented in **Table 3**.

In 2002, Singer and colleagues reviewed a group of 48 GIST patients who underwent resection of their tumor and presence of a *KIT* exon 11 deletion/insertion was an independent predictor of recurrence-free survival (52). Patients with *KIT* exon 11 missense mutation experienced a five-year recurrence-free survival (5-year RFS) of 89% compared to all other mutations types at 40%. Patients with a *KIT* exon 11 deletion/insertion experienced a 37% 5-year recurrence rate compared to all other types. Multivariate analysis comparing *KIT* mutation type, tumor size, mitotic rate, gender, histologic type, and margin of resection revealed *KIT* exon 11 deletion/insertion to be significantly associated with GIST recurrence, in addition to high mitotic rate (>15/30 hpf), mixed tumor histology, and male gender (52). A population-based study of 177 patients from the same timeframe,

Gene	Mutation at Protein Level	Clinicopathological Factors	Tumour Type	Prognostic Value
<i>KIT</i> -EC (exon 9)	Ala502_Tyr503dup	Strongly associated with intestinal GISTs (>90% of these mutations were identified in small intestinal tumours)	Predominantly spindle cell tumours	No prognostic value in intestinal GISTs
<i>KIT</i> -JM (exon 11)	Trp557_Lys558del	Occur in GISTs from different parts of GI tract	Spectrum of spindle cell and epithelioid tumours	May indicate more malignant behaviour, especially in gastric GISTs
	Deletions Deletion-insertions			May indicate less malignant behaviour in gastric GISTs
	Substitutions			
	Duplications	Associated with gastric GISTs	Predominantly spindle cell tumours	May indicate less malignant behaviour in gastric GISTs
<i>KIT</i> -TK1 (exon 13)	Lys642Glu	Occur in GISTs from different parts of GI tract		May indicate less malignant behaviour in gastric GISTs
<i>KIT</i> -TK2 (exon 17)	Asn822Lys	Two times more frequent in intestinal GISTs		No prognostic value
<i>PDGFRA</i> -JM (exon 12)	Deletions Substitutions	Strongly associated with gastric GISTs (>95% of such mutations identified in tumours from stomach)	Predominantly epithelioid or mixed epithelioid and spindle cell tumours	May indicate less malignant behaviour in gastric GISTs
<i>PDGFRA</i> -TK1 (exon 14)	Substitutions			
<i>PDGFRA</i> -TK2 (exon 18)	Deletions Substitutions			
<i>KIT PDGFRA</i>	Wild-type	Occur in GISTs from different parts of GI tract	Spectrum of spindle cell and epithelioid tumours	No prognostic value
		GISTs in NF1 (intestinal tumours)	Almost exclusively spindle cell tumours	No prognostic value
		GIST in Carney triad and paediatric GISTs (gastric tumours)	Predominantly epithelioid tumours	

*PDGFRA*, Platelet-derived growth factor receptor- $\alpha$ ; GIST, gastrointestinal stromal tumour; EC, extracellular domain; JM, juxtamembrane domain; TK1, TK2, cytoplasmic tyrosine kinase domains I and II.

### Table 3. GIST clinicopathological features

Reprinted by permission from John Wiley and Sons: Histopathology 53:245-266, copyright 2008.



1990-2000 (pre-imatinib), showed that *KIT* mutation type was strongly associated with outcome (82). Half of *KIT* exon 11 deletions belonged to a high risk/overly malignant risk group (49% of *KIT* exon 11 deletions belonged to this group, compared to approximately 30% for *KIT* WT, *KIT* exon 11 missense mutation, or *KIT* exon 11 duplication groups separately). In radically resected patients, two-thirds (65%) of *KIT* exon 11 deletion patients had recurrence of disease (31%) or died of disease (34%) when followed-up at five years, compared to WT *KIT* (17% recurrence, 17% death), *KIT* exon 11 missense mutation (0 recurrence, 13% death), and *KIT* exon 11 duplication (0 recurrence, 13% death) groups, prompting the authors to conclude that *KIT* exon 11 deletions are specifically associated with poor prognosis of GIST patients (82). In pre-imatinib gastric GISTs, an increased frequency of liver metastasis was observed in *KIT* exon 11 deleted tumors compared to *KIT* WT, as well as increased mortality in this group, both facts statistically significant (83). *KIT* exon 11 deletions also showed a trend for greater proliferative potential. Analysis of Ki-67 staining, a marker of proliferation and an independent predictor of prognosis in gastric GISTs, revealed that Ki-67 was highest in *KIT* exon 11 deletion tumors, less in the *KIT* exon 11 substitution group, and lowest in the *KIT* WT group (84). While not statistically significant, this trend, taken together with the significantly higher frequency of liver metastasis and higher mortality from disease, suggests *KIT* exon 11 deletions confer more of an aggressive profile to GIST tumors when present (83). Similar results were reported in a large-scale study of 1765 gastric GISTs by Miettinen and colleagues where a

*KIT* exon 11 deletion group had a significantly higher rate of progressive disease versus a *KIT* exon 11 missense mutation group (7).

*KIT* exon 11 deletions are most commonly a six base pair, two-codon W557\_K558 deletion in as high as 67% of detected mutations (85, 86). Missense mutations and larger deletions that overlap/involve codons 557 and 558, either together or independently, also occur. Examining 162 patients, Martin and colleagues analyzed each codon separately and saw a significant drop in 5-yr RFS when either W557 or K558 was affected (W557: 5-yr RFS 25% vs. 75% without mutation; K558: 5-yr RFS: 19% vs. 76% without mutation;  $p < 0.0001$  for each). Examining only *KIT* exon 11 deletions, patients with W557\_K558 deletion had a striking decrease in 5-yr RFS compared with other types of deletions (23% W557/K558 versus 74% all other deletions, **Figure 4**), prompting the hypothesis that W557\_K558 deletion is a significant component of the poor clinical outcome attributed to all *KIT* exon 11 deletions (87). This finding has been reported by two other investigators (88, 89).

Loss of heterozygosity (LOH) of the *KIT* locus and other chromosome 4 loci has been documented in advanced GIST (90). Heterozygous *KIT* exon 11 mutations were noted in small, early primaries, whereas homozygous *KIT* mutations were found in advanced primaries, a majority of which progressed and developed liver and intraabdominal metastatic implants quickly. GISTs with *KIT* exon 11 deletions or deletion/insertions were at significantly higher metastatic risk compared with GISTs that expressed heterozygous deletions in the same locations. Loss of *KIT* WT allele and duplication of the *KIT* mutant allele is associated with a malignant

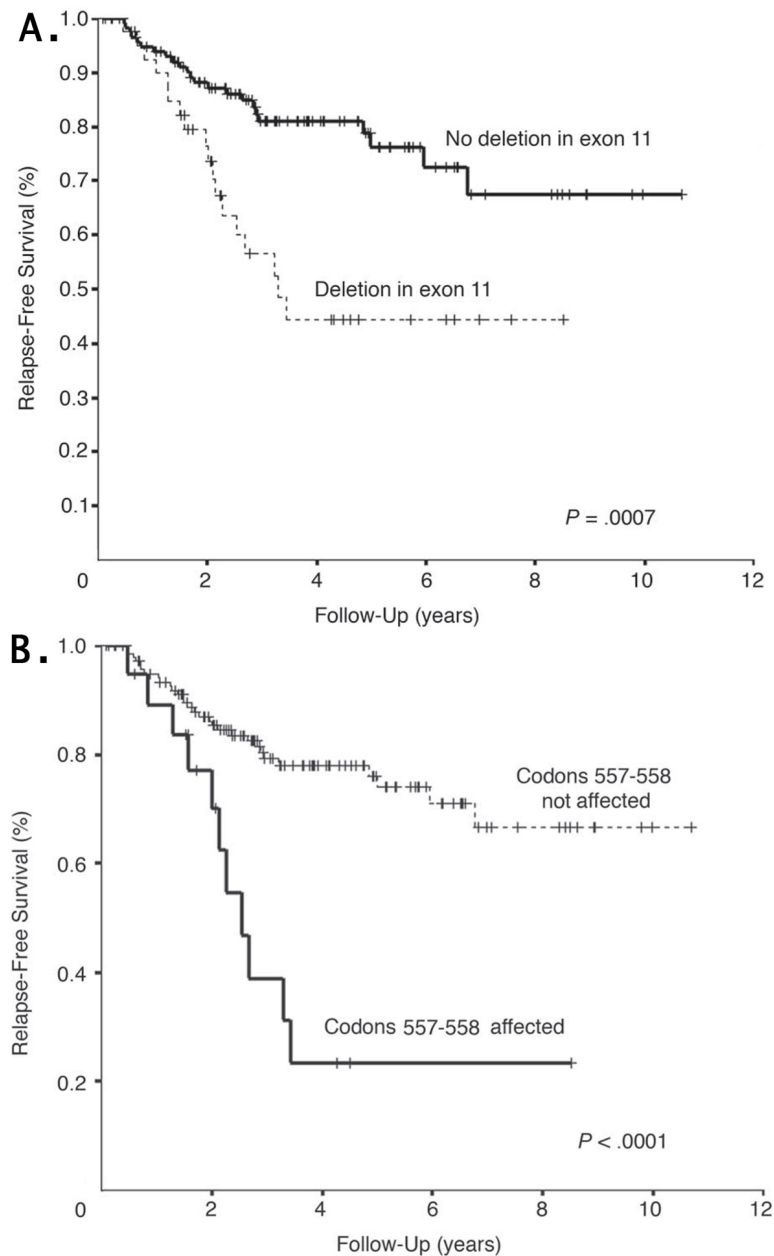


**Figure 4. *KIT* exon 11 deletions portend poor outcome**

Poor outcome likely attributable to W557\_K558 deletion. A) Kaplan-Meier curve for patients with or without *KIT* exon 11 deletion. B) Kaplan-Meier curve for patients with or without a deletion that involves codons 557 to 558 of *KIT* exon 11. Reprinted with permission. © 2008 American Society of Clinical Oncology. All rights reserved. Martin, J et al: J Clin Oncol 23(25) 2005:6190-8.

course of disease (90). *KIT* WT LOH is likely a mechanism of disease progression and metastasis in some advanced GISTs and could be considered an adverse prognostic marker.

### **1.5 *Imatinib Mesylate***

Imatinib was developed out of a drug discovery initiative focused on rational design and discovery of targeted anticancer therapies; rational, in the sense that they selectively targeted genes or gene products that were unique to cancer cells. The first such cancer-specific aberration was discovered in 1960 (91). A translocation of the long-arms of chromosome 9 and 22, called the Philadelphia Chromosome whose resulting fusion gene produced the BCR-ABL protein, was found only in tumor cells and is a primary marker of chronic myelogenous leukemia (CML) (92). Biochemist Nicholas Lydon developed imatinib together with Brian Druker and colleagues at Oregon Health and Science University beginning in 1988. The pair first identified a lead compound from a drug screen of inhibitors against protein kinase C (PKC) (93). During optimization of this lead compound, investigators noticed a structural component that would also inhibit the ATP-binding site of BCR-ABL, but the derivative compounds were poorly soluble in water and had low oral bioavailability at that stage (93). Further structural optimization ensued and the most-promising compound from the optimization, STI-571 (imatinib mesylate, Glivec, Gleevec<sup>™</sup>, Novartis Pharma, Basel, Switzerland) was found to readily inhibit ABL activity at an IC<sub>50</sub> 0.1-0.3 $\mu$ M and possess both high specificity and oral bioavailability (94). It was also noted that imatinib selectively inhibited KIT

and PDGFRA kinase activity by competing for the adenosine triphosphate (ATP)–binding site of these receptors, found within the kinase domain (95, 96).

Selective inhibition of tyrosine kinases is possible through the specific structural/conformational differences they each possess. To inhibit KIT, imatinib binds to the ATP-binding pocket, occupying the nucleotide-binding cleft, and competitively displaces ATP, thereby hindering KIT autophosphorylation and constraining downstream signaling through its signaling mediators (signaling molecules shown in **Figure 2**) (97). In vitro, autophosphorylation of both wild-type and mutated KIT, is completely abrogated at imatinib concentrations  $\geq 1\text{mM}$  (98). Inhibition of KIT, MAP, and phosphorylation of AKT in GIST cell lines leads to reduced glucose uptake, cell cycle arrest, and induction of apoptosis (99, 100). Targets of imatinib and downstream signaling consequences of its inhibition are summarized in **Table 4**. The pharmacokinetics and metabolism of imatinib are discussed in a subsequent section, below.

Following rapid clinical investigation, imatinib received US Food and Drug Administration (FDA) approval in May 2001. An overview of the development timeline of imatinib is presented in **Figure 5**. To date, imatinib is now approved in Ph+ CML, GIST, as well as chronic eosinophilic leukemia, Ph+ acute lymphoblastic leukemia, dermatofibrosarcoma protuberans, systemic mastocytosis, and myelodysplastic/myeloproliferative disorders (101). There are currently 86 active clinical trials with imatinib ongoing in the United States (November 2010) (102).

Gene	Downstream Signaling Factors		Signaling Consequences
BCR-ABL ↓	PI3K, AKT	BAD, MYC	Promote apoptosis
	BAD	BCL-XL, BCL-2	Induce apoptosis
	JAK2	STAT	Prevent cell proliferation
	GRB-2	SOS, RAS, RAF, MEK, ERKs, P90RSK, MSK, ELK-1, STAT	Prevent cell proliferation
	STAT	—	Prevent cell proliferation
Caspase-3 ↑	PARP, DNA-PK, SRE/BP, rho-GDI, <i>et al</i>	—	Cell apoptosis
p38 ↑	PLA2, MNK1, PRAK, Hsp27, STAT1, ELK-1	—	Inhibit proliferation and induce apoptosis by activation of p38 MAPK pathways
Exogenous IL-6 ↓	—	—	Inhibit KIT signaling pathway activated by exogenous interleukin-6
ERK1/2 ↓	p90RSK, MSK, ELK-1, PLA2, MNK1, PRAK, Hsp27, STAT	—	Induce apoptosis and inhibit proliferation by downregulation of ERK pathways
ERK5 ↓	—	—	Inhibit proliferation and induce apoptosis by downregulation of ERK5 pathways
KIT ↓	Decreased autophosphorylation by competing at ATP-binding site	—	Down-regulation of activation of ERK1/2 and AKT, induce apoptosis
PDGFRA ↓	—	—	Down-regulation of activation of ERK1/2 and AKT, induce apoptosis
C-ABL ↓	—	—	Prevent cell proliferation, induce apoptosis
SPRY4A, FZD8, PDE2A, RTP801, FLJ20898, and ARHGEF2 ↓	—	—	Prevent cell proliferation, induce apoptosis
MAFbx ↑	—	—	Prevent cell proliferation, induce apoptosis

**Table 4. Targets of imatinib signaling consequences**

Reprinted by permission from John Wiley and Sons: Cancer 113:1532-1543, copyright 2008.

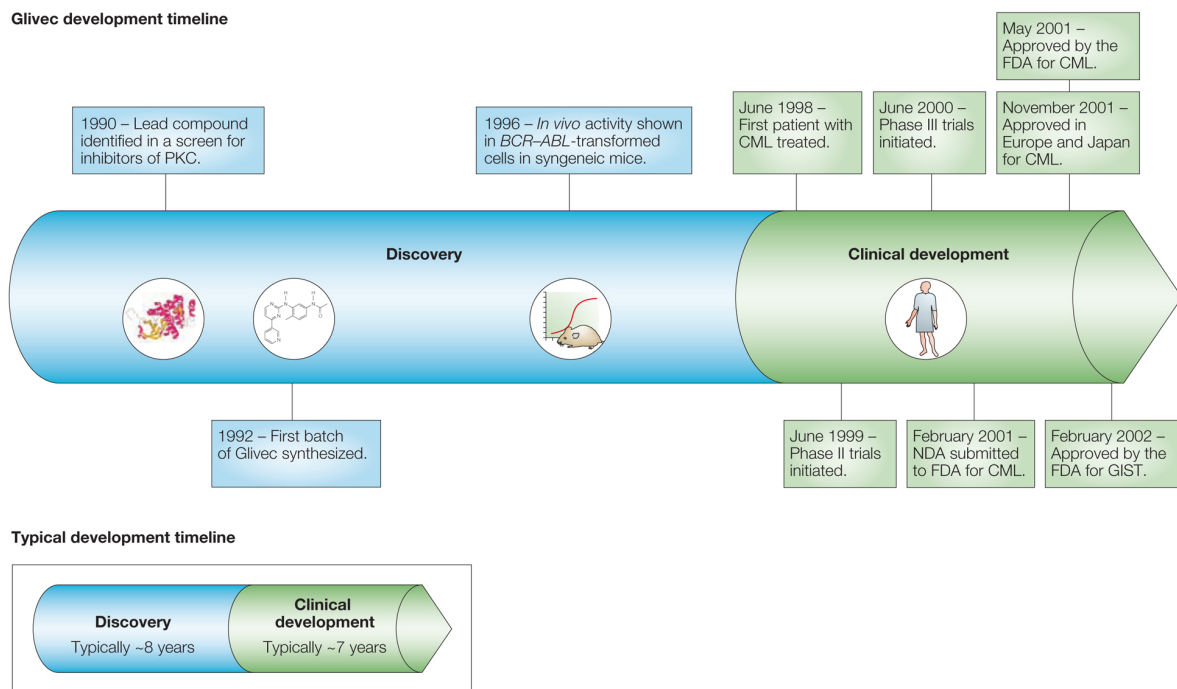


### Figure 5. Timeline of imatinib development

Imatinib was FDA approved in 2001 following rapid clinical development, compared to a typical drug development timeline presented in the inset. Less than three years after treatment of the first CML patient, the new drug application was filed, and FDA approval was granted less than three months after application. GIST, gastrointestinal stromal tumor; PKC, protein kinase C; CML, chronic myelogenous leukaemia. Reprinted by permission from Macmillan Publishers Ltd: *Nat Rev Drug Discov* 1:493-502 copyright 2002.

## **1.6 Imatinib in CML**

CML is a myeloproliferative disorder that affects hematopoietic stem cells. Approximately 20% of all leukemias are CML, and the incidence of this disease appears to be similar worldwide. CML has an annual incidence of 1.6/100,000, there is a slight male predominance (1.4 to 1.3), with a median age at diagnosis of 55 years and few patients under the age of 20 (<10%) (103). Greater than 90% of CML patients possess the Philadelphia chromosomal abnormality (Ph+) (104). CML has three distinct disease phases: it is typically identified when a patient is in the chronic phase (CML-CP), largely asymptomatic but with an elevated granulocyte level, followed by the accelerated phase (CML-AP), where there is a brisk multiplication of granulocytes. CML-AP can lead to a blast phase (CML-BP) similar to acute leukemia wherein metastasis, organ failure, and death can occur (105). Prior to the use of imatinib, cytotoxic chemotherapies controlled the disease, but most patients ultimately progressed to blast phase (105, 106).

Imatinib was quickly moved into clinical trials in 2001 and became the first FDA-approved TKI for treatment of Ph+CML patients in the United States. In a Phase I, dose-escalating trial for patients who had failed interferon- $\alpha$  therapy, 53 of 54 patients saw complete hematologic responses, typically within the first four weeks of therapy, seven patients achieved complete cytogenetic remissions, and no maximum tolerated dose was identified (107). Two phase II studies treating CML-AP and CML-BC patients were highly effective and imatinib showed minimal toxicity in these patient groups (108, 109). Patients were treated with imatinib at 600-800 mg once per day and the maximal tolerated dose was not reached. Interestingly,



subsequent studies showed that increasing the dose above 400-600 mg daily did not produce significantly higher molecular responses (MMR) at 12 months, a point to be examined in contrast to GIST later, and while imatinib remains the first-line therapy in CML, increased dose is not currently supported (110, 111).

While imatinib has transformed treatment of CML, challenges remain as a significant proportion of patients develop intolerance or resistance to therapy (106). Similarly as in GIST, resistance is acquired as patients develop missense mutations in the BCR-ABL fusion gene (112). These mutations affect the conformation of the protein and hinder binding of imatinib, reducing its kinase inhibition of BCR-ABL (113). Sequencing of CML patients resistant to therapy has identified greater than 100 different mutations, and very few of these mutations have been identified prior to therapy, none in CML-CP patients (114, 115). The presence of two or more mutations in a patient, or a particular T315I mutation, has also been shown to infer resistance to other TKI therapies currently available (116-118). While routine mutational analysis is not currently employed in all centers treating CML prior to imatinib therapy failure, the ability to identify those at high-risk of disease progression, or those who would be insensitive to TKI treatment based on mutation status, suggests that mutation testing in CML could be highly informative in the future (116, 117).

### **1.7 *Imatinib in GIST***

Following the observation that imatinib readily inhibited KIT and PDGFRA, a single patient pilot study was carried out in a setting of compassionate use in Finland. A 50-year-old patient with metastatic GIST, who had failed chemotherapy

with six previous agents, was given 400 mg once daily of imatinib beginning March 2000. Response, measured by 2-deoxy-2[F-18]fluoro-D-glucose positron emission tomography (FDG-PET) and computed tomography (CT), showed dramatic metabolic response, shrinkage of the tumor, and myxoid degeneration of the liver metastases, confirmed by biopsy after only four weeks of treatment (119). The patient experienced stable disease for over one year following initiation of imatinib therapy. Phase I clinical study began in the last months of 2000 in three centers in Europe, where 40 patients were administered varying doses of imatinib from 400 mg to 1000 mg once daily (120). The maximum tolerated dose was set at 800 mg based on severe toxicity at the 1000 mg dose, and although not an objective of the study, a partial response rate of 53% was observed.

Two phase II clinical studies followed, both with impressive results in a total of 174 GIST patients. The studies reported an overall objective response rate of 63% and 71%, respectively, with greater than 80% of patients achieving partial response or stable disease in both trials (121, 122). The larger of the two phase II trials compared starting doses of 400 mg and 600 mg in 147 subjects, and reported five-year survival of advanced GIST patients greater than 50%, irrespective of dose (123). This was followed by two large, tandem phase III trials beginning in December 2000.

The first phase III clinical study enrolled 746 patients from 57 treating institutions in the US and Canada with the aim of determining overall survival and response rates of GIST patients at two different doses of imatinib (400 mg versus 800 mg once daily) (124). Patients who progressed at 400 mg were allowed to

crossover to the higher-dose arm of the study. At a median follow-up of 25 months, there were no differences in progression-free survival (50% versus 53%) or overall survival (78% versus 73%) between the two dose groups, 400 mg and 800 mg respectively. There were, however, 106 patients who progressed at the lower dose, increased to 800 mg resulting in 7% partial response and 32% stable disease, demonstrating the efficacy of higher-doses in the context of progression (124). The second phase III trial conducted by a consortium of institutions in Europe and Asia randomized 946 patients to 400 mg and 800 mg daily starting doses (125). At two years, in contrast to the North American study, overall survival was not significantly different between the two arms (69% at 400 mg; 74% at 800 mg), but progression-free survival was significant (44% at 400 mg versus 52% at 800 mg,  $p=0.026$ ), again favoring the outcome of those receiving higher doses of the drug. The reason for the discrepancy between the two studies is unclear, but it is important to mention that *KIT* mutation was not evaluated between the two studies at the time and differences due to race and genetic background may have played a role (4). The European study enrolled more patients and thus may have had greater statistical power to detect such differences. In retrospect, a higher dose of 800 mg showed better response for *KIT* exon 9 patients.

The FDA approved imatinib for treatment in GIST in 2002 and it remains a key first-line treatment in management of GIST today. Patients with local disease (single tumor) are currently treated with surgical removal of the tumor, with negative margins, followed by adjuvant imatinib for up to two years in some cases (10). Adjuvant therapy has proven efficacious in improving recurrence-free survival (RFS)

and overall survival (OS) after GIST resection, likely from treatment of residual micrometastatic disease already present in the patient at the time of primary GIST diagnosis (126). Five studies have examined the benefit of adjuvant imatinib therapy and shown its benefit when considered together with a patient's individual risk of recurrence as well as their tumor's underlying genetic profile (126-130). Similarly, neoadjuvant imatinib ahead of surgery has proven advantageous through the cytoreduction of tumors, decreasing the risk of intraoperative tumor rupture, enabling some unresectable patients the opportunity of later resection, as well as enabling better organ preservation (126). For recurrent or metastatic GIST, imatinib is a first-line therapy and may be followed by resection of residual disease if patients respond. If patients do not respond at a starting dose of imatinib (typically 400-600 mg), imatinib dosing is often increased to 800 mg to elicit response before selecting a second-line TKI. Response in GIST is discussed in a subsequent section. An overview of current GIST management principles is presented in **Table 5**.

Response to imatinib varies greatly based on the underlying mutation type of the patient's tumor. Patients with *KIT* exon 11 mutation experience a significantly higher response rate, increased median and overall survival, and are at reduced risk of progression compared to patients with a *KIT* exon 9 mutation, or no *KIT* mutation at all (**Figure 6**) (54, 127). From early studies of imatinib response, *KIT* exon 9 was identified as the strongest adverse prognostic factor, and it was shown that a higher starting dose of imatinib (800 mg) was more effective in this group of patients (127, 128).

Clinical Scenario	Management
<b>Local disease (one tumour)</b>	<p>Complete surgical removal of the tumour with tumour-free (usually a few centimetre) margins. Avoid tumour rupture.</p> <p>Adjuvant and neoadjuvant treatment with imatinib are being investigated in clinical trials and are considered experimental at present. Neoadjuvant imatinib may be considered for selected patients to achieve organ preservation. Adjuvant imatinib is recommended in case of tumour rupture.</p> <p>Adjuvant radiation therapy or conventional chemotherapy have no proven value.</p>
<b>Recurrent/metastatic disease; first line therapy</b>	<p>Imatinib daily until treatment failure; the starting dose is usually 400–600 mg/day. Monitor blood cell counts, blood chemistry and treatment response (e.g. CT of the abdomen 1 month after starting imatinib, then at about 3-month intervals).</p> <p>Surgical resection of residual tumours of responding patients may be considered in selected cases, but the benefit is unproven. Removal of bleeding, infected or obstructing metastases may be necessary.</p>
<b>GIST progresses during imatinib therapy</b>	<p>(i) Escalate imatinib dose up to 800 mg/day if feasible. Consider surgery for solitary growing metastases.</p> <p>(ii) Sunitinib considered for second-line therapy (especially when KIT exon 9 mutation is present).</p> <p>(iii) Consider participation in a clinical trial with novel agents.</p> <p>(iv) Many patients may benefit from imatinib despite of GIST progression during imatinib therapy. Consider palliative surgery or radiation therapy in selected cases.</p>

*CT, computed tomography scan*

**Table 5. Key principles in the clinical management of GIST**

Reprinted from Joensuu H et al, Gastrointestinal Stromal Tumor (GIST), *Annals of Oncology* 2006, 17(Suppl 10): 208-6 by permission of Oxford University Press.

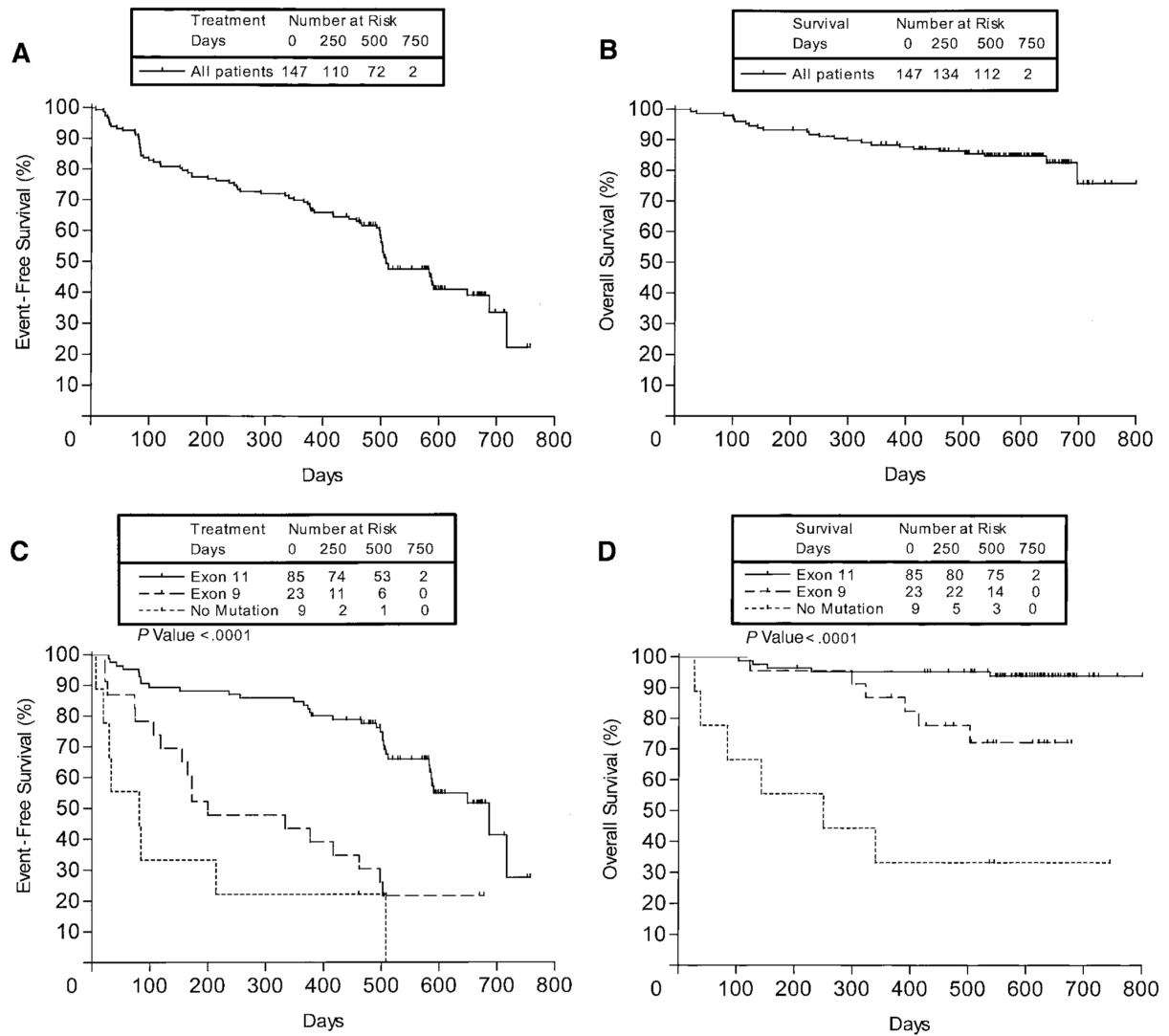


### Figure 6. *KIT* exon 11 mutation portends better response

Genotype of GIST correlates with event-free survival and overall survival. *KIT* exon 11 mutation portends better response (C) and outcome (D) on imatinib compared to that of *KIT* exon 9 or wild-type *KIT* for GIST patients in the CSTI571B 2222 phase II study. Reprinted with permission. © 2008 American Society of Clinical Oncology. All rights reserved. Heinrich, MC et al: J Clin Oncol. 2003 Dec 1;21(23):4342-9.

Resistance to imatinib can occur through the acquisition of secondary mutations, discussed in Section 1.3. These mutations are not usually detected in the pre-imatinib, nonresistant primary tumor, but rather in recurrent nodules or metastatic disease exposed to imatinib, and are associated with activated KIT levels similar or even higher than those in untreated GISTs (133-137). Secondary mutations typically arise in exons 13 and 17 of *KIT*, as was previously shown in **Figure 3**. Not all mutations in this region are identical however, and responsiveness of some *KIT* exon 13 mutations (albeit typically primary 13) to imatinib have been reported (129, 130). Functional analyses and molecular modeling of different mutations in *KIT* has provided meaningful evidence as to why secondary, and even different primary, mutations exhibit discordant influence on the inhibition by imatinib: each mutation affects the complex ultrastructure of the KIT protein and can alter the imatinib:ATP-binding pocket interaction significantly and uniquely (131). Not all secondary mutations might inhibit in the same manner, as a *KIT* exon 13 T670I alteration was found to modify the binding pocket considerably, whereas a *KIT* exon 13 V654A mutation resulted in minor, relatively confined structural changes (131). *KIT* exon 17, which encodes the activation loop, makes close physical contact with imatinib. Mutations such as D820Y and N822K stabilize the active form of the receptor and this, in turn, impedes the binding of imatinib (132-134). Sub-groups of primary *KIT* exon 11 mutations have been reported that have reduced response to imatinib in some cases, such as the *KIT* exon 11 mutation L576P (142, 143). This missense mutation in the juxtamembrane region places considerable constraint upon the ATP-binding pocket was computationally

predicted to be two-times less sensitive to imatinib than wild-type KIT (135). *KIT* exon 9 mutations are thought to distort an anti-dimerization motif in the extracellular region and promote spontaneous dimerization of KIT (49, 53). In both situations, it is understandable to hypothesize that higher concentrations of the competitive inhibitor would be required and that a higher dose of imatinib could be more effective to overcome either binding target constraint or increased KIT dimerization.

### **1.8 Therapeutic Drug Monitoring of Imatinib in GIST**

Therapeutic drug monitoring (TDM) by sampling the levels of a particular drug of interest in the serum or plasma of a patient can be important to ensure that patient stays within a therapeutic range, thereby maximizing a drug's therapeutic effect. TDM also serves to minimize toxicity and assess patient adherence to oral therapies (136, 137). Therapeutic range means the area between the curve where drug levels are to have a therapeutic effect, with minimal toxicity (illustrated in **Figure 7**). After administration and absorption, within a few hours a drug reaches its maximum concentration ( $C_{max}$ ) in the blood. This peak may be associated with some toxicity. Over time, as the drug is metabolized and eliminated by the body, the concentration decreases and reaches its minimum concentration ( $C_{min}$ ), also called the "trough". Generally, a patient achieves the trough level at the time their next dose is scheduled. This trough level is important that it remain above the lowest therapeutically effective concentration (see **Figure 8**). In this study, TDM was used to determine a patient's trough level and dose adjustment may follow to optimize this level. The time needed for the drug concentration to decrease in the blood by 50% is referred to as the half-life of that drug. After a patient has received



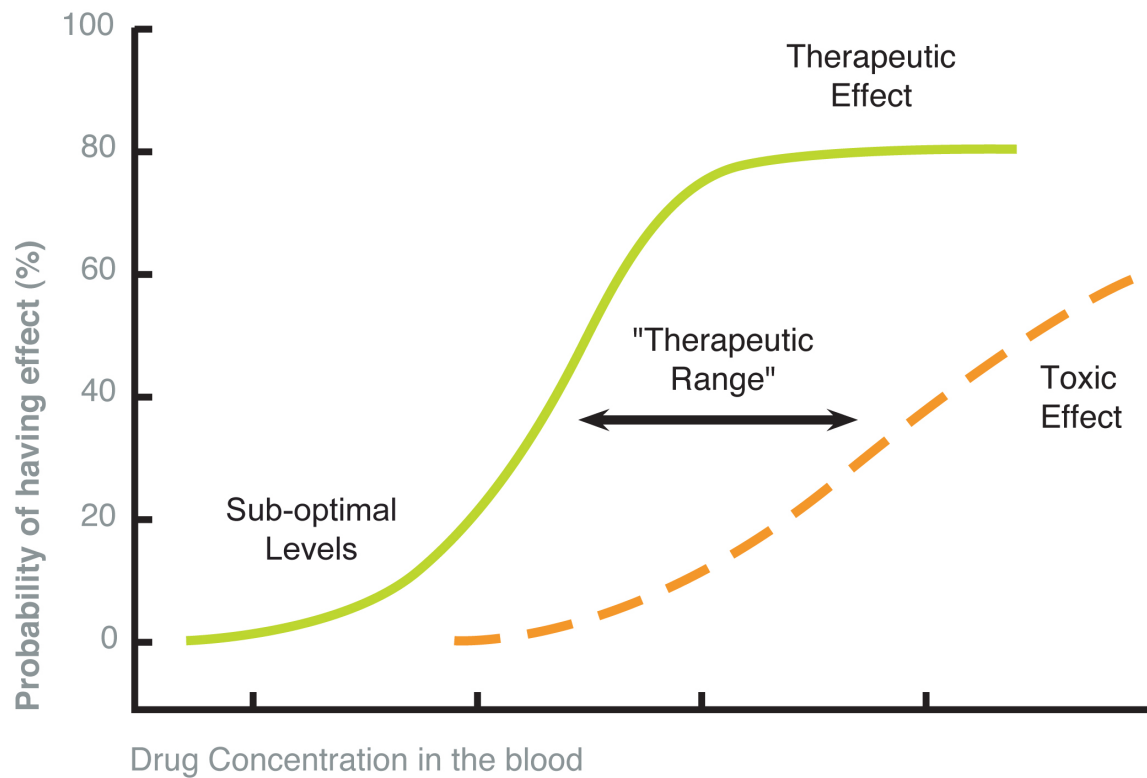


**Figure 7. Therapeutic range**

Therapeutic range of a drug is the region between the effective curve of drug concentration and the concentration that is associated with toxicity. Reprinted with permission. © Test Positive Aware Network 2005; Anderson, P. Positively Aware (6):3-7.

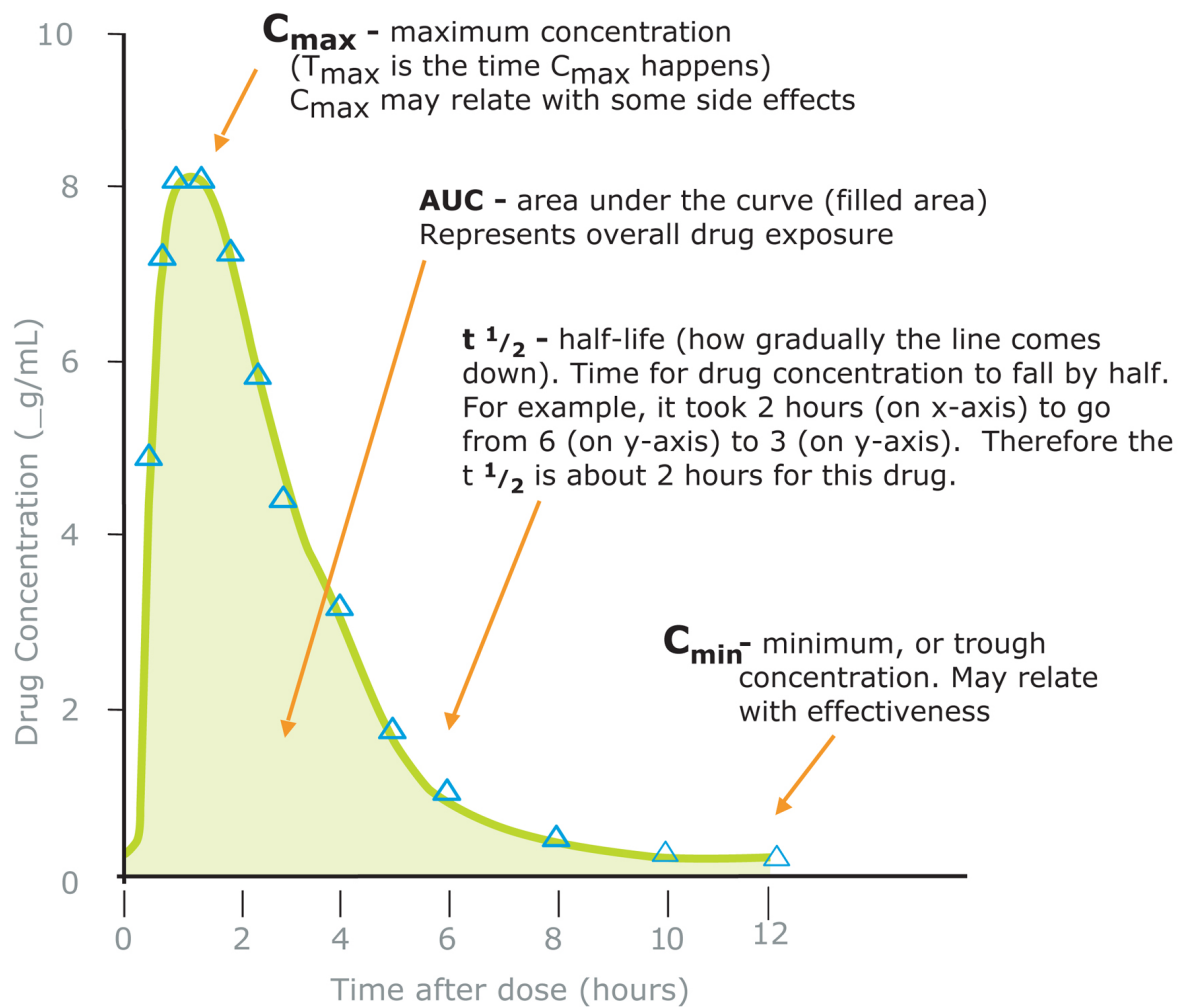


**Figure 8. Blood levels of a drug over time**

A drug will reach  $C_{max}$  within a few hours following administration and absorption.  $C_{max}$  may be associated with some toxicity. Drug concentration decreases over time as it is metabolized and eliminated by the body until  $C_{min}$  ("trough"). Trough level should remain above therapeutic minimum concentration for effectiveness. Reprinted with permission. © Test Positive Aware Network 2005; Anderson, P. Positively Aware (6):3-7.

a drug for some time, the patient is said to be at steady-state when the rate of drug administration and drug elimination are equal. Steady-state is usually achieved within four to five days, or in about five to seven half-lives of imatinib (138). At steady-state, each subsequent dose of a drug would result in identical  $C_{\max}$ ,  $C_{\min}$ , and area under the curve (AUC) (**Figure 9**).

Recently, significant focus has been placed upon monitoring the plasma imatinib levels of GIST patients after studies in CML showed that accelerated-phase patients benefitted from increased plasma imatinib levels. CML-AP patients receiving 400 mg or 600 mg who achieved major molecular response (MMR) had significantly higher mean imatinib trough levels ( $1452 \pm 649$  ng/mL for MMR versus  $869 \pm 427$  ng/mL for non-responders) (139). Dose level did not, however, correlate with this rate of MMR, indicating that not all patients at identical dose may achieve similar trough levels of imatinib. Similarly, a study of 351 CML-CP patients showed that higher steady-state imatinib plasma levels were associated with complete cytogenetic response, and a therapeutic minimum imatinib plasma level for CML was suggested at 1002 ng/mL (139, 140). Again, patients at identical dose experienced a diverse range of imatinib plasma levels, illustrated in **Figure 10**.

In GIST, notable interpatient variability of plasma imatinib levels was similarly observed in a recent, retrospective analysis of patients who received either 400 mg or 600 mg imatinib and dose was not associated with statistically significant differences in median PFS, overall survival or response (141, 142). Dividing the patients into quartiles based on increasing plasma imatinib level, however, revealed that patients with the lowest plasma levels of imatinib (quartile 1) experienced

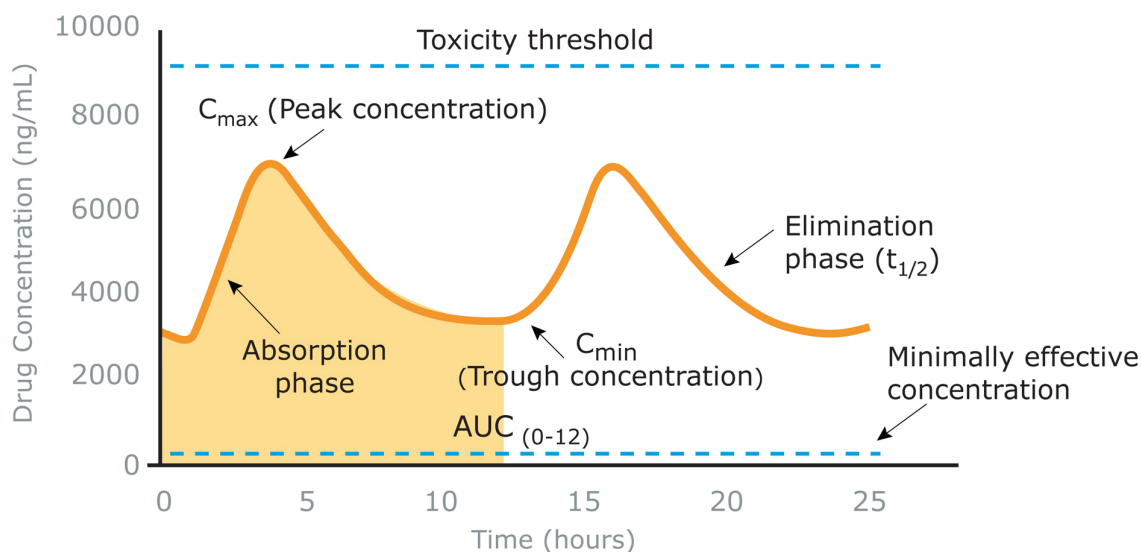


**Figure 9. Concentration time curve at steady-state**

Steady-state is achieved when the rate of drug administration and drug elimination are equal, usually within one to two weeks, or in about five half-lives of a particular drug (143). At steady-state, each subsequent dose of a drug would result in identical  $C_{max}$ ,  $C_{min}$ , and area under the curve (AUC). Reprinted with permission. © Test Positive Aware Network 2005; Anderson, P. Positively Aware (6):3-7.

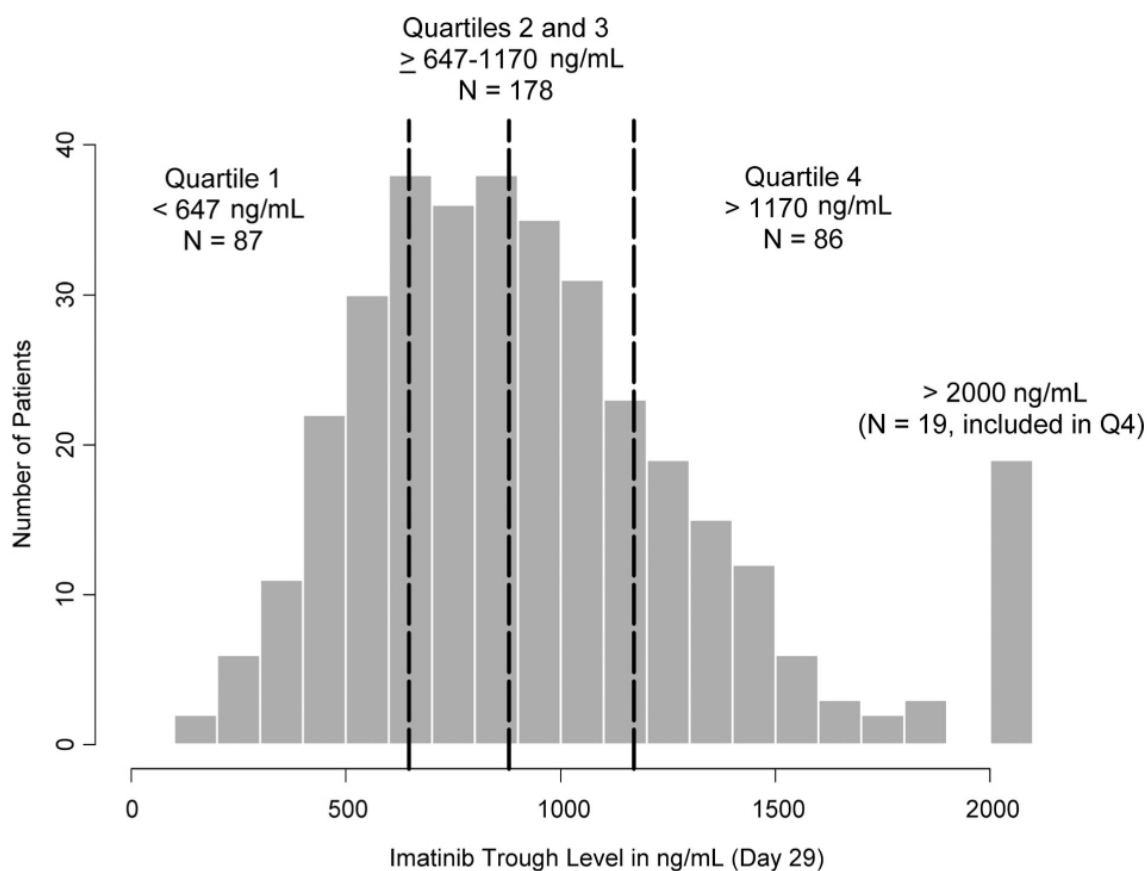


**Figure 10. Patients experience diverse trough imatinib levels**

Distribution of trough imatinib levels at 400 mg daily at steady-state on day 29 ( $n=351$ ). The vertical dashed lines represent 25th, 50th (median), and 75th percentiles. Reprinted with permission of The American Society of Hematology (ASH) from Larson et al. Imatinib pharmacokinetics and its correlation with response and safety in chronic-phase chronic myeloid leukemia: a subanalysis of the IRIS study. *Blood* 111:4022-4028, 2008; permission conveyed through Copyright Clearance Center, Inc.

a significantly shorter time to progression, displayed in **Figure 11**, and Demetri and colleagues assigned a therapeutic lower threshold of 1100 ng/mL which corresponded to the cutoff of this lower quartile (142). A benefit for those with *KIT* exon 9 mutation was not observed in this study due to the low number of patients included. A subsequent small study by Widmer and colleagues did observe a longer time to progression for *KIT* exon 9 patients treated with 800 ng/mL imatinib, but further analysis of the response in relation to plasma imatinib level is required in this group (144, 145).

### **1.9 Pharmacokinetics of Imatinib**

Imatinib mesylate has favorable pharmacokinetic (PK) characteristics in both GIST and CML (146). The drug is rapidly absorbed and has a high oral bioavailability (<97% for both solution or capsule form) (147). Serum proteins avidly bind the drug upon absorption and peak serum concentrations are reached two to four hours following administration (148). Imatinib has a linear dose-exposure relationship in population-PK models, its terminal half-life is approximately 20 hours allowing for once-daily dosing (4). After once-daily dosing, drug accumulation of 1.5 to three-fold is observed and steady-state is achieved within four to five days (149).

The metabolism of many medications, including imatinib, is dependant upon the cytochrome P450 (CYP450) enzymes found in the liver and less extensively in the gastrointestinal tract (150). There are greater than 50 CYP450 enzymes, but over 90% of drugs are metabolized by the following isoenzymes: CYP1A2, CYP2C9, CYP2D6, CYP3A4, CYP3A5 (151, 152). Clinically significant drug interactions are largely a result of altered CYP450 metabolism and close monitoring

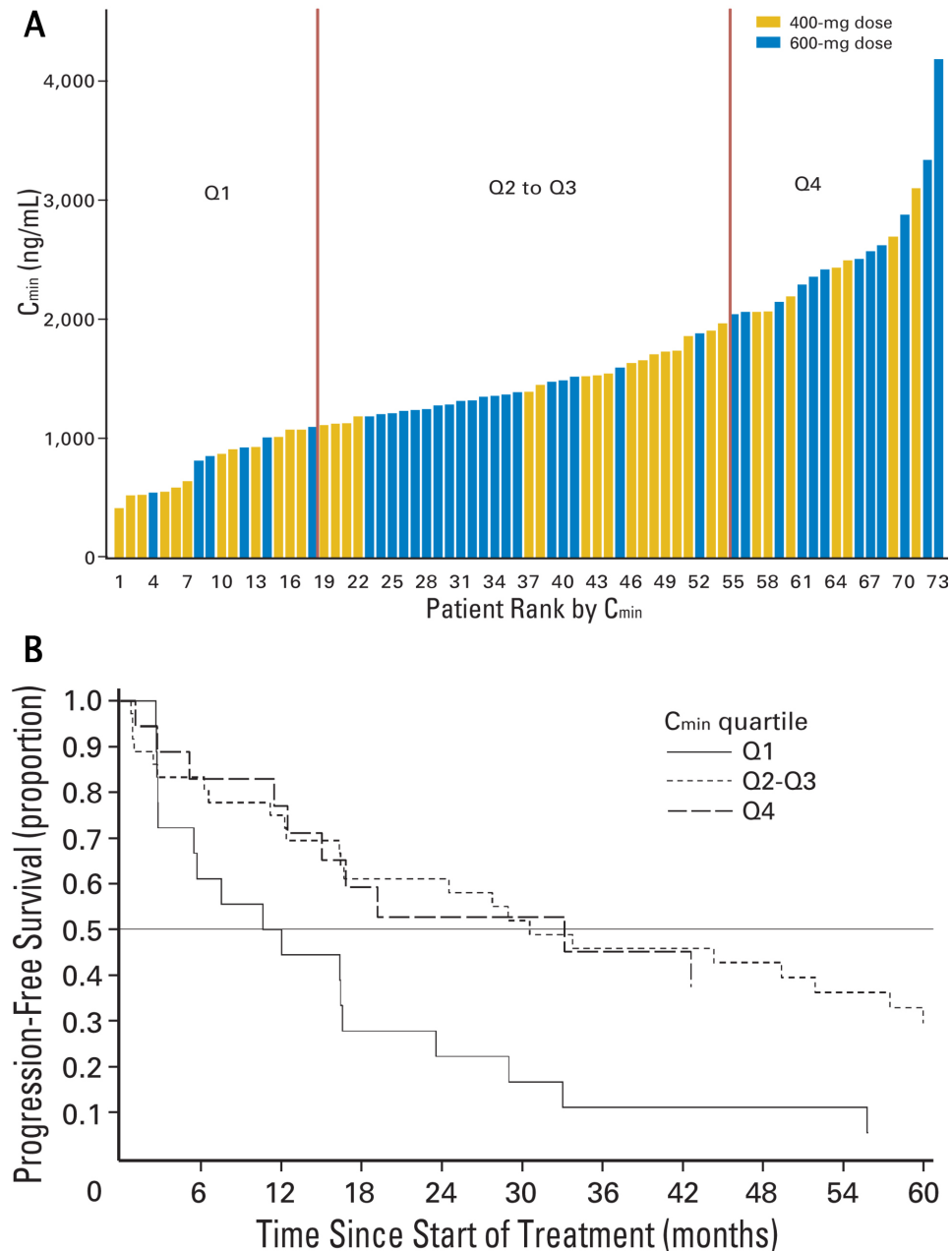


**Figure 11. Distribution of trough imatinib levels**

Plasma levels correlate to response in a group of unresectable/metastatic GIST patients. A) Distribution of imatinib trough concentration of GIST patients at steady-state receiving either 400 mg or 600 mg daily. Investigators subdivided by quartile for efficacy analysis and determined a 1100 ng/mL recommended minimum, which corresponded to the lowest quartile. B) Kaplan-Meier comparing time to progression for the four quartiles shows that patients with lower imatinib trough levels progress faster. Reprinted with permission. © 2008 American Society of Clinical Oncology. All rights reserved. Demetri, G et al. 27(19), 2009: 3141-3147.

is required when patients are given one or more drugs that influence CYP450 metabolism to avoid interaction and/or therapeutic failure (153-158). A drug that causes inhibition of any CYP450 enzyme is referred to as a “CYP450 inhibitor.” Inhibition usually occurs quickly after an inhibitor drug is added to a patient’s medications and resolves upon clearance of the drug. A drug that increases CYP450 enzyme activity is called a “CYP450 inducer” and this occurs via increased enzyme synthesis. Unlike inhibitors, CYP450 induction may take from days to several weeks as more enzyme is produced upon initiation of a CYP450-inducing drug; likewise, a delay may exist for induction to cease once that drug is discontinued (150).

There are several patterns of drug-drug interactions to consider when sequentially adding or removing drugs from a drug regimen, but the interactions that are potentially important in the case of imatinib are as follows (159):

*CYP450 inhibitor added to a CYP450 substrate* - adding a CYP3A4 or CYP3A5 inhibitor to imatinib (a CYP3A4/3A5 substrate) could result in higher plasma imatinib levels. Additionally, stopping a CYP3A4/3A5 inhibitor that a patient received prior to induction of imatinib may result in lower plasma imatinib levels. Conversely, as imatinib is itself a CYP3A4/CYP2D6 inhibitor, one might experience higher levels of both imatinib and any other CYP3A4 or CYP2D6 substrate drug with which it was co-administered. Higher imatinib plasma levels may result in increased efficacy as well as toxicity.



*CYP450 inducer added to a CYP450 substrate* - adding a CYP3A4 or CYP3A5 inducer to imatinib could result in decrease plasma imatinib levels and this drop may be delayed as mentioned above. Decreased plasma imatinib levels below a therapeutic minimum could be associated with decreased efficacy.

*Removal of CYP450 inhibitor* – discontinuation of a CYP3A4 or CYP3A5 inhibitor may result in a decrease of plasma imatinib levels. Again, decreased plasma imatinib levels below a therapeutic minimum could be associated with decreased efficacy.

*Removal of CYP450 inducer* - discontinuation of a CYP3A4 or CYP3A5 inducer may result in increased plasma imatinib levels, with possible delay. As before, higher imatinib plasma levels may result in increased efficacy or toxicity.

Keeping these patterns of interaction in mind, therapeutic drug monitoring of GIST patients may be critically important to ensure that they a) maintain a therapeutic minimum plasma level, and b) do not experience any adverse drug reactions with concomitant medications, and c) do not experience intolerable toxicity while on imatinib. Dose adjustment may be necessary based on clinical judgment. Interactions of significant effect with imatinib are discussed, following.

Imatinib is a substrate of the CYP3A4 and CYP3A5 isoenzymes, and it is an inhibitor of CYP3A4 and CYP2D6 as well, effects of which are discussed below (160). Imatinib is extensively metabolized the cytochrome P450 (CYP) enzymes of the liver into its major metabolite, N-desmethyl-imatinib (CPG74588) and other

metabolites, then eliminated via biliary/fecal excretion (138). At steady-state, the concentration of CPG74588 is approximately 17% that of imatinib and CGP74588 retains the antitumor properties of imatinib; it is currently unclear if the additional metabolites are active (4).

It has been shown that co-administration of rifampicin, a CYP450 inducer, increases the clearance of imatinib (161). Similarly, St. John's Wort, an over the counter herbal medication commonly used for depression, increases imatinib clearance by up to 43% (162). Imatinib is an inhibitor of CYP3A4, as well as CYP2D6 and co-administration of imatinib with simvastatin, a 3-hydroxy-3-methylglutaryl-coenzyme A (HMG-CoA) reductase inhibitor, results in elevated levels of both drugs (163). Ritonavir, a potent CYP3A4 inhibitor, has been shown to have little effect on imatinib steady-state levels (164). Several other pharmaceuticals for cancer patients may achieve toxic levels when co-administered with imatinib, such as alprazolam, clindamycin, clonazepam, cortisol, ethinyl estradiol, and verapamil (163). Imatinib shares a biotransformation route with acetaminophen via CYP3A4 and preclinical studies have suggested an interaction between the two drugs leading to irreversible hepatotoxicity (165, 166). Patients are anecdotally advised to avoid daily use or excessive amounts of acetaminophen (167).

Patients with GIST commonly experience gastric upset, both from their disease and as a side effect of treatment with imatinib, making co-administration of antacids or proton-pump inhibitors (PPI) common. The PPI omeprazole does not significantly affect imatinib pharmacokinetics compared to another TKI used in

GIST, dasatinib, where PPI can decrease peak concentrations as much as two-fold (168). Similarly, magnesium/aluminum-based antacids have shown no effect on the pharmacokinetics of imatinib (169).

### ***1.10 Response Evaluation of GIST by CT***

Multiple imaging modalities have proven informative in assessing response or GIST to therapy. In 2000, international guidelines for the size-based evaluation of tumor response were published, entitled the Response Evaluation Criteria of Solid Tumors (RECIST) (170). RECIST identified contrast-enhanced CT and magnetic resonance imaging (MRI) as the best-reproducible methods for target lesion measurement in solid tumors, including GIST. Additionally, positron emission tomography (PET) employing fluorine-18—fluorodeoxyglucose ( $^{18}\text{FDG}$ ) is highly sensitive in visualizing changes in tumor glucose metabolism and shows GIST early response (171). In patients with KIT-expressing metastatic GIST, early response to imatinib treatment, as measured by  $^{18}\text{FDG}$ -PET, correlates with significantly improved progression-free survival after one year (172, 173). Unfortunately,  $^{18}\text{FDG}$ -PET is not universally accessible and is cost-prohibitive. Additionally, some small GISTs (<4.7 cm) have no discernable uptake of FDG, make them inutile as baseline images or comparators to post-treatment imaging (174). Contrast-enhanced CT is widely available, less expensive, and particularly with the latest-generation multidetection scanners, provides significant anatomic detail and spatial resolution compared to PET, making it the imaging modality of choice in GIST (175, 176).

Gastrointestinal stromal tumors can occur throughout the GI tract; the most frequent site of metastasis is the liver and the peritoneum (177). These highly

vascular tumors have significant contrast enhancement when visualized by CT (176). GISTs responding to treatment by imatinib generally decrease in size, which may not be appreciable for several weeks (178). Some responding GIST tumors actually increase in size and current opinion attributes this to intratumoral hemorrhage, necrosis, and myxoid degeneration within the tumor (176). Enhancing nodules within the tumor resolve, vascularity decreases, and GISTs become homogenous and hypodense in response to effective therapy. Changes in density are appreciable within one to four weeks of treatment initiation (178). An example of response to imatinib therapy in GIST is shown in **Figure 12**.

Surveillance of GIST during and post-treatment with contrast-enhanced CT is also important to detect evidence of recurrence or progression, which may occur in the form of clonal, resistant nodules (179). The appearance of intratumoral enhancing nodules within a hypodense lesion are often a sign of progression and these may occur without a size change in the overall tumor (176). Often, these enhancing lesions represent clonal development of tumor cells bearing additional resistance mutations in *KIT* (180-182). Appearance of focal progression within a principally-responding GIST tumor do not necessarily signal that imatinib therapy should be stopped, as alternative, complementary therapies may be available, such as radio frequency ablation (RFA) (176).

Recent studies have proven that evaluating GIST using traditional size-based criteria can dramatically underestimate response (173, 183-185). Using WHO criteria (sum of the products of two-dimensional tumor measurements) or RECIST criteria (sum of the longest unidimensional tumor measurement), one might

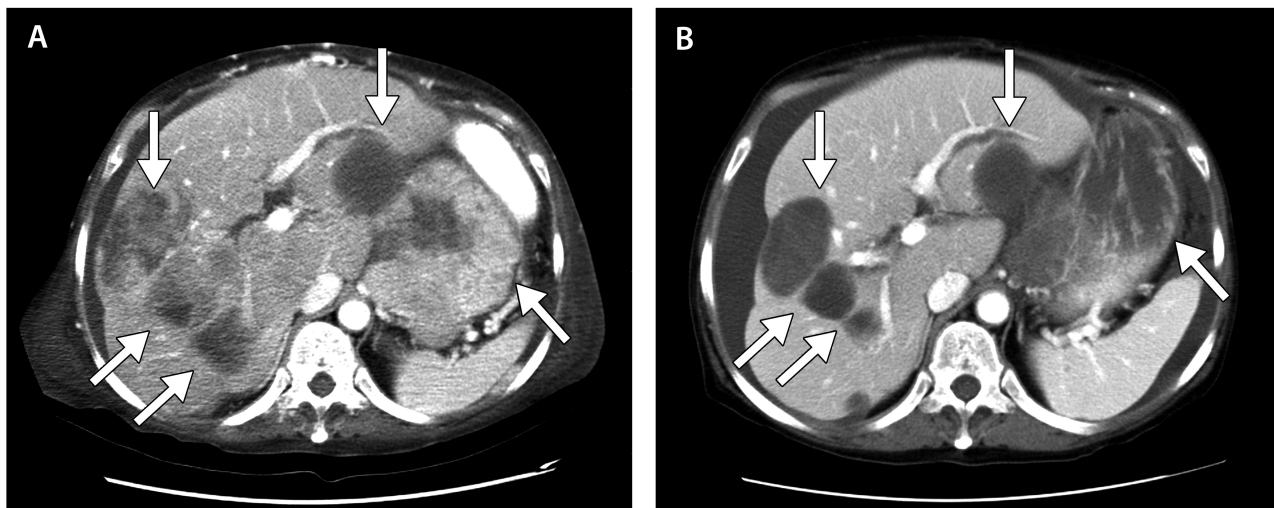


**Figure 12. Representative response of GIST metastases**

Advanced GIST with multiple hepatic and peritoneal metastases in a 61-year old woman with recurrent small bowel GIST. A) Pre-treatment contrast-enhanced CT reveals multiple, bulky, heterogeneous, hypervascular masses in the liver and peritoneum (arrows). B) Follow-up CT after six months of 400 mg imatinib daily shows that the lesions have reduced in size and have become significantly hypodense. Such results typify good response to imatinib.

misclassify a responding GIST as stable disease or even progressing upon size enhancement with imatinib therapy (176). Subjective evaluation criteria account for tumor size, extent/degree of CT enhancement, presence of tumor vessels, and presence of solid nodules within the tumor and are thought to best indicate overall response of a GIST tumor, yet such subjective criteria are not wholly quantitative and require an experienced radiologist familiar with the response patterns of GIST. Modified, objective criteria have been developed which predict response with greater accuracy in GIST compared to RECIST, hereinafter referred to as “Choi criteria”. Choi criteria consider a 10% (or greater) decrease in summed unidimensional tumor size or 15% decrease in tumor radiodensity a more sensitive qualifier of response in GIST (186). These criteria for response are summarized in **Table 6**. Though Choi criteria have been validated and RECIST shown to be an inadequate measure of clinical benefit, most if not all studies evaluating prognostic and predictive markers in GIST still use RECIST (184).

Response	Definition
<b>CR</b>	Disappearance of all lesions No new lesions
<b>PR</b>	A decrease in size* of $\geq 10\%$ or a decrease in tumor density (HU) $\geq 15\%$ on CT No new lesions No obvious progression of nonmeasurable disease
<b>SD</b>	Does not meet the criteria for CR, PR, or PD No symptomatic deterioration attributed to tumor progression
<b>PD</b>	An increase in tumor size of $\geq 10\%$ and does not meet criteria of PR by tumor density (HU) on CT New lesions New intratumoral nodules or increase in the size of the existing intratumoral nodules

*Abbreviations:* CR, complete response; PR, partial response; HU, Hounsfield unit; CT, computed tomography; SD, stable disease; PD, progression of disease; RECIST, Response Evaluation Criteria in Solid Tumors.

\* The sum of longest diameters of target lesions as defined in RECIST.

#### **Table 6. Modified Choi response criteria of GIST**

Criteria defining radiologic characteristics of complete response (CR), partial response (PR), stable disease (SD), and progressive disease (PD) are presented. Reprinted from Choi, H et al: J Clin Oncol 25 (13), 2007: 1753-1759; Reprinted with permission. © 2008 American Society of Clinical Oncology. All rights reserved.

### **1.11 Specific Aims of the Study**

There are a number of clinical challenges in the optimal treatment of GIST patients. Since *KIT* genotype influences the binding of imatinib (129), the optimal plasma trough concentration of imatinib is likely to vary based on the *KIT* genotype of the individual patient. Patients' genotype may influence the type of response that is appreciable by clinical evaluation, for example, by CT. Patient clinical response, if not homogenous and clear-cut in reflex to imatinib treatment should be carefully defined so as to better recognize effective treatment and/or earlier no-response of patients based on genotype.

Even though imatinib is an orally administered therapy, it is unclear whether patients who have received gastrectomy or small bowel resection absorb adequate levels of imatinib. Although standard of care is to increase imatinib dose at the time of progression, there is no data to show that a dose escalation results in an increase in the plasma trough concentration of imatinib in GIST patients.

The objectives of this study are to determine effects of genotype on the type of response appreciable by current imaging criteria, to determine the distribution of plasma imatinib levels in patients with GIST, to determine factors that correlate with plasma imatinib level, to determine the incremental effects of imatinib dose escalation; and to explore the median plasma levels and outcomes of patients with *KIT* exon 9 mutation. To that end, we have the following specific aims:

**1. To determine whether specific *KIT* mutations correlate with clinical outcomes of GIST patients treated with imatinib.** *Hypothesis:* Patients with *KIT* exon 11 mutations affecting codon 557 respond to imatinib with maximal reductions



in tumor size and greater decreased radiodensity compared to other *KIT* exon 11 mutations. If the hypothesis is true, then patients with *KIT* exon 11 mutation affecting codon 557 will respond to imatinib with a decrease in tumor IV contrast uptake on CT and significant decrease in tumor size. If the hypothesis is not true, then other *KIT* exon 11 codons, other exons of *KIT*, and specific types of mutational changes will be evaluated for type of CT response.

**2. To determine whether imatinib plasma levels correlate with clinical outcomes of GIST patients treated with imatinib - Hypothesis:** standard dosing of imatinib in GIST patients results in sub-therapeutic treatment levels for some patients. Higher imatinib plasma levels correlate with better clinical response. If the hypothesis is true, then clinical response, as assessed by CT (Choi Criteria), will be associated with higher imatinib plasma levels, irrespective of imatinib dose. If the hypothesis is not true, then this may indicate resistance to the drug in some patients (ie secondary mutation present), which could be screened.

## Chapter 2. Materials and Methods

### 2.1 *Plasma Level Testing and Calculation of Adj-C<sub>min</sub>*

From May 2008 to September 2010, patients with gastrointestinal stromal tumor (GIST) underwent therapeutic drug monitoring (TDM) at the University of Texas M.D. Anderson Cancer Center (UTMDACC), in Houston, Texas. Patients received a variety of doses ranging from 100 to 1200 mg based on clinical indication. Dose escalation occurred following disease progression, identification of *KIT* exon 9 mutation, or in patients with a notably low imatinib plasma level as per current clinical practice guidelines. Dose reduction occurred in the setting of unacceptable toxicity.

Plasma imatinib levels were determined using a validated liquid chromatography-tandem mass spectrometry assay by Avantix Laboratories, Newark, DE. Per patient, at least 5mL of blood was collected in K<sub>2</sub>-EDTA tubes by direct venipuncture, centrifuged at 1500Xg for ten minutes to achieve plasma separation, and plasma samples stored below -20°C until analysis. Protein precipitation/dilution samples were prepared using 100 µ L of patient sample, followed by isocratic separation on a Sepax GP-C18, 3 µ m, 2.1 x 100 mm LC column (3.5 minutes run time @ 0.4 mL/min). Samples were then analyzed by LC/MS/MS (MRM, electrospray positive ion mode) with an internal calibration method to detect both imatinib ST1571 (from 10 – 7500 ng/mL in plasma) and its metabolite CGP74588 (from 50 – 1500 ng/mL in plasma) in the samples.

Samples were drawn over a wide time window and adjusted trough imatinib concentrations ( $\text{Adj-C}_{\min}$ ) were calculated from the observed trough levels according to the algorithm validated by Y Wang and colleagues (187).

$$\text{Adj-C}_{\min} = C_{\text{measured}} \cdot \exp(0.041 \Delta\tau)$$

where  $C_{\text{measured}}$  is the observed plasma level at the time of sampling, and  $\Delta\tau$  is the time since last imatinib dose. Adjustment of trough levels is achieved by multiplying the observed plasma imatinib level ( $C_{\text{measured}}$ ) and time since last dose ( $\Delta\tau$ ) by an elimination rate constant, ( $k_e$ ), determined using the clearance and volume of distribution for imatinib. Since it is assumed that the actual  $k_e$  is not known in each patient in the clinical setting, the algorithm is corrected using a typical  $k_e$  of  $0.041\text{hr}^{-1}$ . For patients with typical  $k_e$ , blood samples can be collected at any time point in the elimination phase and correctly adjusted using the algorithm with no error, whereas patients with high  $k_e$  should conservatively be drawn within  $\pm 6\text{hrs}$  normal dose time to keep the residual error of the adjusted trough low (187).

No patient was drawn more than twelve hours after his or her regularly scheduled dosing time,  $\tau$ . Samples were excluded from patients who were non-adherent to therapy (by patient report) or had experienced dose interruption within five days of sampling, and from those who took imatinib too close to the sampling time less than six hours for all dose schedules).

## **2.2 Patient Response Assessment**

Response to therapy, measured by CT, was assessed at baseline, two months and four months after first imatinib exposure. CT was performed with a LightSpeed or Hi-Speed Advantage helical scanner (GE Healthcare) using a monophasic scanning technique. The abdomen and pelvis were scanned at 5.0- or 7.0-mm collimation from the level of the diaphragm to the pubic symphysis. The scanning delay was 60 seconds after the start of administration of 150 mL of 60% nonionic contrast agent (Optiray 320, Mallinckrodt) at a rate of 3 mL/sec. Triphasic scanning technique was used in some patients, with scanning delays of 30, 60, and 120 sec for the early arterial, late arterial, and portal venous phases, respectively, after IV injection of the contrast agent at a rate of 5 mL/sec.

Using an independent workstation available in Diagnostic Imaging UTMDACC, the CT attenuation coefficient (radiodensity) of each tumor was measured in Hounsfield units by drawing a region of interest circumscribing the margin of the tumor in post-contrasted images. In patients scanned using triphasic techniques, the portal venous phase images were used for the tumor density measurement. The tumor density change (%) from the pretreatment evaluation to the two- and four-month evaluation was computed for each lesion, and the average percentage of change was then computed for each patient.

Tumor size was then measured at the longest cross-sectional dimension of each lesion. The percentage of change in the sum of the longest dimensions from the pretreatment evaluation to the two- and four-month evaluation was then computed for each patient.

Response was classified according to Choi criteria as complete response (CR, no radiographic evidence of GIST) partial response (PR,  $\geq 10\%$  decrease in GIST size or a  $\geq 15\%$  decrease in GIST radiodensity), stable disease (SD, less than 10% decrease or increase in GIST size and does not meet criteria of PR by radiodensity), progressive disease (PD,  $\geq 10\%$  increase in GIST size), or no data (ND, patient underwent resection and no response could be assessed) (184).

### **2.3 GIST Genotyping**

Genotype of GIST patient samples were characterized in the Molecular Diagnostics Laboratory at UTMDACC for clinical purposes or in the sarcoma research laboratory at our institution. Tumor tissue was assayed for *KIT* and *PDGFRA* mutation as previously described. Specific paraffin blocks containing tumor were identified and hematoxylin and eosin (H&E)-stained and unstained four mm-thick sections were obtained. Areas containing viable tumors were marked on the H&E slides and the slides were submitted for molecular analysis. Genomic DNA samples were isolated from microdissected paraffin-embedded slides using a QIAamp DNA minikit (Qiagen, Germantown, MD, USA) according to the manufacturer's instructions. One milligram Chelex-100 resin (Bio-Rad, Hercules, CA, USA) was added, mixed to a slurry, and incubated at room temperature for fifteen minutes. After centrifugation at 10,000 *g* for five minutes, the supernatant was decanted for use.

Polymerase chain reaction (PCR) for sequencing of *KIT* and *PDGFRA* was carried out using the following oligonucleotides:

<i>KIT</i> exon 9 (180bp product)	F 5'-TTTCCTAGAGTAAGCCAGGGC-3'
	R5'-GTTGTAAGCCTTACATTCAACCG-3'
<i>KIT</i> exon 11 (193bp)	F 5'-CTATTTTTCCTTTCTCCCC-3'
	R5'-TACCCAAAAAGGTGACATGG-3'
<i>KIT</i> exon 13 (176bp)	F 5'-TTTGCCAGTTGTGCTTTTTG-3'
	R5'-CAGCTTGGACACGGCTTTAC-3'
<i>KIT</i> exon 17 (185bp)	F 5'-TGGTTTTCTTTTCTCCTCCAA-3'
	R5'-TGCAGGACTGTCAAGCAGAG-3'
<i>PDGFRA</i> exon 12 (261bp)	F 5'-TCCAGTCACTGTGCTGCTTC-3'
	R5'-GCAAGGGAAAAGGGAGTCTT-3'
<i>PDGFRA</i> exon 18 (252bp)	F 5'-ACCATGGATCAGCCAGTCTT-3'
	R5'-TGAAGGAGGATGAGCCTGACC-3'

PCR was carried out in a total volume of 25  $\mu$ L containing 50 to 100 ng of genomic DNA and 0.25 acral lentiginous DNA polymerase (Bioline, London, UK). Mutations in these genes were identified by sequencing the PCR products on a 3730  $\times$  1 DNA analyzer (Applied Biosystems, Carlsbad, CA, USA) in the Molecular Diagnostic Laboratory or the Nucleic Acid Core Facility at UTMDACC. Control wild-type *KIT* and *PDGFRA* sequences were used for comparison to evaluate for mutation using FinchTV 1.4.0 software (Geospiza, Inc., Seattle, WA) on Mac Operating System 10.5.8. Sequencing was carried out for *KIT* exons 9 and 11 first, followed by *KIT* exons 13 and 17 if no results, then followed by sequencing of *PDGFRA* exons 12

and 18 if *KIT* was wild-type. Incomplete sequencing of *PDGFRA* is available, as a result.

## **2.4 Statistical Analysis**

The minimum study size was determined as follows: assuming exponential PSF and at least 12 months median PFS, then 90 patients would be sufficient to detect a 100% difference in PFS of 24 months with 83% power, based on a one-sided 0.025 level test. These estimates are based on the study by Demetri and colleagues (142).

Patients undergoing a planned dose escalation, for example following surgery, who were at a known less-than therapeutic dose at the time of TDM analysis were used only for the PK analysis and were excluded from any long-term outcome analysis.

The statistical association between immunohistochemical expression of KIT, *KIT* genotype, and diagnoses was investigated using Fisher's exact test, Kruskal–Wallis test, and the Spearman's rank correlation when the ordering of both factors was important. The level of significance was set at 5%. Covariates analyzed included: age, gender, race, body surface area (BSA), *KIT* mutation status (wild-type, exon 11 mutation, exon 9 mutation, or other), location of the primary tumor (esophageus, stomach, small bowel, or colon/rectum), primary tumor versus metastatic disease, lab values on the day of TDM such as total bilirubin, aspartate aminotransferase (AST), alanine aminotransferase (ALT), and presence of co-medications classified as cytochrome P450 (CYP450) inducers, inhibitors, or substrates. We also analyzed whether presence of full gastrectomy, proximal partial

gastrectomy, or distal partial gastrectomy correlated with altered plasma imatinib concentrations.

The distribution of each continuous variable was summarized by its mean, standard deviation and range. The distribution of each categorical variable was summarized in terms of its frequencies and percentages.

Since multiple measurements from a patient were collected/evaluated, a linear mixed model accounting for within-patient correlation was used. Marginal effect model and random effect model were conducted separately (188). Marginal effect model means the average response over the sub-population that shares a common value of the covariate. The coefficient was to describe the change in the average response for a unit change in the covariate for the entire population. As for the random effect model, the underlying idea is that a natural heterogeneity exists between individuals and this heterogeneity can be represented by a probability distribution. The coefficient under the random effect model describes the change in the average response for a unit change in the covariate for a particular subject.

Covariate distributions for this cohort and the retrospective patients were compared using generalized Fisher exact tests for categorical variables and Wilcoxon tests for numerical valued variables. Logistic regression was conducted to evaluate the effect of various factors on patient response. Kaplan-Meier curves (1958) were used to estimate unadjusted OS and PFS (189). Log rank tests were used to compare each time-to-event variable between groups like mutation groups. The Cox proportional hazards regression model (1972) was used to evaluate the ability of patient prognostic variables or treatment group to predict OS and PFS time



(190). The  $t$ -test was conducted to assess if there is difference between different sites (liver vs. peritoneal) regarding size change and density change; the ANOVA test was used to assess if there is difference across mutation types (9, 11, and wild type) regarding liver/peritoneal size and density change. All computations and were carried out in SAS version 9.1 and S-Plus version 8.0.

## **Chapter 3. Specific *KIT* Mutations Correlate with Clinical Outcomes of GIST Patients Treated with Imatinib**

### **3.1 *Introduction***

Genotype of GIST is significantly associated with progression-free survival, rate of recurrence, response to therapy (imatinib or other), as well as pathological correlates (54, 129). Genotype, and *KIT* mutation subtype, is associated with differential mitotic rate and histology of different GISTs (87). It is therefore logical to investigate whether genotype influences response to imatinib therapy, as measured by CT.

We hypothesize that patients with *KIT* exon 11 mutations affecting codon 557 are more sensitive to the antitumor activity of imatinib in GIST. Therefore, GISTs will respond to imatinib with maximal reductions in tumor size and greater decrease in radiodensity compared to other *KIT* exon 11 mutations. If the hypothesis is true, then GIST patients with *KIT* exon 11 mutation affecting codon 557 will be more likely to have better clinical outcomes such as progression-free survival and down staging of the tumor to enable surgical resection. If the hypothesis is not true, then other *KIT* exon 11 codons, other *KIT* exons, and specific types of mutational changes will be evaluated in order to identify the genotype with best clinical outcome.

### 3.2 Results

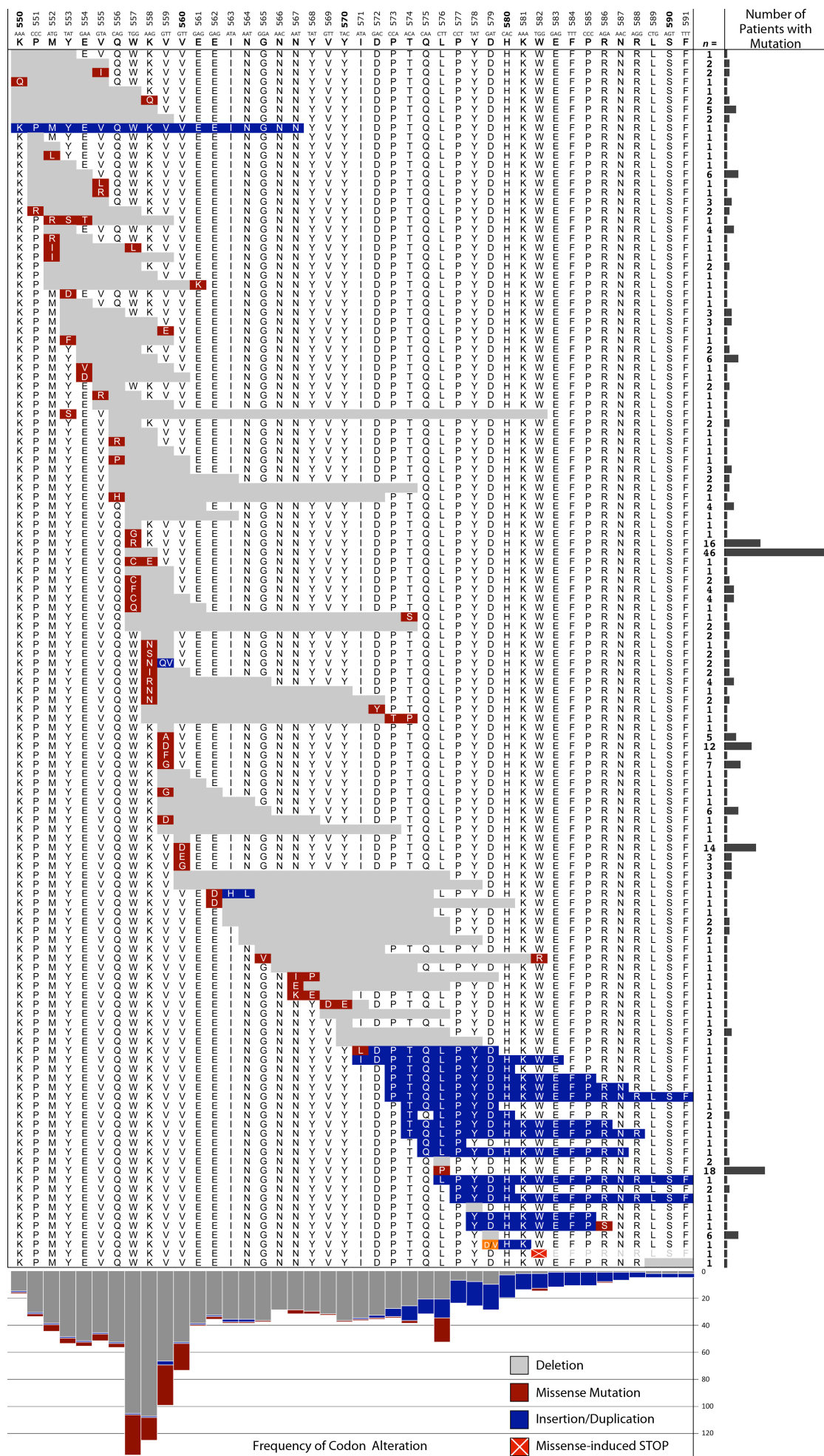
In total, 531 consecutive GIST patients whose pathology was reviewed at UTMDACC were sequenced for the presence of *KIT* and *PDGFRA* mutations as previously described. In all, 321 *KIT* exon 11 mutations were identified, 49 *KIT* exon 9 mutations, 10 *KIT* exon 13 mutations, 9 *KIT* exon 17 mutations, and 11 *PDGFRA* mutations (exon 12  $n=3$ , exon 18  $n=8$ ) were identified. *KIT* was determined wild-type in 51 samples (no *KIT* exon 9, 11, 13, or 17 mutation identified) and incomplete sequencing was obtained on 80 samples where, for example, *KIT* exons 9 and 11 were negative, but insufficient material was available for further sequencing. A summary of sequencing findings is presented in **Table 7**.

*KIT* exon 11 mutations represented a majority of mutations identified and significant diversity was observed in the type of mutations across this region. Deletions were identified in 158 cases, 82 cases displayed a missense mutation of one or more codons, deletions plus missense mutation accounted for 59 cases, while duplications and duplication with missense mutation occurred in 17 and 5 cases, respectively. The most frequent *KIT* exon 11 mutations identified, of any type, were a W557\_K558 deletion ( $n=46$ ), an L576P missense mutation ( $n=18$ ), and a W557G missense mutation ( $n=16$ ). All mutations identified were mapped together and sorted by earliest codon affected, represented in **Figure 13**. While some exceptions were noted, deletions were observed most frequently in the N-terminal to mid-region of the exon. The majority of missense mutations also occurred in the N-terminal to mid-region of the exon, excluding L576P. Duplications clustered primarily in the C-terminal region of the exon.

Type of Mutation			<i>n</i> =	( % )
<b>No Mutations</b> ( <i>wild-type</i> )			<b>51</b>	( <b>9.6</b> )
<b>No Mutations</b> ( <i>incomplete seq</i> )			<b>80</b>	( <b>15.1</b> )
<b><i>KIT</i></b>			<b>389</b>	( <b>73.3</b> )
Exon 11				
	Deletion		158	( 29.8 )
	Missense		82	( 15.4 )
	Deletion + Missense		59	( 11.1 )
	Duplication		17	( 3.2 )
	Duplication + Missense		5	( 0.9 )
Exon 9				
	Duplication		47	( 8.9 )
	Missense		2	( 0.4 )
Exon 13				
	Missense		10	( 1.9 )
Exon 17				
	Missense		9	( 1.7 )
<b><i>PDGFRA</i></b>			<b>11</b>	( <b>2.1</b> )
Exon 12				
	Missense		3	( 0.6 )
Exon 18				
	Deletion		4	( 0.8 )
	Missense		4	( 0.8 )

**Table 7. Mutations identified in 528 GIST patients**

Sequencing results from 531 GIST reviewed at UTMDACC are presented. Incomplete sequencing of 80 cases, where only partial *KIT* testing could be obtained for various reasons are included in the combined percentages. *Note:* a single case where W582[stop] was identified in *KIT* exon 11 has been accounted as a deletion in this table.



(previous page)

**Figure 13. Frequency of *KIT* exon 11 mutations in our population**

*KIT* exon 11 alterations of 132 distinct types were identified in 321 patients. A wild-type *KIT* exon 11 codon sequence map appears at the top of the diagram. Below the wild-type sequence is each of the 132 distinct mutations identified in the order of earliest codon affected. The number of **patients** identified for each mutation type is displayed on the right-hand side of the figure, while the frequency of each **mutation** to each individual *KIT* exon 11 codon is represented graphically at the bottom. While some exceptions were noted, deletions were observed most frequently in the N-terminal to mid-regions of *KIT* exon 11. The majority of missense mutations also occurred in the N-terminal to mid-regions, excluding L576P. Insertions and duplications clustered primarily in the C-terminal region.

Forty-six patients with GIST were found to have the most common *KIT* exon 9 mutation in GIST, a duplication of A502-Y503. Two new *KIT* exon 9 mutations were identified in 3 GIST patients: two patients had S476I while one patient had A507-F508 duplication (**Figure 14** A, B). Identification of the two S476I mutations verifies one previously reported case, whereas the A507\_F508 duplication was found to be unique (186-188). Although these novel mutations have not been proven to be oncogenic, they are in the region of *KIT* exon 9 that is aberrant in GIST.

From this database of GIST sequencing information, patients were identified for whom clinical demographics, imatinib treatment information, and contrast-enhanced CT (baseline, two months and four months post imatinib initiation) were available. From the mutational dataset, patients were excluded for the following reasons: a) patient received mutation testing at our institution, but clinical treatment at an outside center, b) GIST patient did not receive imatinib, c) patient was missing baseline, two-month, or four-month follow-up CT imaging, d) only non-contrast CT or very poor quality OSF CT was available for the patient, e) the patient underwent resection and there was no evidence of disease, f) the tumor contained air-fluid/barium and was difficult to measure density and compare size, g) the existing lesions were too small (<2cm). Thus, we identified 95 patients for whom complete information was evaluable.

Characteristics of the patients evaluated in this study are presented in **Table 8** ( $n=95$ ). Males were slightly more frequent (52 men (55%) and 43 women (45%)) and the average age at treatment initiation was approximately 59 years old.

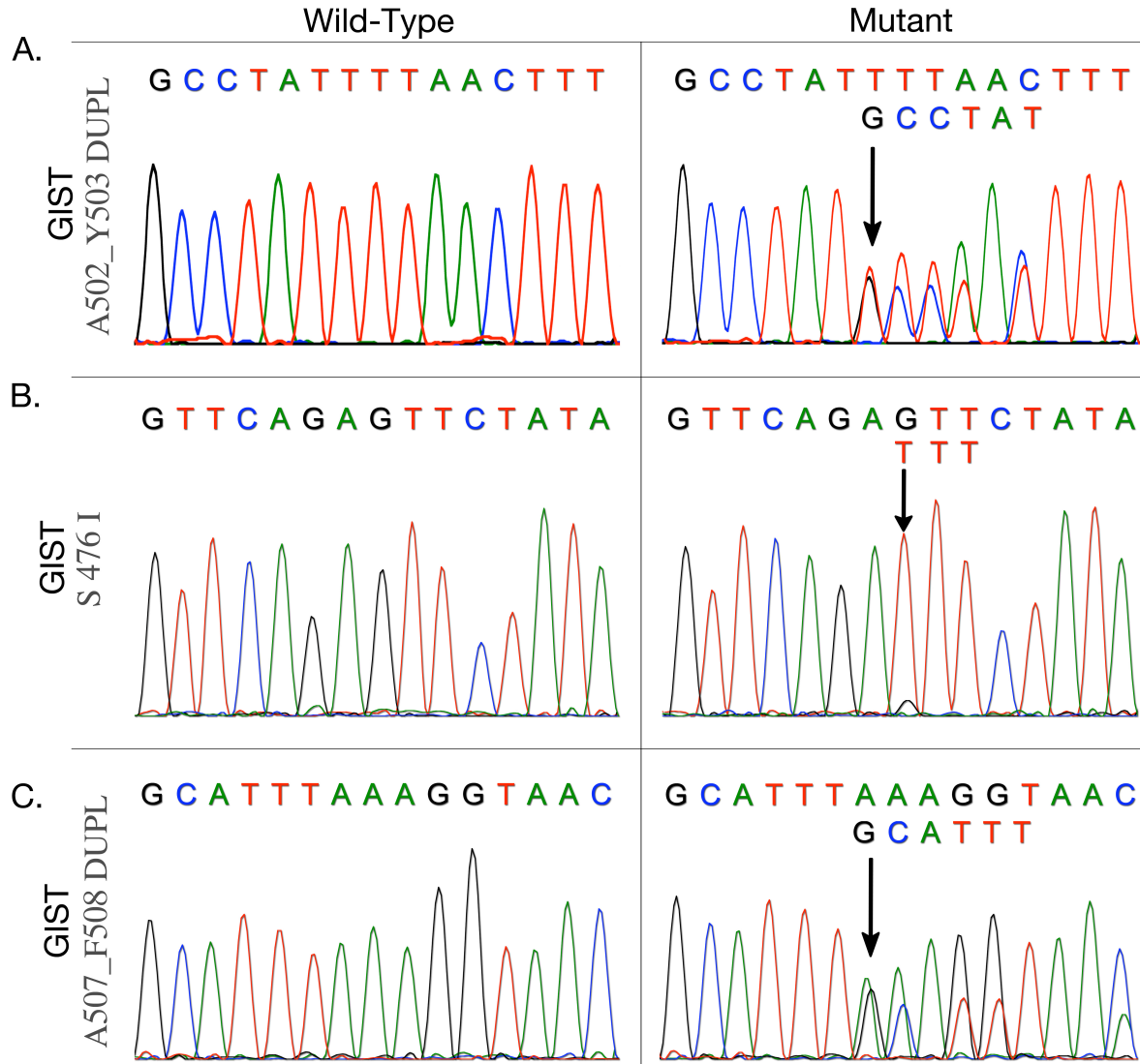


**Figure 14. Unique *KIT* exon 9 mutations identified**

(A) Sequencing trace output is shown from *KIT* exon 9. Most *KIT* exon 9 mutations reported to date in GIST are a single A502\_Y503 duplication/insertion, shown on the right; (B) Two GIST patients exhibited the same S467I point mutation; (C) one GIST patient experienced a unique, previously-unreported six base-pair in-frame insertion that resulted in a A507\_F508 duplication.



<b>Patient Characteristics</b>		<b><i>KIT</i> WT</b>	<b><i>KIT</i> exon 9</b>	<b><i>KIT</i> exon 11</b>
	<i>n</i> ( % )	<i>n</i> ( % )	<i>n</i> ( % )	<i>n</i> ( % )
Gender				
Female	43 ( 45.3 )	7 ( 41.2 )	4 ( 50.0 )	32 ( 45.7 )
Male	52 ( 54.7 )	10 ( 58.8 )	4 ( 50.0 )	38 ( 54.3 )
Mean Age				
Female	58.4			
Male	59.5			
Ethnicity				
Caucasian	76 ( 80.0 )	14 ( 82.4 )	7 ( 87.5 )	55 ( 78.6 )
African American	11 ( 11.6 )	2 ( 11.8 )	1 ( 12.5 )	8 ( 11.4 )
Hispanic	5 ( 5.3 )	1 ( 5.9 )	0	4 ( 5.7 )
Asian	3 ( 3.2 )	0	0	3 ( 4.3 )
<b>Tumor Characteristics</b>		<b><i>KIT</i> WT</b>	<b><i>KIT</i> exon 9</b>	<b><i>KIT</i> exon 11</b>
	<i>n</i> ( % )	<i>n</i> ( % )	<i>n</i> ( % )	<i>n</i> ( % )
Primary Tumor Site				
Stomach	39 ( 41.1 )	10 ( 58.8 )	0	29 ( 41.4 )
Small Bowel	42 ( 44.2 )	5 ( 29.4 )	5 ( 62.5 )	32 ( 45.7 )
Colon / Rectum	12 ( 12.6 )	2 ( 11.8 )	2 ( 25.0 )	8 ( 11.4 )
Esophagus	2 ( 2.1 )	0	1 ( 12.5 )	1 ( 1.4 )
Metastatic Site				
Liver	37 ( 38.9 )	7 ( 41.2 )	3 ( 37.5 )	27 ( 38.6 )
Peritoneum	28 ( 29.5 )	6 ( 35.3 )	2 ( 25.0 )	20 ( 28.6 )
Both	15 ( 15.8 )	1 ( 5.9 )	1 ( 12.5 )	13 ( 18.6 )
Other	15 ( 15.8 )	3 ( 17.6 )	2 ( 25.0 )	10 ( 14.3 )
Genotype				
<i>KIT</i> exon 11	70 ( 73.7 )			
<i>KIT</i> exon 9	8 ( 8.4 )			
<i>KIT</i> wild-type	17 ( 17.9 )			
<b>Response Characteristics</b>		<b><i>KIT</i> WT</b>	<b><i>KIT</i> exon 9</b>	<b><i>KIT</i> exon 11</b>
	<i>n</i> ( % )	<i>n</i> ( % )	<i>n</i> ( % )	<i>n</i> ( % )
Δ Size Change	-20.3	-3.9	-7.0	-25.8
Δ Density Change	-30.1	-19.6	-25.8	-33.2
Choi Response				
Y	84 ( 88.4 )	11 ( 64.7 )	7 ( 87.5 )	66 ( 94.3 )
N	11 ( 11.6 )	6 ( 35.3 )	1 ( 12.5 )	4 ( 5.7 )

**Table 8. Study Characteristics**

Characteristics of patients used for CT response assessment. As previously reported, *KIT* genotype was statistically associated with different primary tumor locations ( $p=0.042$  by Fisher's exact).

The majority of patients ( $n=76$ ) were Caucasian (80%), with 11, 5, and 3 African American, Hispanic, and Asian patients included, respectively. Tumors occurred most frequently in gastric and small bowel tissues (41.1% and 44.2% of cases), while there were 12 tumors of the colorectum (12.6%), and 2 esophageal tumors (2.1%) identified.

In total, 264 lesions from 95 patients were evaluated by CT. Size (in centimeters) and density (in Hounsfield Units (HU)) measured at initiation of imatinib treatment were compared to two- and four-month follow-up CT scans. All available lesions that were disease-characteristic, both primary and metastatic, were examined and measured per patient. The most frequent site of metastasis was the liver ( $n=37$  patients, 40%), followed by the peritoneum in 28 patients (30%). 15 (16%) patients had metastasis at both these sites. Another 15 (16%) patients were found to have disease elsewhere, including in lung, bone, lymph node and recurrent primary lesions.

There were 70 patients whose tumor had *KIT* exon 11 mutation, 8 patients with *KIT* exon 9 mutation and 17 with wild-type *KIT* (74%, 8%, and 18% of patients, respectively). Overall, 84 (88%) patients were considered responsive to imatinib treatment, as evaluated by either density or size alterations that met the Choi criteria for response (please refer to **Table 6** for criteria summary), whereas 11 patients did not respond and were classified as either SD or PD. Subgroup analyses were then carried out to further stratify the data.

The change in tumor size for each patient from baseline at imatinib treatment initiation to the four-month follow-up is presented in **Figure 15** (A). 69 patients (73%) achieved a Choi PR by size change alone. Less than 10% decrease, no change, or an increase in tumor size was observed in 26 patients (27%). The change in tumor density over the same period is shown in **Figure 15** (B), where density decreases qualified 73 patients as Choi PR (77%) and 22 patients (23%) experienced less than 15% decrease or an increase in tumor density.

In order to better understand the interactions between tumor size and density of GIST patients treated with imatinib, a graded combination measure of response was evaluated. Patients' combined percentage density and size changes were plotted together and scored according to the combined change of the tumor, presented in **Figure 16**. Combined response Grade 1 was assigned to Choi responders with decreases  $\leq 15\%$ , Grade 2 corresponded to decreases 16-20%, Grade 3 decrease was 21-30%, Grade 4 was 31-40%, Grade 5 was 41-50% and so forth with each grade spanning 10 percentage points up to Grade 8. No penalty was assigned for increases in size or density, since decreases in tumor size can associate with increased tumor density in GIST and vice versa. Natural breakpoints emerged which grouped Grade 1-4 ( $n=25$ ), Grade 5-7 ( $n=32$ ) and Grade 8 + ( $n=27$ ). While exceptions were noted, the Grade 1-4 group included patients whose tumors moderately responded to imatinib, as well as a majority of responders whose tumor size/density responded in opposite fashion. The Grade 5-7 group included patients most of whom had a response to imatinib, whereas the Grade 8+ group patients all experienced a robust response in both size and density decreases.

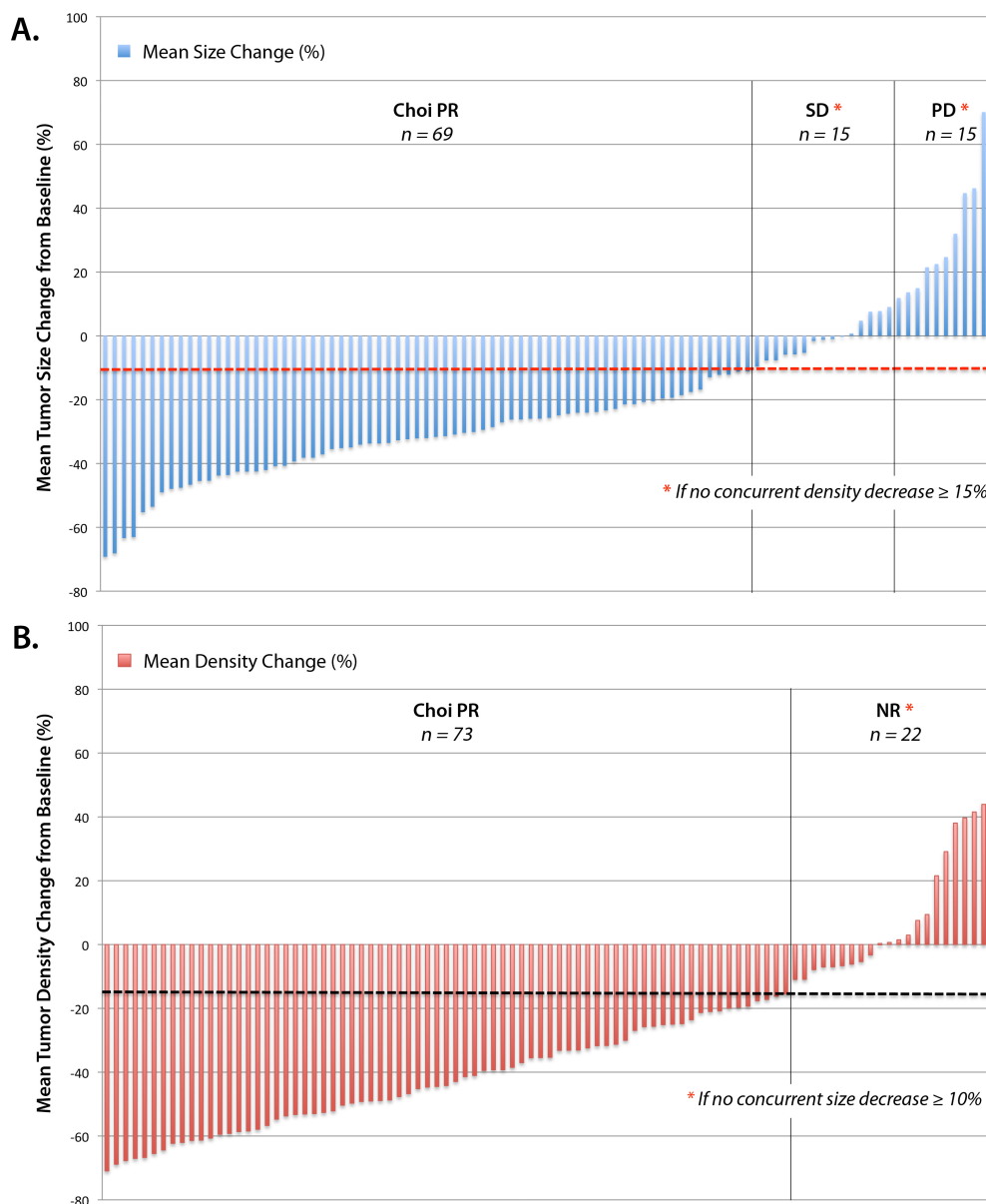


**Figure 15. CT response changes in size and density**

(A) A waterfall plot of mean tumor size change (%) from baseline. The dashed line indicates  $\geq 10\%$  size decrease. Size decreases in 69 patients (73%) qualified as PR by Choi, compared to minimal size changes in 15 patients and size increases in 11 patients; (B) A waterfall plot of mean tumor density change (%) from baseline. The dashed line indicates  $\geq 15\%$  decrease, observed in 73 patients (77%).

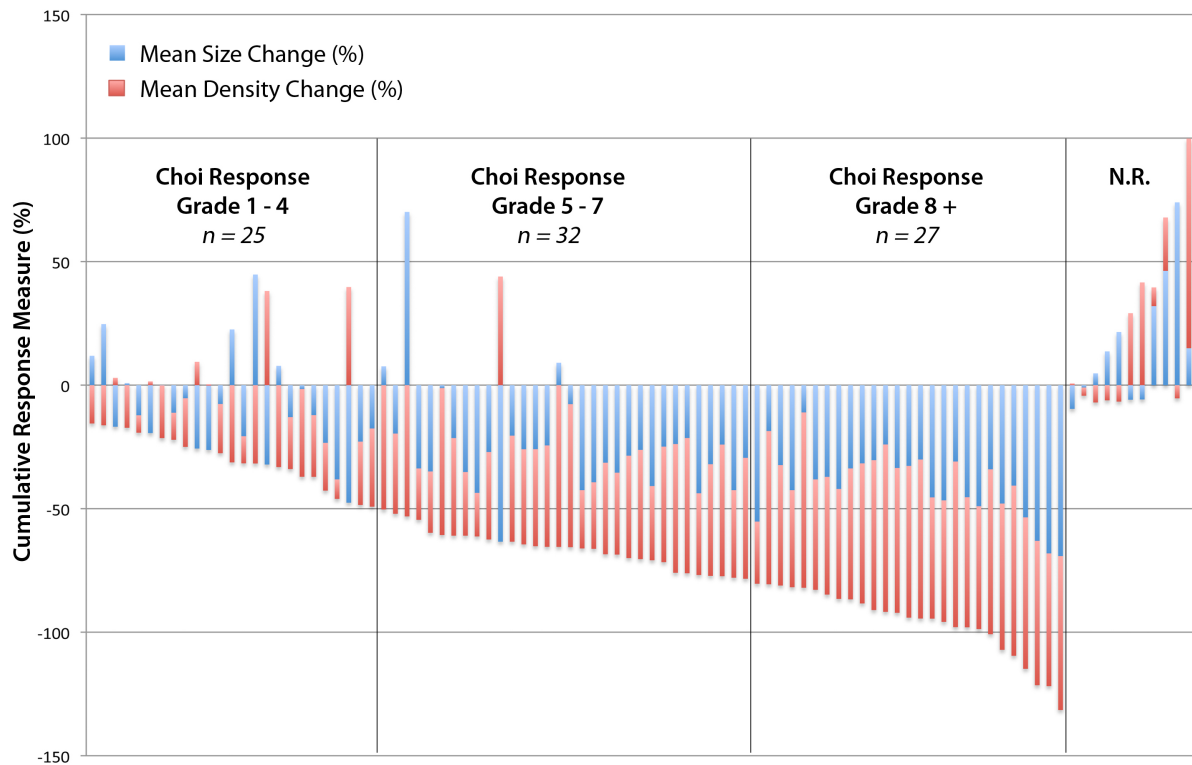


**Figure 16. Cumulative response comparison**

Percent change in density and size of GIST tumors are compared. A cumulative grade was assigned to Choi responders based on decreases in size and density. Group 1-4 ( $n=25$ ) had the most patients with mixed response, Grade 5-7 ( $n=32$ ) experienced response, and Grade 8+ ( $n=27$ ) patients were all combined responders and displayed the greatest decreases in size but also were found to have decreases in density.

To examine whether *KIT* mutation influences the type of response in these GIST patients, as measured by CT, mutation characteristics such as location of individual mutations, specific codon altered, and type of alteration (missense, duplication, deletion) were each examined using the Choi response subgroups. First, patients with *KIT* exon 11 mutation (of any type,  $n=60$ ) were compared to those expressing *KIT* exon 9 mutation ( $n=8$ ) or wild-type *KIT* ( $n=17$ ). As summarized in **Table 9**, *KIT* genotype was significantly associated with type of response measured by CT ( $p=0.001$  by Fisher's exact test for Choi responder subgroups vs. non-responders). While wild-type patients, whose tumors primarily responded with density changes, were fairly equally distributed between response groups, a majority of *KIT* exon 9 patients responded in the lowest response class (62.5% Response Grade 1-4). On the other hand, patients with *KIT* exon 11 mutant GIST responded with the largest size and density decreases, and 81.7% attained a response Grade 5 or higher (**Figure 17**).

Next, subgroup analysis stratified *KIT* exon 11 patients into regions of focus of their mutation within *KIT* exon 11: N-terminus included all mutations affecting K550 to V560 ( $n=57$ ), "M/C" included mutations altering the mid-region or C-terminus of *KIT* exclusively, from E561 to V569 for mid-region, and Y570 to F591 for C-terminal region ( $n=10$  for mutations residing in both regions). These regions were distinguished by the natural pattern of mutation that was observed in the larger mutation group (see **Figure 13**). Finally, a small group ( $n=3$ ) of mutations that disrupted the entire length of *KIT* exon 11 were included for analysis ("pan"). These pan-exon mutations deleted portions of all three regions of *KIT* exon 11 and patients

<b>A. KIT Mutation Type</b>		<b>KIT WT</b>	<b>KIT exon 9</b>	<b>KIT exon 11</b>	
		<i>n</i> ( % )	<i>n</i> ( % )	<i>n</i> ( % )	
Choi Responder		11 ( 64.7 )	7 ( 87.5 )	56 ( 80.0 )	b a
Response Grade 1 - 4		3 ( 17.6 )	5 ( 62.5 )	7 ( 11.7 )	
Response Grade 5 - 7		3 ( 17.6 )	1 ( 12.5 )	28 ( 46.7 )	
Response Grade 8 +		5 ( 29.4 )	1 ( 12.5 )	21 ( 35.0 )	
Choi Non-responder		6 ( 35.3 )	1 ( 12.5 )	4 ( 6.7 )	
<b>Fisher T-Test p =</b>		<b>a) p = 0.008</b>		<b>b) p = 0.001</b>	

<b>B. Mutation region (exon 11)</b>		<b>Pan-mut</b>	<b>M/C</b>	<b>N-term</b>	
		<i>n</i> ( % )	<i>n</i> ( % )	<i>n</i> ( % )	
Choi Responder		2 ( 66.7 )	9 ( 90.0 )	55 ( 96.5 )	
Response Grade 1 - 4		0	4 ( 40.0 )	13 ( 22.8 )	
Response Grade 5 - 7		2 ( 66.7 )	4 ( 40.0 )	22 ( 38.6 )	
Response Grade 8 +		0	1 ( 10.0 )	20 ( 35.1 )	
Choi Non-responder		1 ( 33.3 )	1 ( 10.0 )	2 ( 3.5 )	
<b>Fisher T-Test p =</b>		<b>a) p = 0.08 ns</b>		<b>b) p = 0.109 ns</b>	

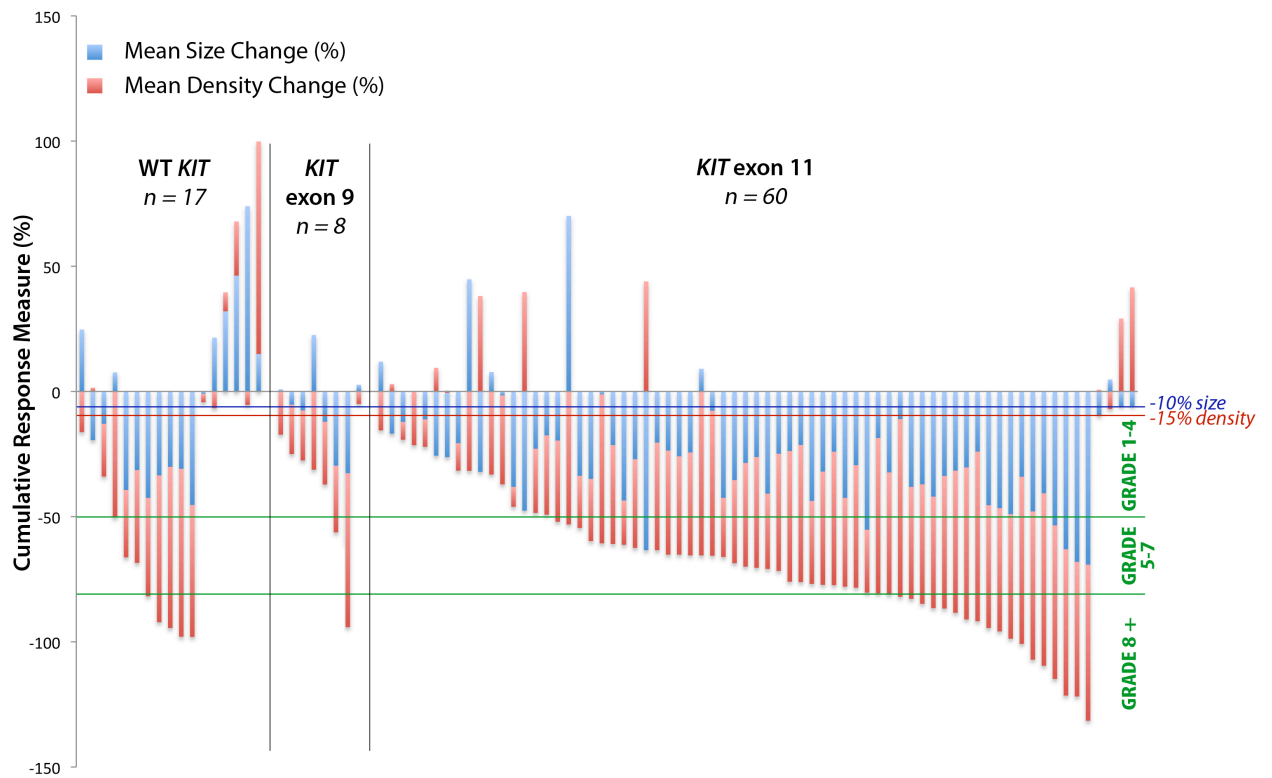
<b>C. Specific Codon Affected (exon 11)</b>		<b>L576</b>	<b>V559/V560</b>	<b>W557</b>	
		<i>n</i> ( % )	<i>n</i> ( % )	<i>n</i> ( % )	
Choi Responder		6 ( 85.7 )	14 ( 87.5 )	36 ( 100.0 )	
Response Grade 1 - 4		3 ( 42.9 )	6 ( 37.5 )	6 ( 16.7 )	
Response Grade 5 - 7		2 ( 28.6 )	2 ( 12.5 )	19 ( 52.8 )	
Response Grade 8 +		1 ( 14.3 )	6 ( 37.5 )	11 ( 30.6 )	
Choi Non-responder		1 ( 14.3 )	2 ( 12.5 )	0 ( 0.0 )	
<b>Fisher T-Test p =</b>		<b>a) p = 0.08 ns</b>		<b>b) p = 0.013</b>	

<b>D. Mutation Type (exon 11)</b>		<b>Dup/Ins</b>	<b>Missense</b>	<b>Deletion</b>	
		<i>n</i> ( % )	<i>n</i> ( % )	<i>n</i> ( % )	
Choi Responder		4 ( 100 )	22 ( 95.7 )	39 ( 90.7 )	
Response Grade 1 - 4		3 ( 75.0 )	6 ( 26.1 )	8 ( 19.0 )	
Response Grade 5 - 7		1 ( 25.0 )	9 ( 39.1 )	17 ( 40.5 )	
Response Grade 8 +		0	7 ( 30.4 )	14 ( 33.3 )	
Choi Non-responder		0 ( 0.0 )	1 ( 4.3 )	3 ( 7.1 )	
<b>Fisher T-Test p =</b>		<b>a) p = 1.0 ns</b>		<b>b) = 0.504 ns</b>	

**Table 9. Factors evaluated for radiographic response correlation**

For each comparison A-D, Choi response group versus non-responders were compared (a), then sub-groups of Choi responders were statistically considered against non-responders and each other (b).



**Figure 17. Genotype is associated with grade of radiographic response**

KIT genotype was significantly associated with type of response measured by CT ( $p=0.001$  by Fisher's exact test for Choi responder sub-groups vs. non-responders).



with this mutation responded exclusively by size. This comparison was not statistically significant ( $p=0.109$  by Fisher's exact test for Choi responder subgroups vs. non-responders). This may indicate that location of the mutation within *KIT* exon 11 may not be a predictive marker of imatinib response.

Next, mutations that altered particular codons within *KIT* exon 11 were compared as to their relationship types of radiographic response to imatinib. Codons of interest were W557, V559/V560 (considered together), and L576 since these are the most common distinct mutations in *KIT* exon 11 of GIST. Both W557 and V559/V560 reside in the N-terminal region of *KIT* and are frequent points of alteration in GISTs, together representing 74% of *KIT* exon 11 mutations in our analysis. W557\_K558 is one of the most frequent alterations overall, and more mutations affect this codon through larger deletion in the region or missense mutation of W557. Any change to W557 in this case, deletion or missense mutation was included ( $n=36$ , 51% of all *KIT* exon 11 mutations in this study). Likewise, missense mutations affecting V559 or V560, and deletions affecting one or both valines were grouped together ( $n=16$ , 23%). Finally, seven patients with alterations affecting L576 in the C-terminus were included. Often a missense mutation, one duplication that affected L576 and one deletion were included (10% of our *KIT* exon 11 group). Radiographic response, when examined by response grade group versus non-responders, was significantly influenced by the type of codon changes examined ( $p=0.013$  by Fisher's exact test). Over 80% of W557-altered tumors responded with a Grade 5 or higher, whereas nearly half of L576-mutated tumors fell in Grade 1-4, as shown in **Figure 18**. V559/V560-mutations were split evenly

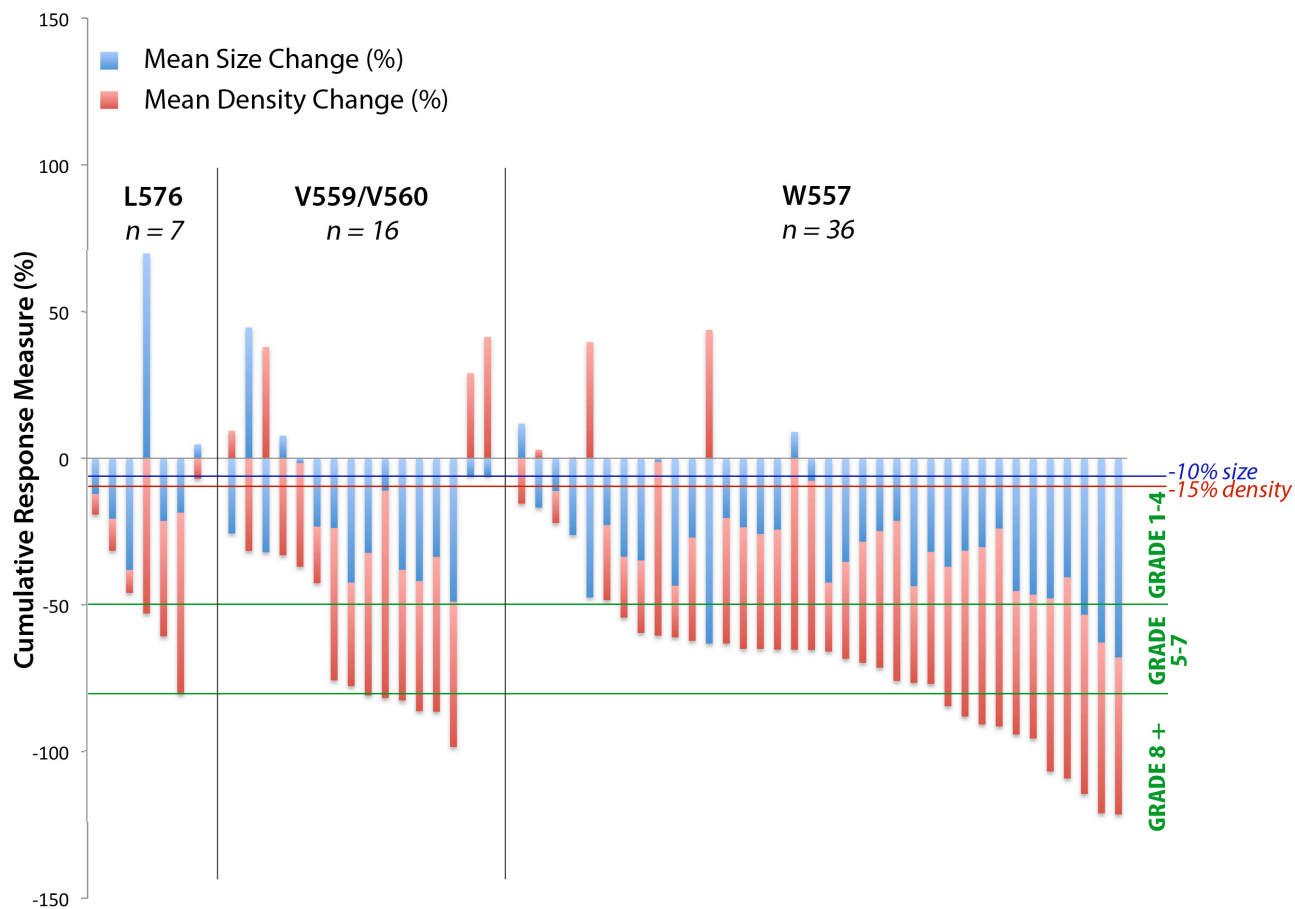


**Figure 18. Specific codon alterations of *KIT* exon 11 correlate with response**

Over 80% of W557-altered tumors responded with a Grade 5 or higher, whereas nearly half of L576-mutated tumors fell in Grade 1-4 ( $p=0.013$  by Fisher's exact test).

between the lowest and highest response categories, which may indicate that an alteration to V559 does not affect V560 similarly, or again, specific types of alterations may discern the difference.

In a fourth question, the type of mutational alteration in *KIT* exon 11, missense mutation, versus any deletion, versus duplication/insertions was examined. As previously discussed, the frequency of these mutational changes does seem to correlate with region of *KIT* exon 11. Only 1 of 23 point mutations, 3 of 40 deletions, and none of the four duplications were non-responders by Choi, and the comparison to radiographic response sub-groups was non-significant ( $p=0.504$ ).

Focus on specific density and size changes in patients' metastases led to an inquiry about type of response in different metastatic sites. Comparing patients who had both liver and peritoneal implants, it was noted that both metastatic sites maintained the same type of response within a given patient. That is to say that both liver and peritoneal implants responded similarly in their size and density changes, in both responders and non-responders.

Statistical comparison of all size changes showed no significant difference in size of liver implants as a group ( $-16.2\pm 29.6\%$  mean change) versus peritoneal implants ( $-25.8\pm 25.3\%$  mean change;  $p=1.0$ ). Likewise, density was not statistically significant between the two metastatic locations: liver  $-28.5\pm 24.7\%$  mean change versus peritoneal  $-34.5\pm 27.5\%$  mean change,  $p=0.27$ .

Primary mutation was then used to stratify radiographic response by metastatic location. *KIT* exon 11 mutant GIST responded, as before, with decreases in size and density in both metastasis sites of 20-30%. Comparing the

change in *KIT* exon 9 and wild-type revealed that density was not a significant factor, yet size changes were distinctly different. *KIT* exon 9 size decreased less than 5% in liver and increased 2.5% in peritoneal while WT conversely increased in liver (mean 12.4%) and decreased in peritoneal tissues (-8.3%). ANOVA statistic showed both size alterations significant at  $p<0.01$  for liver changes and  $p=0.01$  for peritoneum. The summary of these analyses is presented in **Table 10**.

Liver vs Peritoneal changes		<i>n</i>	<i>mean</i>	( <i>stdev</i> )	<i>p-value</i>
<b>Size</b>					
Liver		52	-16.2	( 29.6 )	<b><i>p</i> = 0.1</b>
Peritoneal		43	-25.8	( 25.3 )	
<b>Density</b>					
Liver		52	-28.5	( 24.7 )	<b><i>p</i> = 0.27</b>
Peritoneal		43	-34.5	( 27.5 )	
		<i>KIT</i> WT	<i>KIT</i> exon 9		<i>KIT</i> exon 11
Liver vs Peritoneal +Mutation		<i>mean</i> ( <i>stdev</i> )	<i>mean</i> ( <i>stdev</i> )	<i>mean</i> ( <i>stdev</i> )	
<b>Liver</b>					
Size		12.4 ( 51.5 )	-4.8 ( 6.2 )	-22.5 ( 21.0 )	<i>a</i>
Density		-16.7 ( 19.6 )	-17.1 ( 7.9 )	-31.2 ( 26.0 )	<i>b</i>
	<b>ANOVA F-test <i>p</i> =</b>	<b>&lt;0.01</b>	<i>a</i>		
	<b>ANOVA F-test <i>p</i> =</b>	<b>0.20</b>	<i>b</i>		
<b>Peritoneal</b>					
Size		-8.3 ( 36.9 )	2.5 ( 32.7 )	-31.5 ( 19.4 )	<i>a</i>
Density		-23.2 ( 35.7 )	-19.1 ( 16.6 )	-38.0 ( 26.3 )	<i>b</i>
	<b>ANOVA F-test <i>p</i> =</b>	<b>0.01</b>	<i>a</i>		
	<b>ANOVA F-test <i>p</i> =</b>	<b>0.30</b>	<i>b</i>		

**Table 10. Characteristics that influence response**

Liver and peritoneal metastases did not experience distinct size or density changes when compares by location. Stratified by *KIT* genotype, size changes were statistically different, where *KIT* wild-type tumors increased in liver and decreased in peritoneum and *KIT* exon 9 had conversely decreased size in liver compared to a slight mean increase in peritoneum.

## Chapter 4. Relationship of Imatinib Plasma Level to Outcome

### 4.1 Introduction

In patients with GIST, radiographic responses and PFS are correlated with imatinib trough level exposure. However, limited data are available regarding steady-state, adjusted imatinib levels ( $\text{Adj-C}_{\min}$ ) in patients with gastrectomy, patients undergoing dose escalation, by patient dose level, and by subtype of *KIT* mutation (eg *KIT* exon 9), and GIST patients receiving concomitant medications. Therefore, we examined  $\text{Adj-C}_{\min}$  in 197 GIST patients to determine distribution in our patient population by dose level, after dose escalation, over time, and by modified response criteria (Choi Criteria). We hypothesize that standard dosing of imatinib in GIST patients results in sub-therapeutic treatment levels for some patients. Higher imatinib plasma levels correlate with better clinical response. If the hypothesis is true, then clinical response, as assessed by CT (Choi Criteria), will be associated with higher imatinib plasma levels, irrespective of imatinib dose. If the hypothesis is not true, then this may indicate resistance to the drug in some patients (ie secondary mutation present), which could be screened.

### 4.2 Results

From May 2008 to September 2010, information was collected from 197 GIST patients who underwent imatinib TDM at UTMDACC. The baseline patient characteristics, characteristics of these patients' disease and treatment characteristics are provided in **Table 11**. There was a slight male predominance in

<b>Patient Characteristics</b>	<i>n</i>	( % )	( <i>Range</i> )
Gender			
Female	89	( 45.2 )	
Male	108	( 54.8 )	
Ethnicity			
Caucasian	164	( 83.2 )	
African American	17	( 8.6 )	
Hispanic	9	( 4.6 )	
Asian	7	( 3.6 )	
Median Age at Diagnosis (yrs)			55 ( 19 - 87 )
Mean BSA (m <sup>2</sup> )			2.0 ( 1.3 - 3.0 )
Female			1.9 ( 1.3 - 2.8 )
Male			2.1 ( 1.6 - 3.0 )
<b>Tumor Characteristics</b>	<i>n</i>	( % )	
Primary Tumor Site			
Stomach	80	( 40.6 )	
Small Bowel	92	( 46.7 )	
Colon / Rectum	23	( 11.7 )	
Esophagus	2	( 1.0 )	
Primary Tumor	88	( 44.7 )	
Metastatic Tumor	109	( 55.3 )	
Genotype			
<i>KIT</i> exon 11	112	( 56.9 )	
<i>KIT</i> exon 9	15	( 7.6 )	
<i>KIT</i> wild-type	28	( 14.2 )	
Other / unavailable	42	( 21.3 )	
<b>Treatment Characteristics</b>	<i>n</i>	( % )	
Gastrectomy	53	( 26.9 )	
Total Gastrectomy	4	( 2.0 )	
Gastrectomy, partial, proximal	32	( 16.2 )	
Gastrectomy, partial, distal	17	( 8.6 )	
Imatinib Dose			
< 400 mg *	8	( 4.1 )	
400 mg	142	( 72.1 )	
600 mg	18	( 9.1 )	
800 mg	29	( 14.7 )	

**Table 11. TDM patient, disease, and treatment characteristics**

the group (108 M/89 F), patients were primarily Caucasian (83.2%) with median age at diagnosis of 55 and mean BSA of 2.0m<sup>2</sup>. Mean BSA for men was 2.1m<sup>2</sup>, whereas mean BSA for women was 1.9m<sup>2</sup> in this group. Most patients experienced a gastric or small bowel primary tumor (40.6% and 46.7%, respectively) with a small number located in the colorectum (11.7%). Two patients had primary GIST of the esophagus (1.0%). Patients with metastatic disease accounted for 55.3% of the group (109 patients). More than half of patients exhibited a *KIT* exon 11 mutation (112 patients, 56.9%), and 15 patients were identified with *KIT* exon 9 mutation. Twenty-eight patients were considered *KIT* wild-type (*KIT* exon 9, 11, 13, and 17 negative), whereas mutation information was unavailable in 42 patients (either no tissue available or incomplete *KIT* sequencing to date). There were no *PDGFRA* mutations identified in this cohort. Less than 30% of patients underwent gastrectomy, partial or complete, as shown in **Table 11**. Starting imatinib doses in the group varied from 100 mg daily up to 800 mg daily, with a majority of patients (142) receiving 400 mg daily. Patients underwent TDM over time and 48 patients experienced dose escalation as clinically indicated. Individual imatinib trough levels were used for correlative analyses whereas a mean trough imatinib level at identical dose was obtained for each patient used in outcome analyses.

Trough imatinib levels (Adj-C<sub>min</sub>) were obtained at 245 different patient time points, as shown in **Table 12**. Mean Adj-C<sub>min</sub> increased as dose increased in these patients, where patients receiving less than 400 mg imatinib daily corresponded to 851 ng/mL mean Adj-C<sub>min</sub> (*n*=20; range 200-2073 ng/mL), 400 mg daily imatinib corresponded to mean Adj-C<sub>min</sub> of 1224 ng/mL (*n*=151; range 189-3476 ng/mL),



<b>Plasma Levels Observed</b>	<b><i>n</i></b>	<b>Mean AdjCmin</b>	<b>Median ( Range )</b>
Imatinib Dose			
< 400 mg *	20	851	882 ( 200 - 2073 )
400 mg	151	1224	1157 ( 189 - 3476 )
600 mg	34	1793	1742 ( 320 - 4088 )
800 mg or above	40	2773	2466 ( 679 - 7088 )

**Table 12. Range of trough imatinib levels observed**

Trough imatinib levels were measured at 245 different doses. Broad interpatient variability of Adj-C<sub>min</sub> was observed, but while ranges overlapped, Adj-C<sub>min</sub> increased as dose increased. \*Patients at known subtherapeutic levels due to tolerance were excluded from efficacy analysis.

600 mg daily imatinib corresponded to mean Adj- $C_{min}$  of 1793 ng/mL ( $n=34$ ; range 320-4088 ng/mL), and 800 mg daily imatinib or greater corresponded to mean Adj- $C_{min}$  of 2773 ng/mL ( $n=40$ ; range 679-7088 ng/mL). (Note total doses equal to 245 for the 197 patients due to clinically-indicated dose escalation in some patients). While ranges overlapped, imatinib dose escalation corresponded with incremental Adj- $C_{min}$  means, as expected ( $p < 0.0001$ , **Table 12**).

Covariate analysis revealed factors that correlated with imatinib plasma level included age of the patient ( $p=0.0003$ ), gender ( $p < 0.0001$ ), and imatinib dose ( $p < 0.0001$ ), represented in **Table 13**. Age of the patient was shown to be a significant covariate, where every 10-year increase in age correlated with approximately 129 ng/mL increase in trough level for similar patients at the same imatinib dose. Gender was also indicated to be a significant influencing covariate, where women experienced an estimated 388.1 ng/mL higher trough imatinib level compared with male patients ( $p<0.0001$ ). Modeling estimated that increasing imatinib dose would increase imatinib plasma concentrations by an estimated 430 ng/mL per 100 milligram imatinib ( $p<0.0001$ ). Reduced hepatic function examined through bilirubin ( $>1.2$  mg/dL) and ALT ( $>56$  IU/L) did not significantly influence Adj- $C_{min}$ , however AST ( $>48$  IU/L), available in only a subset of cases, was significantly associated with higher Adj- $C_{min}$  and estimated to increase levels as much as 221.1 ng/mL ( $p=0.04$ ). Renal metabolism of imatinib accounts for  $<10\%$ , so it was not included in the analysis but may affect covariates. While mean BSA was significantly different between women and men ( $p<0.0001$ ), marginal effects modeling did not show BSA

Final Marginal Effects Model		Estimated $\Delta$ Trough (ng/mL)	( Standard Error )	F-statistics	p-value
Age	(per year)	12.9	( 3.6 )	13.18	0.0003
Gender	(Female)	388.1	( 86.6 )	20.1	<0.0001
Imatinib Dose	(per mg)	4.3	( 0.18 )	540.1	<0.0001
CYP Inducer	(if drug is present)	-320.3	( 129.7 )	6.1	0.01
CYP Inhibitor	(if drug is present)	97.4	( 76.1 )	1.6	0.2
CYP Substrate	(if drug is present)	266.9	( 71.5 )	13.9	0.002
AST > 48 *	(if above 48 IU/L)	221.1	( 106.6 )	4.3	0.04

**Table 13. Covariates of trough imatinib level**

Covariates of trough imatinib level are summarized. The estimated change in trough imatinib level (estimated Adj- $C_{\min}$  change in ng/mL) for a unit change in the covariate is shown.

to significantly correlate with trough imatinib level, so gender is significant independent of BSA but could be affected by other unknown covariates.

Since GIST patients frequently are co-administered drugs that are either CYP450 inhibitors or CYP450 inducers, which may inhibit or induce function of particular CYP450 isoenzymes, we examined the effect of CYP450 inhibitor, inducer, substrate drugs upon imatinib Adj- $C_{min}$ . The metabolism of many medications, including imatinib, is dependant upon the CYP450 enzymes found in the liver, as well as in the gastrointestinal tract. Clinically significant drug interactions are largely a result of altered CYP450 metabolism and close monitoring is required when patients are given one or more drugs influenced by CYP450 metabolism to avoid interaction and/or therapeutic failure. Over half of patients were taking one or more CYP450 inhibitor (54.31%) or CYP450 substrate (61.93%) concomitant medications together with imatinib (**Table 14**). While 40 percent of patients took one or more CYP450 inducers, only 9.14 percent of these patients took CYP450 inducers known to be relevant to imatinib metabolism. Marginal effects modeling showed that CYP450 inhibitors in this group did not statistically influence Adj- $C_{min}$  ( $p=0.2$ ). The presence of one or more CYP450 inducers or substrates did, however, influence Adj- $C_{min}$  significantly ( $p=0.01$  and  $p=0.0002$  for inducers and substrate comedications, respectively). The presence of a CYP450 inducer drug in addition to imatinib was estimated to decrease Adj- $C_{min}$  by 320 ng/mL. The presence of a CYP450 substrate drug was estimated to increase Adj- $C_{min}$  by 267 ng/mL, which is of uncertain clinical relevance and may be due to competitive metabolism (**Table 13**).

	Inhibitors	Inducers	Substrates
<b>CYP1A2</b>	acyclovir, ciprofloxacin, citalopram, diltiazem, ethinyl estradiol, famotidine, ketoconazole, levofloxacin, omeprazole, paroxetine <b>n=36</b> (18.27%)	ciprofloxacin, esomeprazole, insulin, lansoprazole, omeprazole, pantoprazole, pheytoin <b>n=77</b> (39.09%)	azelastine, clopidogrel, diazepam, estradiol, haloperidol, verapamil <b>n=13</b> (6.60%)
<b>CYP2C9</b>	clopidogrel, fenofibrate, fluconazole, fluoxetine, gemfibrozil, <b>imatinib</b> , ketoconazole, lovastatin, omeprazole, paroxetine, sertraline <b>n=41</b> (20.81%)*	phenytoin <b>n=1</b> (0.51%)	celecoxib, citalopram, diazepam, fluoxetine, montelukast, omeprazole, phenytoin, sulfamethoxazole <b>n=36</b> (18.27%)
<b>CYP2C19</b>	azelastine, citalopram, esomeprazole, fluconazole, fluoxetine, ketoconazole, letrozole, omeprazole, pantoprazole, paroxetine, sertraline, topiramate <b>n=76</b> (38.58%)	phenytoin, prednisone, topiramate <b>n=7</b> (3.55%)	azelastine, escitalopram, esomeprazole, lansoprazole, omeprazole, pantoprazole, phenytoin, progesterone <b>n=78</b> (39.59%)
<b>CYP2D6</b>	azelastine, bupropion, celecoxib, chlorpheniramine, citalopram, diphenhydramine, doxepin, duloxetine, escitalopram, fluoxetine, haloperidol, <b>imatinib</b> , metoclopramide, paroxetine, sertraline <b>n=54</b> (27.41%)*	pheytoin <b>n=1</b> (0.51%)	azelastine, doxepin, duloxetine, fluoxetine, haloperidol, hydrocodone, methadone, metoclopramide, paroxetine, venlafaxine <b>n=40</b> (20.30%)
<b>CYP3A4</b> <b>CYP3A5</b>	azelastine, ciprofloxacin, diltiazem, ethinyl estradiol, fluconazole, fluoxetine, <b>imatinib</b> , ketoconazole, prednisone, sertraline, verapamil <b>n=27</b> (13.71%)*	phenytoin, pantoprazole <b>n=18</b> (9.14%)	atorvastatin, azelastine, cetirizine, chlorpheniramine, citalopram, clopidogrel, diazepam, diltiazem, esomeprazole, estrogen, ethinyl estradiol, haloperidol, hydrocodone, <b>imatinib</b> , ketoconazole, lansoprazole, letrozole, lovastatin, methadone, montelukast, omeprazole, pantoprazole, prednisone, sertraline, simvastatin, verapamil <b>n=116</b> (58.88%)*
<b>CYP2C8</b>	gemfibrozil, montelukast, trimethoprim <b>n=6</b> (3.05%)		phenytoin, verapamil <b>n=2</b> (1.02%)
<b>Any CYP450 Inhibitor, Inducer, or Substrate Drug</b>	<b>n=107</b> <b>(54.31%)*</b>	<b>n=80</b> <b>(40.61%)</b>	<b>n=122</b> <b>(61.93%)*</b>

CYP = Cytochrome P450

\* Excluding imatinib mesylate

## Table 14. Concomitant medications

Number of patients, percentage and type of coadministered CYP450 inhibitors, inducers, or substrates of are shown for each isozyme class. \*Note: imatinib is itself an inhibitor of CYP2C9, CYP2D6, CYP3A4, and is processed by CYP3A4/3A5. Imatinib is excluded from these percentages, since all patients received imatinib.

Interestingly, factors that did not achieve statistical significance included BSA of the patient, duration of imatinib therapy, race, and gastrectomy, the latter of which could be due to the small patient sample.

Patients undergoing a planned dose escalation, for example following surgery, who were at a known less-than therapeutic dose at the time of TDM analysis were used for PK analysis exclusively and were excluded from any long-term outcome analysis.

The distribution of Adj- $C_{min}$  in a subset of GIST patients with metastatic or unresectable disease ( $n=126$ ), irrespective of dose, ranged from 272 ng/mL to 4582 ng/mL with a mean of 1367 ng/mL (**Figure 19**). The increasing distribution of Adj- $C_{min}$  were then subdivided into quartiles for comparison (Q), where Q1 Adj- $C_{min}$  mean was 628 ng/mL ( $n=32$ ; range 272-803 ng/mL), Q2 Adj- $C_{min}$  mean was 982 ng/mL ( $n=31$ ; range 803-1166 ng/mL), Q3 Adj- $C_{min}$  mean was 1449 ng/mL ( $n=32$ ; range 1173-1758 ng/mL), and Q4 Adj- $C_{min}$  mean was 2429 ng/mL ( $n=31$ ; range 1772-4582 ng/mL).

The trough imatinib level distribution in these patients with unresectable disease was examined by Choi response four months after initiation of imatinib therapy. Response in GIST, assessed by Choi, is delineated by complete response (CR) or partial response (PR), whereas stable disease (SD) and progressive disease (PD) do not represent response, by definition (summarized previously in **Table 6**). Two-thirds of patients experienced a PR ( $n=82$  (65.1%)), whereas 21.4% exhibited SD ( $n=27$  (21.4%)) and one patient was classified as PD ( $n=1$  (0.8%)) at this time point. Choi response was undeterminable in 16 patients (ND, 12.7%) who

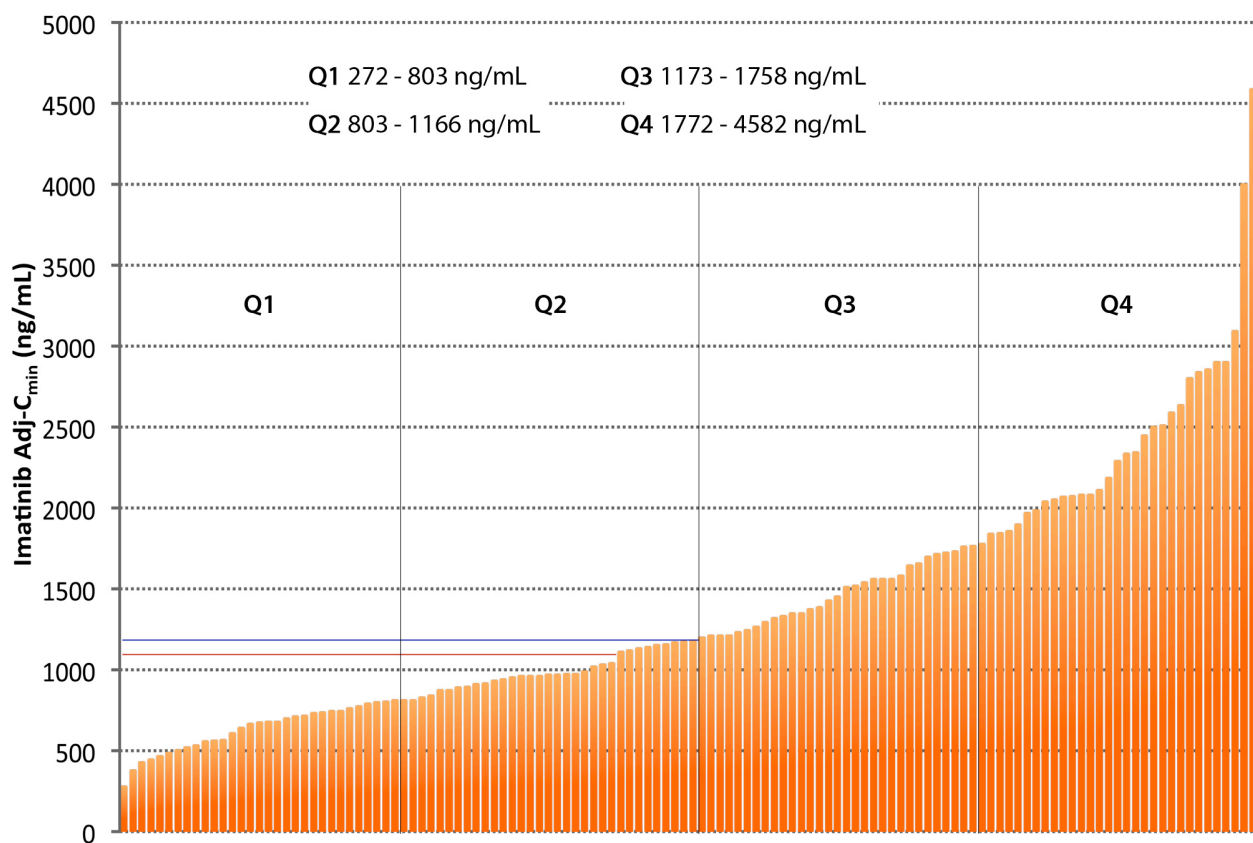


**Figure 19. Distribution of plasma levels in unresectable patients**

Distribution of trough imatinib levels in patients with metastatic or unresectable GIST ( $n=126$ ). Quartile cutoffs and ranges are shown. The median Adj- $C_{min}$  in this group (1170 ng/mL) is shown in blue. The first-quartile cutoff (1100 ng/mL) suggested by Demetri et al(142) is represented in red for comparison.

underwent resection and were receiving adjuvant imatinib therapy and two patients who received a known sub-therapeutic imatinib dose due to toxicity were excluded from this evaluation. Patients who experienced PR had a significantly higher Adj- $C_{min}$  than those in the combined SD/PD group, where PR mean Adj- $C_{min}$  equaled 1503.6 ng/mL compared to SD/PD mean Adj- $C_{min}$  of 1116.6 ng/mL ( $p=0.02$ ). While exceptions were noted, a majority of Choi non-responders clustered in the Q1 to mid-Q2 range (**Figure 20**).

Overall in this group of patients, *KIT* exon 11 mutation was identified in 66 patients, *KIT* exon 9 mutation in 10 patients, and 16 patients were considered *KIT* wild-type (no *KIT* exon 9, 11, 13, or 17 mutation was identified). Of those, 78 patients had CT response measured and the distribution of Adj- $C_{min}$  combined with response and mutation is shown in **Figure 21**. SD/PD responders included 6 of 14 *KIT* wild-type (42.8%), 2 of 8 exon 9 (25%) and 14 of 56 *KIT* exon 11 mutations (25%). While a trend of more *KIT* wild-type was represented in this comparison, it was non-significant ( $p=0.393$  by Fisher's exact test).



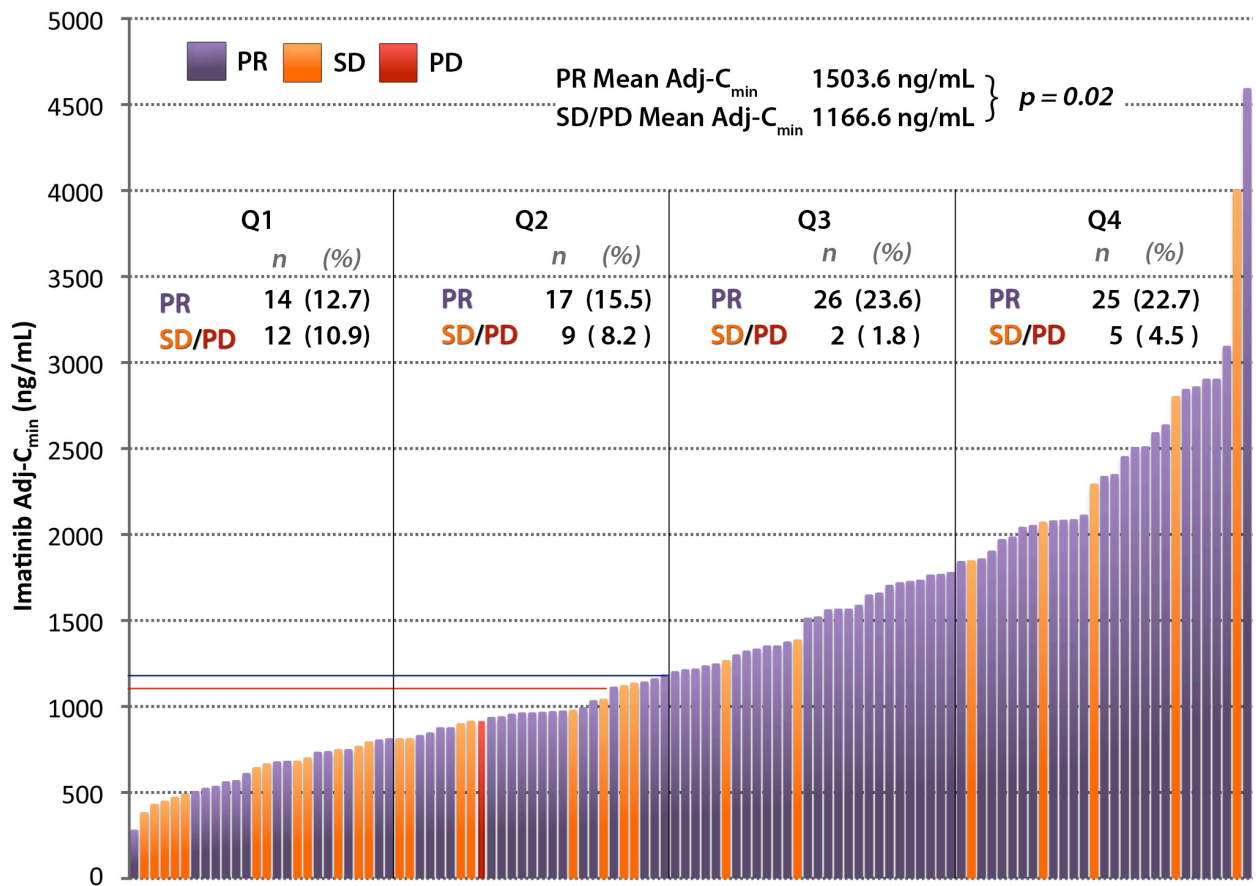
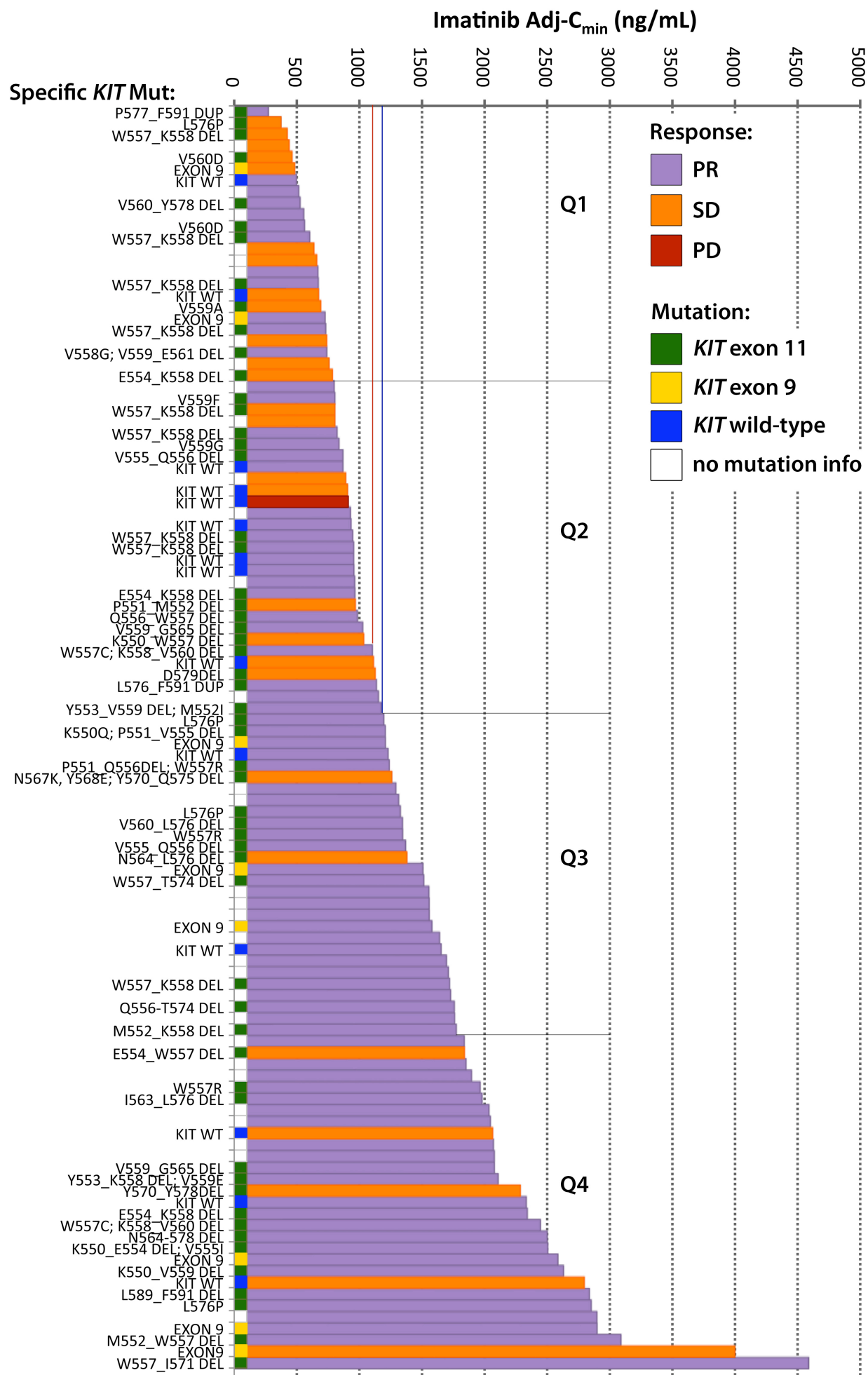


**Figure 20. Distribution of Adj-C<sub>min</sub> and Outcome**

Distribution of Adj-C<sub>min</sub> and Outcome: Response (Choi) is significantly associated with higher trough imatinib levels where PR versus SD/PD (mean Adj-C<sub>min</sub> 1503.6 ng/mL versus 1166.6 ng/mL,  $p=0.02$ ). While exceptions were noted, a majority (75%) of SD/PD responders clustered in the lower two quartiles. Quartile cutoffs were established using the overall distribution of trough imatinib levels in 126 patients with unresectable disease. Patients inevaluable by CT ( $n=16$ ) are excluded in this comparison. The median Adj-C<sub>min</sub> of the overall distribution (1170 ng/mL) is shown in blue. The first-quartile cutoff (1100 ng/mL) suggested by Demetri et al(142) is represented in red for comparison.



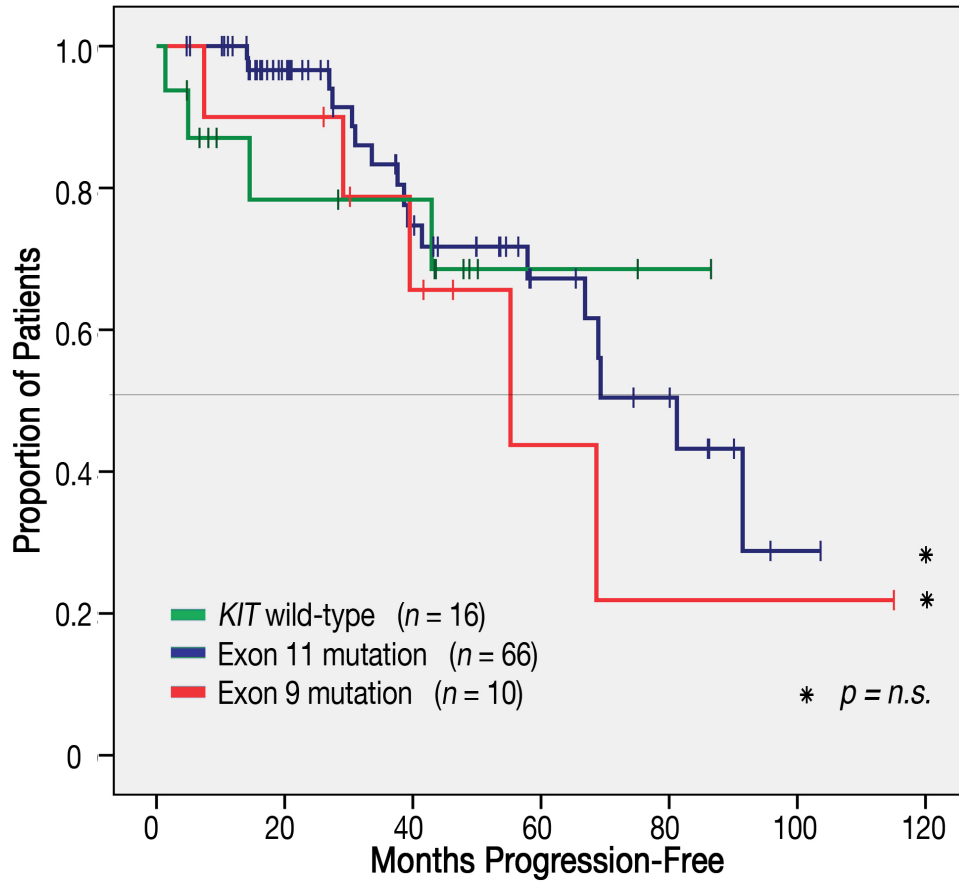
(previous page)

**Figure 21. Response distribution with *KIT* mutation**

*KIT* mutation was available in 92 patients included in efficacy analyses. Where available, *KIT* mutation group (exon 11, exon 9 or wild-type) are represented graphically beneath each graph column, whereas the actual mutation identified is listed vertically on the left. While a higher percentage of *KIT* wild-type patients were resented in the SD/PD response group, there was no statistical correlation.

Comparable to previous studies, patients with wild-type *KIT* progressed first and *KIT* exon 11 patients experienced a median PFS of 81 months (**Figure 22**). Interestingly, patients with *KIT* exon 9 mutation experienced a progression-free survival similar to that of *KIT* exon 11 mutation patients, likely due to the 800 mg imatinib baseline dose given this group upon identification of the mutation at UTMDACC (*KIT* exon 11 median PFS  $81.2 \pm 10.7$  SEM, *KIT* exon 9 PFS  $55.2 \pm 15.0$  SEM). As expected, *KIT* exon 9 patients experienced a higher imatinib Adj- $C_{min}$ , as summarized in the table below, showing that higher trough imatinib levels correlate with response in this mutation sub-group.

Finally, OS and PFS for patients used in efficacy analysis, presented herein, are representative for GIST patients and indicate that our population is what one would expect clinically. Analyses of overall and progression-free survival are provided in **Figure 23**. The PFS of these patients sub-divided by quartile of the Adj- $C_{min}$  distribution was evaluated, presented in **Figure 24**. There was no significant difference in PFS of Q1-Q4, unlike similar studies, and this likely represents a selection bias in our population (190). Having already observed that patients with PR have a significantly higher Adj- $C_{min}$  than those with SD/PD response, and that patients with *KIT* exon 9 mutation experienced higher PFS with higher doses of imatinib, a prospective trial would best address the long-term potential benefits of increased plasma imatinib concentration on response.



<i>KIT</i> Genotype	<i>n</i>	Median Dose	( Range )	Mean Adj-Cmin	( Range )
<i>KIT</i> exon 9	10	800	( 200 - 800 )	1668.5	( 482 - 3995 )
<i>KIT</i> exon 11	66	400	( 300 - 800 )	1353.5	( 423 - 4582 )
<i>KIT</i> wild-type	16	400	( 300 - 800 )	1302.3	( 497 - 2793 )
Other/ND	34	400	( 300 - 600 )	1333.8	( 438 - 2044 )

### Figure 22. Improved PFS with higher imatinib exposure

Patients harboring *KIT* exon 9 mutations experienced a PFS not statistically distinct from *KIT* exon 11 mutation patients when treated at higher imatinib doses (*KIT* exon 11 median PFS 81.2±10.7SEM, *KIT* exon 9 PFS 55.2±15.0SEM). *KIT* exon 9 mutation patients treated at higher doses experience increased trough imatinib levels compared to other groups. ND: no mutation information.

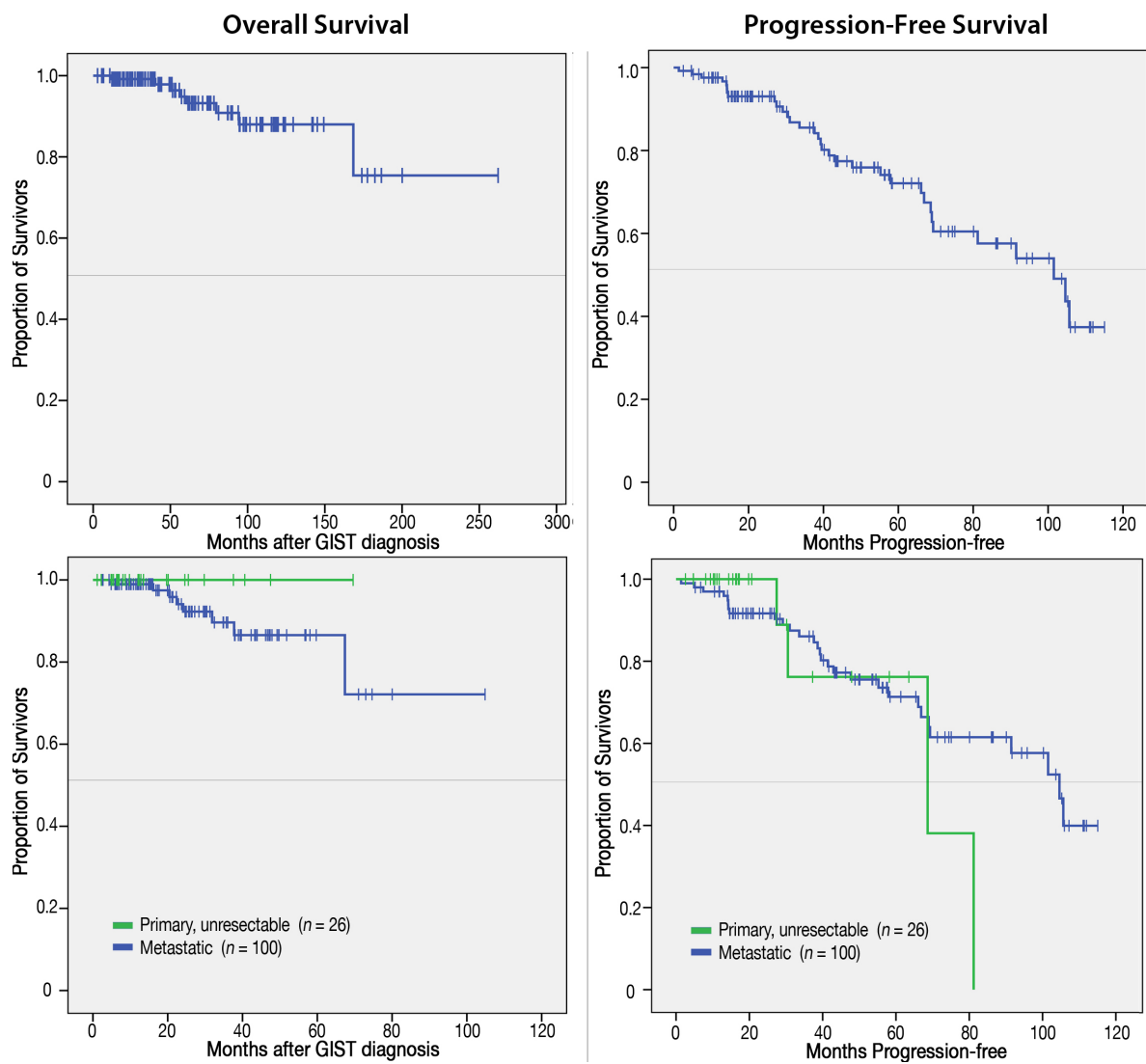


**Figure 23. OS and PFS of patients included in efficacy analyses**

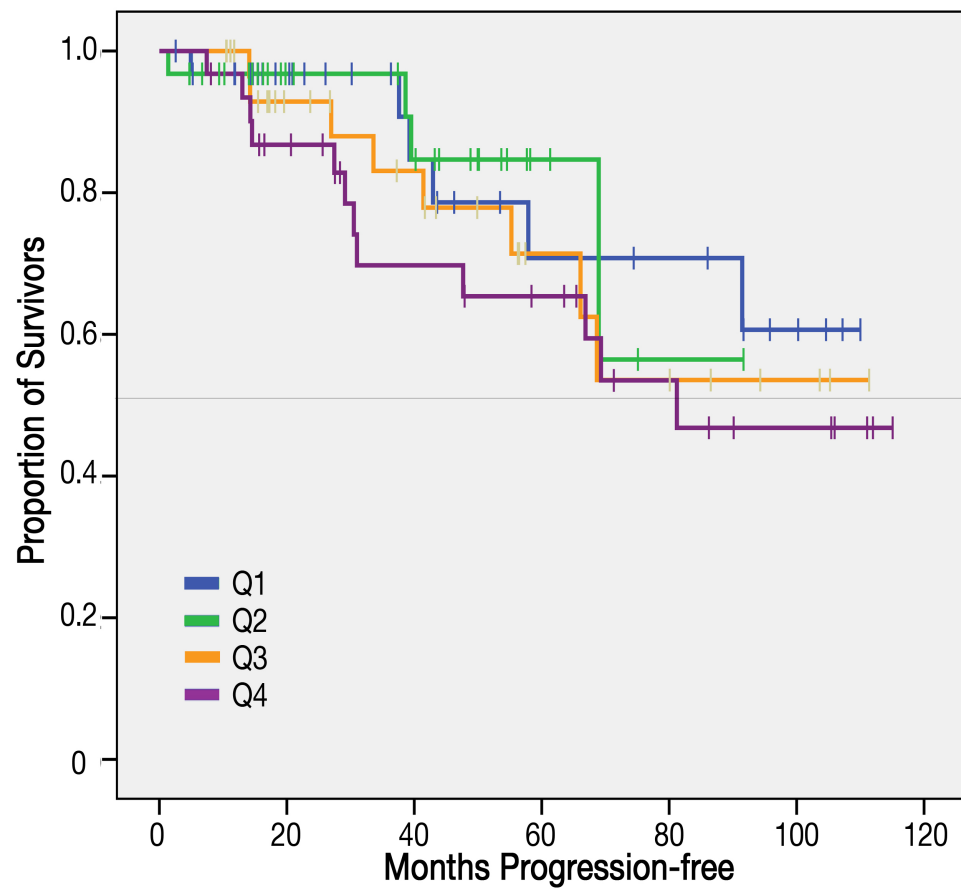


**Figure 24. PFS of patients by Adj-C<sub>min</sub> quartile**

## Chapter 5. Discussion and Conclusions

These investigations have indicated that *KIT* genotype is significantly associated with the type of response determined by clinical evaluation, in this case CT. Moreover, this observation was found to be independent of imatinib dose. Patients with *KIT* exon 11 mutations exhibited the most robust response, with decreases in both size and density (81.7% attained response grade 5 or higher), whereas patients harboring *KIT* exon 9 mutations responded more subtly, with over half in the lowest response group (62.5%). Interestingly patients with no identified *KIT* mutation appeared to stratify into two distinct groups by CT response ( $p=0.001$ ), an observation that has not yet been reported. The presence of a group of patients with WT *KIT* that appeared to benefit from therapy with imatinib may indicate the presence of a mutation in an alternate exon of *KIT* that was not tested or mutation in another kinase susceptible to the inhibitor imatinib.

Comparison of *KIT* exon 11 mutations in GIST patients reviewed at UTMDACC revealed that mutations clustered within regions across the exon where missense mutations and deletions were more frequent in the N-terminal region, insertion/duplications were commonly in the mid- to C-terminal region, and a few large deletions spanned across all three domains (“pan” group). Analysis of radiographic response stratified by any mutation identified in one of these three regions was conducted, followed by response stratified by what type of change occurred (deletion versus missense mutation or insertion/duplication). Both of these analyses were not statistically associated with radiographic response, so codons most frequently affected by mutation were examined (*KIT* exon 11 codons W557,



V559/V560, and L576). Within *KIT* exon 11, mutations altering specific codons were significantly associated with radiographic response when examined using the graded response criteria. Over 80% of W557-altered tumors responded with a Grade 5 or higher, whereas nearly half of L576-mutated tumors fell in Grade 1-4 ( $p=0.013$ ). This may indicate that the specific codon change is a superior predictor of imatinib response than where on *KIT* exon 11 the mutation occurs or whether the mutation is a deletion, insertion, or point mutation, further bolstered by the fact that regional comparison (n-terminal *KIT* exon 11 mutations versus mid/C-terminal) and mutations grouped by type (deletion or missense mutation versus insertion) was not statistically associated with clinical response. Mutations in *KIT* induce conformational changes which not only activate the tyrosine kinase, but may also affect the interaction between imatinib and its binding sites on KIT (129). *In silico* experiments with L576P have shown that this mutation renders a protein that harbors an imatinib binding affinity that is two times less than wild-type KIT (135). It is conceivable that L576P alterations may require higher imatinib concentrations, or even alternate TKIs to achieve the same efficacy as imatinib against mutations at W557, although further research is necessary.

Radiographic response in metastases varied based on location and *KIT* genotype. Wild-type *KIT* metastases increased in size in liver, on average, while decreasing in the peritoneum (mean size change 12.4% versus -8.3%, respectively). In the context of *KIT* exon 9 mutation, size decreased only moderately in liver but increased in the peritoneum (mean size change -4.8% versus 2.5%, respectively). These changes were significant ( $p \leq 0.01$  for both liver

and peritoneum) compared to *KIT* exon 11 mutant GIST, which responded with decreases in size and density in both hepatic and peritoneal sites of 20 to 30%. The rationale as to why differential responses would be observed is not known. This may be due to the biology of the tumor cells that preferentially metastasize to the liver or peritoneum. Alternatively, it may be due to the tissue environment that determines the changes in tumor size and density after imatinib therapy. This is critical in the assessment of response rates that may be different between organs. Perhaps response criteria should be different for liver as compared to peritoneal metastases. This is an area in need of further multidisciplinary investigation.

Recently, there has been significant interest in establishing whether exposure of patients to imatinib, as measured by imatinib trough level ( $\text{Adj-C}_{\min}$ ) may correlate with outcome. Since *KIT* genotype influences the binding of imatinib (129), the optimal plasma trough concentration of imatinib is likely to vary based on the *KIT* genotype of the individual patient. In a group of metastatic or unresectable GIST patients presented herein, trough imatinib levels ranged from 256 – 4582 ng/mL with a first quartile cutoff of 803 ng/mL, much lower than the published literature (142). Examining response in this group, as measured by Choi, revealed that nearly 75% of non-responders (SD/PD) clustered in the lower two quartiles (<1166 ng/mL) and that patients who achieved a Choi response at four months experienced a significantly higher trough imatinib level (PR versus SD/PD mean  $\text{Adj-C}_{\min}$  1503.6ng/mL vs. 1116.6ng/mL,  $p=0.02$ ) irrespective of underlying genotype. In chronic myelogenous leukemia where imatinib therapy is a standard of care for its inhibition of BCR-ABL, two studies have associated higher trough

imatinib levels with better cytogenetic and molecular responses, and improved event-free survival (139, 140). This association was independent of imatinib dose, as highly variable plasma levels were observed at both 400 mg and 600 mg doses (139). CML patients who achieved a complete cytogenetic response (CCyR) experienced significantly higher imatinib trough levels (mean  $1009 \pm 554$  ng/mL) than those who did not achieve a CCyR (mean  $812 \pm 409$  ng/mL) (140). Both studies suggested a therapeutic minimum threshold above 1000 ng/mL for trough imatinib level (139, 140). Recently, in a study of 73 patients with advanced GIST who had been randomized to either imatinib 400 mg or imatinib 600 mg per day, Demetri and colleagues identified that patients in the lowest trough imatinib quartile ( $<1100$  ng/mL) had a significantly shorter median time to progression (11.3 months) when compared to patients in the other three quartiles (30.6 months,  $p=0.0029$ ) (142).

Mutation of *KIT* serves as an important predictive factor for clinical outcome. Previous studies have established rationale for initiating high-dose imatinib treatment in patients harboring *KIT* exon 9 mutations. Therefore, *KIT* mutation testing is determined clinically at many centers (53, 123, 133). Patients with *KIT* exon 9 mutation in our cohort received a median dose of 800 mg, experienced higher trough imatinib levels, and experienced a PFS that was not statistically different from that of patients whose tumors had a mutation in exon 11 of the *KIT* gene. The previous GIST study identified that patients with *KIT* exon 11 mutations in the upper three quartiles (trough imatinib  $>1100$  ng/mL), had a significantly higher clinical benefit rate than patients with *KIT* exon 11 mutations in the lowest quartile

(142). This was not observed in our study, but this may be due to differences in the treatment groups, survival bias, and patient selection.

Analyses were performed and identified a number of novel factors that correlate with trough imatinib levels. For instance, older patients had higher trough imatinib levels than that of younger patients. Moreover, female gender was associated with higher trough imatinib levels, which may explain a somewhat better clinical response in women as reported by others (123). However, this observation may be a result of other covariates, such as renal function, body mass index, or other pharmacokinetic variables and should be studied in prospective trials. High interpatient variability of trough imatinib levels independent of dose was observed, concordant with a smaller study in GIST (142). AST (>48 IU/L) was shown to be associated with higher trough imatinib levels, which may be due to tissue or cellular damage in some patients. Finally, imatinib trough levels were lower when co-administered with CYP450 inducer drugs, whereas CYP450 substrates were associated with higher imatinib trough levels. Taken together, these data suggest should be studied prospectively to determine clinical utility.

## Bibliography

1. Mazur, M. T., and H. B. Clark. 1983. Gastric stromal tumors. Reappraisal of histogenesis. *Am J Surg Pathol* 7:507-519.
2. Hirota, S., K. Isozaki, Y. Moriyama, K. Hashimoto, T. Nishida, S. Ishiguro, K. Kawano, M. Hanada, A. Kurata, M. Takeda, G. Muhammad Tunio, Y. Matsuzawa, Y. Kanakura, Y. Shinomura, and Y. Kitamura. 1998. Gain-of-function mutations of c-kit in human gastrointestinal stromal tumors. *Science* 279:577-580.
3. Nilsson, B., P. Bèumming, J. M. Meis-Kindblom, A. Odâen, A. Dortok, B. Gustavsson, K. Sablinska, and L. G. Kindblom. 2005. Gastrointestinal stromal tumors: the incidence, prevalence, clinical course, and prognostication in the preimatinib mesylate era--a population-based study in western Sweden. *Cancer*. 103:821-829.
4. D'Amato, G., D. M. Steinert, J. C. McAuliffe, and J. C. Trent. 2005. Update on the biology and therapy of gastrointestinal stromal tumors. *Cancer control : journal of the Moffitt Cancer Center*. 12:44-56.
5. KindBlom LG, M.-K. J., Bumming P. 2002. Incidence, prevalence, phenotype and biologic spectrum of gastrointestinal stromal cell tumors (GIST): a population-based study of 600 cases. *Annals of Oncology* 13 , Supplement 5:157: Abstract 5770.

6. Clary, B. M., R. P. DeMatteo, J. J. Lewis, D. Leung, and M. F. Brennan. 2001. Gastrointestinal stromal tumors and leiomyosarcoma of the abdomen and retroperitoneum: a clinical comparison. *Ann Surg Oncol* 8:290-299.
7. Miettinen, M., L. H. Sobin, and J. Lasota. 2005. Gastrointestinal stromal tumors of the stomach: a clinicopathological, immunohistochemical, and molecular genetic study of 1765 cases with long-term follow-up. *American Journal of Surgical Pathology* 29:52-68.
8. Nilsson, B., P. Bumming, J. M. Meis-Kindblom, A. Oden, A. Dortok, B. Gustavsson, K. Sablinska, and L. G. Kindblom. 2005. Gastrointestinal stromal tumors: the incidence, prevalence, clinical course, and prognostication in the preimatinib mesylate era--a population-based study in western Sweden. *Cancer* 103:821-829.
9. Kim, K. M., D. W. Kang, W. S. Moon, J. B. Park, C. K. Park, J. H. Sohn, J. S. Jeong, M. Y. Cho, S. Y. Jin, J. S. Choi, and D. Y. Kang. 2005. Gastrointestinal stromal tumors in Koreans: it's incidence and the clinical, pathologic and immunohistochemical findings. *J Korean Med Sci* 20:977-984.
10. Joensuu, H. 2006. Gastrointestinal stromal tumor (GIST). *Ann Oncol* 17 Suppl 10:x280-286.
11. Kindblom, L. G., H. E. Remotti, F. Aldenborg, and J. M. Meis-Kindblom. 1998. Gastrointestinal pacemaker cell tumor (GIPACT): gastrointestinal stromal tumors show phenotypic characteristics of the interstitial cells of Cajal [see comments]. *Am J Pathol* 152:1259-1269.

12. Miettinen, M., and J. Lasota. 2001. Gastrointestinal stromal tumors--definition, clinical, histological, immunohistochemical, and molecular genetic features and differential diagnosis. *Virchows Arch* 438:1-12.
13. Fletcher, C. D., J. J. Berman, C. Corless, F. Gorstein, J. Lasota, B. J. Longley, M. Miettinen, T. J. O'Leary, H. Remotti, B. P. Rubin, B. Shmookler, L. H. Sobin, and S. W. Weiss. 2002. Diagnosis of gastrointestinal stromal tumors: a consensus approach. *International Journal of Surgical Pathology* 10:81-89.
14. Blay, P., A. Astudillo, J. M. Buesa, E. Campo, M. Abad, J. Garcia-Garcia, R. Miquel, V. Marco, M. Sierra, R. Losa, A. Lacave, A. Brana, M. Balbin, and J. M. Freije. 2004. Protein kinase C theta is highly expressed in gastrointestinal stromal tumors but not in other mesenchymal neoplasias. *Clin Cancer Res* 10:4089-4095.
15. Duensing, A., N. E. Joseph, F. Medeiros, F. Smith, J. L. Hornick, M. C. Heinrich, C. L. Corless, G. D. Demetri, C. D. Fletcher, and J. A. Fletcher. 2004. Protein Kinase C theta (PKCtheta) expression and constitutive activation in gastrointestinal stromal tumors (GISTs). *Cancer Res* 64:5127-5131.
16. Motegi, A., S. Sakurai, H. Nakayama, T. Sano, T. Oyama, and T. Nakajima. 2005. PKC theta, a novel immunohistochemical marker for gastrointestinal stromal tumors (GIST), especially useful for identifying KIT-negative tumors. *Pathol Int* 55:106-112.

17. Chirieac, L. R., J. C. Trent, D. M. Steinert, H. Choi, Y. Yang, J. Zhang, S. R. Patel, R. S. Benjamin, and A. K. Raymond. 2006. Correlation of immunophenotype with progression-free survival in patients with gastrointestinal stromal tumors treated with imatinib mesylate. *Cancer* 107:2237-2244.
18. Eisenberg, B. L. 2006. Combining imatinib with surgery in gastrointestinal stromal tumors: rationale and ongoing trials. *Clin Colorectal Cancer* 6 Suppl 1:S24-29.
19. DeMatteo, R. P., J. J. Lewis, D. Leung, S. S. Mudan, J. M. Woodruff, and M. F. Brennan. 2000. Two hundred gastrointestinal stromal tumors: recurrence patterns and prognostic factors for survival. *Ann Surg* 231:51-58.
20. Pierie, J. P., U. Choudry, A. Muzikansky, B. Y. Yeap, W. W. Souba, and M. J. Ott. 2001. The effect of surgery and grade on outcome of gastrointestinal stromal tumors. *Arch Surg* 136:383-389.
21. Plager, C., N. Papadopolous, P. salem, and R. Benjamin. 1991. Adriamycin based chemotherapy for leiomyosarcoma of the stomach and small bowel. In *Proceedings of the American Society of Clinical Oncology, American Society of Clinical Oncology*. 352.
22. Patel, S., S. Legha, P. Salem, C. Plager, N. Papadopolous, and R. Benjamin. 1991. Evaluation of ifosfamide in metastatic leiomyosarcomas of gastrointestinal origin. In *Proceedings of the American Society of Clinical Oncology, American Society of Clinical Oncology*. 352.



23. Edmonson, J., R. Marks, J. Buckner, and M. Mahoney. 1999. Contrast of response D-MAP + sargramostatin between patients with advanced malignant gastrointestinal stromal tumors and patients with other advanced leiomyosarcomas. In Proceedings of the American Society of Clinical Oncology. American Society of Clinical Oncology. 541a.
24. Carson, W., C. Karakousis, H. Douglass, U. Rao, and M. L. Palmer. 1994. Results of aggressive treatment of gastric sarcoma. *Ann Surg Oncol* 1:244-251.
25. Tuveson, D. A., N. A. Willis, T. Jacks, J. D. Griffin, S. Singer, C. D. Fletcher, J. A. Fletcher, and G. D. Demetri. 2001. STI571 inactivation of the gastrointestinal stromal tumor c-KIT oncoprotein: biological and clinical implications. *Oncogene* 20:5054-5058.
26. Rubin, B. P., S. Singer, C. Tsao, A. Duensing, M. L. Lux, R. Ruiz, M. K. Hibbard, C. J. Chen, S. Xiao, D. A. Tuveson, G. D. Demetri, C. D. Fletcher, and J. A. Fletcher. 2001. KIT activation is a ubiquitous feature of gastrointestinal stromal tumors. *Cancer Research* 61:8118-8121.
27. Kitamura, Y., and S. Hirota. 2004. Kit as a human oncogenic tyrosine kinase. *Cell Mol Life Sci* 61:2924-2931.
28. Besmer, P., J. E. Murphy, P. C. George, F. H. Qiu, P. J. Bergold, L. Lederman, H. W. Snyder, Jr., D. Brodeur, E. E. Zuckerman, and W. D. Hardy. 1986. A new acute transforming feline retrovirus and relationship of its oncogene v-kit with the protein kinase gene family. *Nature* 320:415-421.

29. Yarden, Y., W. J. Kuang, T. Yang-Feng, L. Coussens, S. Munemitsu, T. J. Dull, E. Chen, J. Schlessinger, U. Francke, and A. Ullrich. 1987. Human proto-oncogene c-kit: a new cell surface receptor tyrosine kinase for an unidentified ligand. *Embo J* 6:3341-3351.
30. Chabot, B., D. A. Stephenson, V. M. Chapman, P. Besmer, and A. Bernstein. 1988. The proto-oncogene c-kit encoding a transmembrane tyrosine kinase receptor maps to the mouse W locus. *Nature* 335:88-89.
31. Geissler, E. N., M. A. Ryan, and D. E. Housman. 1988. The dominant-white spotting (W) locus of the mouse encodes the c-kit proto-oncogene. *Cell* 55:185-192.
32. Maeda, H., A. Yamagata, S. Nishikawa, K. Yoshinaga, S. Kobayashi, and K. Nishi. 1992. Requirement of c-kit for development of intestinal pacemaker system. *Development* 116:369-375.
33. Linnekin, D. 1999. Early signaling pathways activated by c-Kit in hematopoietic cells. *Int J Biochem Cell Biol* 31:1053-1074.
34. Reith, A. D., C. Ellis, S. D. Lyman, D. M. Anderson, D. E. Williams, A. Bernstein, and T. Pawson. 1991. Signal transduction by normal isoforms and W mutant variants of the Kit receptor tyrosine kinase. *EMBO J* 10:2451-2459.
35. Crosier, P. S., S. T. Ricciardi, L. R. Hall, M. R. Vitas, S. C. Clark, and K. E. Crosier. 1993. Expression of isoforms of the human receptor tyrosine kinase c-kit in leukemic cell lines and acute myeloid leukemia. *Blood* 82:1151-1158.
36. Mol, C. D., D. R. Dougan, T. R. Schneider, R. J. Skene, M. L. Kraus, D. N. Scheibe, G. P. Snell, H. Zou, B. C. Sang, and K. P. Wilson. 2004. Structural

- basis for the autoinhibition and STI-571 inhibition of c-Kit tyrosine kinase. *J Biol Chem* 279:31655-31663.
37. Mol, C. D., K. B. Lim, V. Sridhar, H. Zou, E. Y. Chien, B. C. Sang, J. Nowakowski, D. B. Kassel, C. N. Cronin, and D. E. McRee. 2003. Structure of a c-kit product complex reveals the basis for kinase transactivation. *The Journal of biological chemistry* 278:31461-31464.
  38. Lemmon, M. A., D. Pinchasi, M. Zhou, I. Lax, and J. Schlessinger. 1997. Kit receptor dimerization is driven by bivalent binding of stem cell factor. *J Biol Chem* 272:6311-6317.
  39. Paulhe, F., B. A. Imhof, and B. Wehrle-Haller. 2004. A specific endoplasmic reticulum export signal drives transport of stem cell factor (Kitl) to the cell surface. *J Biol Chem* 279:55545-55555.
  40. Ashman, L. K. 1999. The biology of stem cell factor and its receptor C-kit. *Int J Biochem Cell Biol* 31:1037-1051.
  41. Huang, E. J., K. H. Nocka, J. Buck, and P. Besmer. 1992. Differential expression and processing of two cell associated forms of the kit-ligand: KL-1 and KL-2. *Mol Biol Cell* 3:349-362.
  42. Longley, B. J., L. Tyrrell, Y. Ma, D. A. Williams, R. Halaban, K. Langley, H. S. Lu, and N. M. Schechter. 1997. Chymase cleavage of stem cell factor yields a bioactive, soluble product. *Proc Natl Acad Sci U S A* 94:9017-9021.
  43. Pandiella, A., M. W. Bosenberg, E. J. Huang, P. Besmer, and J. Massague. 1992. Cleavage of membrane-anchored growth factors involves distinct

- protease activities regulated through common mechanisms. *J Biol Chem* 267:24028-24033.
44. Heissig, B., K. Hattori, S. Dias, M. Friedrich, B. Ferris, N. R. Hackett, R. G. Crystal, P. Besmer, D. Lyden, M. A. Moore, Z. Werb, and S. Rafii. 2002. Recruitment of stem and progenitor cells from the bone marrow niche requires MMP-9 mediated release of kit-ligand. *Cell* 109:625-637.
  45. Hsu, Y. R., G. M. Wu, E. A. Mendiaz, R. Syed, J. Wypych, R. Toso, M. B. Mann, T. C. Boone, L. O. Narhi, H. S. Lu, and K. E. Langley. 1997. The majority of stem cell factor exists as monomer under physiological conditions. Implications for dimerization mediating biological activity. *J Biol Chem* 272:6406-6415.
  46. Hong, L., V. Munugalavadla, and R. Kapur. 2004. c-Kit-mediated overlapping and unique functional and biochemical outcomes via diverse signaling pathways. *Mol Cell Biol* 24:1401-1410.
  47. Saul, S. H., M. L. Rast, and J. J. Brooks. 1987. The immunohistochemistry of gastrointestinal stromal tumors. Evidence supporting an origin from smooth muscle. *Am J Surg Pathol* 11:464-473.
  48. Heinrich, M. C., D. C. Dooley, A. C. Freed, L. Band, M. E. Hoatlin, W. W. Keeble, S. T. Peters, K. V. Silvey, F. S. Ey, D. Kabat, R. Maziarz, and G. Bagby. 1993. Constitutive expression of steel factor gene by human stromal cells. *Blood* 82:771-783.
  49. Heinrich, M. C., C. Corless, G. D. Demetri, C. D. Blanke, M. von Mehren, H. Joensuu, L. S. McGreevey, C. J. Chen, A. D. Van de Abbeele, B. J. Druker,

- B. Kiese, B. Eisenberg, P. J. Roberts, S. Singer, C. D. Fletcher, S. Silberman, S. Dimitrijevic, and J. A. Fletcher. 2003. Kinase mutations and imatinib response in patients with metastatic gastrointestinal stromal tumor. *JCO* 21:4342-4349.
50. Lennartsson, J., T. Jelacic, D. Linnekin, and R. Shivakrupa. 2005. Normal and oncogenic forms of the receptor tyrosine kinase kit. *Stem cells* (Dayton, Ohio) 23:16-43.
  51. Lasota, J., and M. Miettinen. 2008. Clinical significance of oncogenic KIT and PDGFRA mutations in gastrointestinal stromal tumours. *Histopathology* 53:245-266.
  52. Singer, S., B. P. Rubin, M. L. Lux, C. J. Chen, G. D. Demetri, C. D. Fletcher, and J. A. Fletcher. 2002. Prognostic value of KIT mutation type, mitotic activity, and histologic subtype in gastrointestinal stromal tumors. *Journal of Clinical Oncology* 20:3898-3905.
  53. Debiec-Rychter, M., R. Sciot, A. Le Cesne, M. Schlemmer, P. Hohenberger, A. T. van Oosterom, J. Y. Blay, S. Leyvraz, M. Stul, P. G. Casali, J. Zalcberg, J. Verweij, M. Van Glabbeke, A. Hagemeijer, I. Judson, E. S. T. a. B. S. Group, G. The Italian Sarcoma, and G. Australasian GastroIntestinal Trials. 2006. KIT mutations and dose selection for imatinib in patients with advanced gastrointestinal stromal tumours. *European Journal of Cancer* 42:1093-1103.
  54. Heinrich, M. C., C. L. Corless, G. D. Demetri, C. D. Blanke, M. von Mehren, H. Joensuu, L. S. McGreevey, C. J. Chen, A. D. Van den Abbeele, B. J.

- Druker, B. Kiese, B. Eisenberg, P. J. Roberts, S. Singer, C. D. Fletcher, S. Silberman, S. Dimitrijevic, and J. A. Fletcher. 2003. Kinase mutations and imatinib response in patients with metastatic gastrointestinal stromal tumor. *J Clin Oncol* 21:4342-4349.
55. Corless, C. L., L. McGreevey, A. Town, A. Schroeder, T. Bainbridge, P. Harrell, J. A. Fletcher, and M. C. Heinrich. 2004. KIT gene deletions at the intron 10-exon 11 boundary in GI stromal tumors. *J Mol Diagn* 6:366-370.
56. McAuliffe, J. C., A. J. Lazar, D. Yang, D. M. Steinert, W. Qiao, P. F. Thall, A. K. Raymond, R. S. Benjamin, and J. C. Trent. 2007. Association of intratumoral vascular endothelial growth factor expression and clinical outcome for patients with gastrointestinal stromal tumors treated with imatinib mesylate. *Clin Cancer Res* 13:6727-6734.
57. Penzel, R., S. Aulmann, M. Moock, M. Schwarzbach, R. J. Rieker, and G. Mechttersheimer. 2005. The location of KIT and PDGFRA gene mutations in gastrointestinal stromal tumours is site and phenotype associated. *J Clin Pathol* 58:634-639.
58. Lasota, J., C. L. Corless, M. C. Heinrich, M. Debiec-Rychter, R. Sciot, E. Wardelmann, S. Merkelbach-Bruse, H. U. Schildhaus, S. E. Steigen, J. Stachura, A. Wozniak, C. Antonescu, O. Daum, J. Martin, J. G. Del Muro, and M. Miettinen. 2008. Clinicopathologic profile of gastrointestinal stromal tumors (GISTs) with primary KIT exon 13 or exon 17 mutations: a multicenter study on 54 cases. *Mod Pathol* 21:476-484.

59. Lasota, J., and M. Miettinen. 2006. KIT and PDGFRA mutations in gastrointestinal stromal tumors (GISTs). *Seminars in Diagnostic Pathology* 23:91-102.
60. Heinrich, M. C., C. L. Corless, A. Duensing, L. McGreevey, C. J. Chen, N. Joseph, S. Singer, D. J. Griffith, A. Haley, A. Town, G. D. Demetri, C. D. Fletcher, and J. A. Fletcher. 2003. PDGFRA activating mutations in gastrointestinal stromal tumors. *Science* 299:708-710.
61. Corless, C. L., A. Schroeder, D. Griffith, A. Town, L. McGreevey, P. Harrell, S. Shiraga, T. Bainbridge, J. Morich, and M. C. Heinrich. 2005. PDGFRA mutations in gastrointestinal stromal tumors: frequency, spectrum and in vitro sensitivity to imatinib. *J Clin Oncol* 23:5357-5364.
62. Lasota, J., A. Dansonka-Mieszkowska, L. H. Sobin, and M. Miettinen. 2004. A great majority of GISTs with PDGFRA mutations represent gastric tumors of low or no malignant potential. *Lab Invest* 84:874-883.
63. Medeiros, F., C. L. Corless, A. Duensing, J. L. Hornick, A. M. Oliveira, M. C. Heinrich, J. A. Fletcher, and C. D. Fletcher. 2004. KIT-negative gastrointestinal stromal tumors: proof of concept and therapeutic implications. *Am J Surg Pathol* 28:889-894.
64. Hirota, S., T. Nishida, K. Isozaki, M. Taniguchi, K. Nishikawa, A. Ohashi, A. Takabayashi, T. Obayashi, T. Okuno, K. Kinoshita, H. Chen, Y. Shinomura, and Y. Kitamura. 2002. Familial gastrointestinal stromal tumors associated with dysphagia and novel type germline mutation of KIT gene. *Gastroenterology* 122:1493-1499.

65. Nishida, T., S. Hirota, M. Taniguchi, K. Hashimoto, K. Isozaki, H. Nakamura, Y. Kanakura, T. Tanaka, A. Takabayashi, H. Matsuda, and Y. Kitamura. 1998. Familial gastrointestinal stromal tumours with germline mutation of the KIT gene. *Nature Genetics* 19:323-324.
66. Isozaki, K., B. Terris, J. Belghiti, S. Schiffmann, S. Hirota, and J. M. Vanderwinden. 2000. Germline-activating mutation in the kinase domain of the KIT gene in familial gastrointestinal stromal tumors. *American Journal of Pathology* 157:1581-1585.
67. Beghini, A., M. Tibiletti, G. Roversi, A. M. Chiavaralli, G. Serio, C. Capella, and L. Larizza. 2001. Germline mutation in the juxtamembrane domain of the kit gene in a family with gastrointestinal stromal tumors and urticaria pigmentosa. *Cancer* 92:657-662.
68. Maeyama, H., E. Hidaka, H. Ota, S. Minami, M. Kajiyama, A. Kuraishi, H. Mori, Y. Matsuda, S. Wada, H. Sodeyama, S. Nakata, N. Kawamura, S. Hata, M. Watanabe, Y. Iijima, and T. Katsuyama. 2001. Familial gastrointestinal stromal tumor with hyperpigmentation: association with a germline mutation of the c-kit gene. *Gastroenterology* 120:210-215.
69. Chompret, A., C. Kannengeisser, M. Barrois, P. Terrier, P. Dahan, T. Tursz, G. M. Lenoir, and B. Bressac-De Paillerets. 2004. PDGFRA germline mutation in a family with multiple cases of gastrointestinal stromal tumor. *Gastroenterology* 126:318-321.
70. Robson, M. E., E. Glogowski, G. Sommer, C. R. Antonescu, K. Nafa, R. G. Maki, N. Ellis, P. Besmer, M. Brennan, and K. Offit. 2004. Pleomorphic



- characteristics of a germ-line KIT mutation in a large kindred with gastrointestinal stromal tumors, hyperpigmentation and dysphagia. *Clinical Cancer Research* 10:1250-1254.
71. Carballo, M., I. Roig, F. Aguilar, M. A. Pol, M. J. Gamundi, I. Hernan, and M. Martinez-Gimeno. 2005. Novel c-kit germline mutation in a family with gastrointestinal stromal tumors and cutaneous hyperpigmentation. *American Journal of Medical Genetics* 132:361-364.
  72. Li, F., J. A. Fletcher, M. C. Heinrich, J. E. Garber, S. E. Sallan, C. Curiel-Lewandrowski, A. Duensing, M. van de Rijn, L. E. Schnipper, and G. D. Demetri. 2005. Familial gastrointestinal stromal tumor syndrome: phenotypic and molecular features in a kindred. *JCO* 23:2735-2743.
  73. Tarn, C., E. Merkel, A. A. Canutescu, W. Shen, Y. Skorobogatko, M. J. Heslin, B. Eisenberg, R. Birbe, A. Patchefsky, R. Dunbrack, J. P. Arnoletti, M. von Mehren, and A. K. Godwin. 2005. Analysis of KIT mutations in sporadic and familial gastrointestinal stromal tumors: therapeutic implications through protein modeling. *Clinical Cancer Research* 11:3668-3677.
  74. O'Riain, C., C. Corless, M. Heinrich, D. Keegan, M. Vioreanu, D. Maguire, and K. Sheahan. 2005. Gastrointestinal stromal tumors: Insights from a new familial GIST kindred with unusual genetic and pathological features. *American Journal of Surgical Pathology* 29:1680-1683.
  75. Hartmann, K., E. Wardelmann, M. Yongsheng, S. Merkelbach-Bruse, L. M. Pruessner, C. Woolery, S. E. Baldus, T. Heinicke, J. Thiele, R. Buettner, and B. J. Longley. 2005. Novel germline mutation of KIT associated with familial

- gastrointestinal stromal tumor and mastocytosis. *Gastroenterology* 129:1042-1046.
76. Lasota, J., and M. Miettinen. 2006. A new familial GIST identified. *Am J Surg Pathol* 30:1342.
77. Hirota, S., T. Okazaki, Y. Kitamura, P. O'Brien, L. Kapusta, and I. Dardick. 2000. Cause of familial and multiple gastrointestinal autonomic nerve tumors with hyperplasia of interstitial cells of Cajal is germline mutation of the c-kit gene. *American Journal of Surgical Pathology* 24:326-327.
78. Kang, D. Y., C. K. Park, J. S. Choi, S. Y. Jin, H. J. Kim, M. Joo, M. S. Kang, W. S. Moon, K. J. Yun, E. S. Yu, H. Kang, and K. M. Kim. 2007. Multiple gastrointestinal stromal tumors: Clinicopathologic and genetic analysis of 12 patients. *Am J Surg Pathol* 31:224-232.
79. Graham, J., M. Debiec-Rychter, C. L. Corless, R. Reid, R. Davidson, and J. D. White. 2007. Imatinib in the management of multiple gastrointestinal stromal tumors associated with a germline KIT K642E mutation. *Arch Pathol Lab Med* 131:1393-1396.
80. de Raedt, T., J. Cools, M. Debiec-Rychter, H. Brems, N. Mentens, R. Sciot, J. Himpens, I. de Wever, P. Schoffski, P. Marynen, and E. Legius. 2006. Intestinal neurofibromatosis is a subtype of familial GIST and results from a dominant activating mutation in PDGFRA. *Gastroenterology* 131:1907-1912.
81. Pasini, B., L. Matyakhina, T. Bei, M. Muchow, S. Boikos, B. Ferrando, J. A. Carney, and C. A. Stratakis. 2007. Multiple gastrointestinal stromal and other tumors caused by platelet-derived growth factor receptor alpha gene

- mutations: a case associated with a germline V561D defect. *J Clin Endocrinol Metab* 92:3728-3732.
82. Andersson, J., P. Bumming, J. M. Meis-Kindblom, H. Sihto, N. Nupponen, H. Joensuu, A. Oden, B. Gustavsson, L. G. Kindblom, and B. Nilsson. 2006. Gastrointestinal stromal tumors with KIT exon 11 deletions are associated with poor prognosis. *Gastroenterology* 130:1573-1581.
83. Cho, S., Y. Kitadai, S. Yoshida, S. Tanaka, M. Yoshihara, K. Yoshida, and K. Chayama. 2006. Deletion of the KIT gene is associated with liver metastasis and poor prognosis in patients with gastrointestinal stromal tumor in the stomach. *Int J Oncol* 28:1361-1367.
84. Wong, N. A., R. Young, R. D. Malcomson, A. G. Nayar, L. A. Jamieson, V. E. Save, F. A. Carey, D. H. Brewster, C. Han, and A. Al-Nafussi. 2003. Prognostic indicators for gastrointestinal stromal tumours: a clinicopathological and immunohistochemical study of 108 resected cases of the stomach. *Histopathology* 43:118-126.
85. Emile, J. F., N. Theou, S. Tabone, A. Cortez, P. Terrier, M. T. Chaumette, C. Julie, P. Bertheau, A. Lavergne-Slove, J. Donadieu, A. Barrier, A. Le Cesne, B. Debuire, and A. Lemoine. 2004. Clinicopathologic, phenotypic, and genotypic characteristics of gastrointestinal mesenchymal tumors. *Clin Gastroenterol Hepatol* 2:597-605.
86. Taniguchi, M., T. Nishida, S. Hirota, K. Isozaki, T. Ito, T. Nomura, H. Matsuda, and Y. Kitamura. 1999. Effect of c-kit mutation on prognosis of gastrointestinal stromal tumors. *Cancer Res* 59:4297-4300.

87. Martin, J., A. Poveda, A. Llombart-Bosch, R. Ramos, J. A. Lopez-Guerrero, J. Garcia del Muro, J. Maurel, S. Calabuig, A. Gutierrez, J. L. Gonzalez de Sande, J. Martinez, A. De Juan, N. Lainez, F. Losa, V. Alija, P. Escudero, A. Casado, P. Garcia, R. Blanco, and J. M. Buesa. 2005. Deletions affecting codons 557-558 of the c-KIT gene indicate a poor prognosis in patients with completely resected gastrointestinal stromal tumors: a study by the Spanish Group for Sarcoma Research (GEIS). *J Clin Oncol* 23:6190-6198.
88. Ilesalnieks, I., P. Rummele, W. Dietmaier, T. Jantsch, C. Zulke, H. J. Schlitt, F. Hofstadter, and M. Anthuber. 2005. Factors associated with disease progression in patients with gastrointestinal stromal tumors in the pre-imatinib era. *Am J Clin Pathol* 124:740-748.
89. Wardelmann, E., I. Losen, V. Hans, I. Neidt, N. Speidel, E. Bierhoff, T. Heinicke, T. Pietsch, R. Buttner, and S. Merkelbach-Bruse. 2003. Deletion of Trp-557 and Lys-558 in the juxtamembrane domain of the c-kit protooncogene is associated with metastatic behavior of gastrointestinal stromal tumors. *Int J Cancer* 106:887-895.
90. Lasota, J., A. J. vel Dobosz, B. Wasag, A. Wozniak, E. Kraszewska, W. Michej, K. Ptaszynski, P. Rutkowski, M. Sarlomo-Rikala, S. E. Steigen, R. Schneider-Stock, J. Stachura, M. Chosia, G. Ogun, W. Ruka, J. A. Siedlecki, and M. Miettinen. 2007. Presence of homozygous KIT exon 11 mutations is strongly associated with malignant clinical behavior in gastrointestinal stromal tumors. *Lab Invest* 87:1029-1041.

91. Nowell, P. C., and D. A. Hungerford. 1960. Chromosome studies on normal and leukemic human leukocytes. *J Natl Cancer Inst* 25:85-109.
92. Lugo, T. G., A. M. Pendergast, A. J. Muller, and O. N. Witte. 1990. Tyrosine kinase activity and transformation potency of bcr-abl oncogene products. *Science* 247:1079-1082.
93. Capdeville, R., E. Buchdunger, J. Zimmermann, and A. Matter. 2002. Glivec (STI571, imatinib), a rationally developed, targeted anticancer drug. *Nat Rev Drug Discov* 1:493-502.
94. Zimmermann, J., G. Caravatti, H. Mett, T. Meyer, M. Muller, N. B. Lydon, and D. Fabbro. 1996. Phenylamino-pyrimidine (PAP) derivatives: a new class of potent and selective inhibitors of protein kinase C (PKC). *Arch Pharm (Weinheim)* 329:371-376.
95. Druker, B. J., C. L. Sawyers, H. Kantarjian, D. J. Resta, S. F. Reese, J. M. Ford, R. Capdeville, and M. Talpaz. 2001. Activity of a specific inhibitor of the BCR-ABL tyrosine kinase in the blast crisis of chronic myeloid leukemia and acute lymphoblastic leukemia with the Philadelphia chromosome.[see comment][erratum appears in *N Engl J Med* 2001 Jul 19;345(3):232]. *New England Journal of Medicine* 344:1038-1042.
96. Capdeville, R., S. Silberman, and S. Dimitrijevic. 2002. Imatinib: the first 3 years. *European Journal of Cancer* 38 Suppl 5:S77-82.
97. Savage, D. G., and K. H. Antman. 2002. Imatinib mesylate--a new oral targeted therapy. *N Engl J Med* 346:683-693.

98. Heinrich, M. C., D. J. Griffith, B. J. Druker, C. L. Wait, K. A. Ott, and A. J. Zigler. 2000. Inhibition of c-kit receptor tyrosine kinase activity by STI 571, a selective tyrosine kinase inhibitor. *Blood* 96:925-932.
99. Noma, K., Y. Naomoto, M. Gunduz, J. Matsuoka, T. Yamatsuji, Y. Shirakawa, T. Nobuhisa, T. Okawa, M. Takaoka, Y. Tomono, O. Hiroyuki, E. Gunduz, and N. Tanaka. 2005. Effects of imatinib vary with the types of KIT-mutation in gastrointestinal stromal tumor cell lines. *Oncol Rep* 14:645-650.
100. Wardelmann, E., H. U. Schildhaus, S. Merkelbach-Bruse, and R. Buttner. 2006. [Therapeutic targets in gastrointestinal stromal tumors]. *Verh Dtsch Ges Pathol* 90:73-79.
101. Imatinib Mesylate [Internet]. National Cancer Institute (US) [last updated 10/20/2009; cited 11/13/2010] Available from <http://www.cancer.gov/cancertopics/druginfo/imatinibmesylate>.
102. Clinical Trials Results [Internet]. National Cancer Institute (US) [last updated 10/18/2010; cited 11/13/2010] Available from <http://www.cancer.gov/search/ResultsClinicalTrials.aspx?protocolsearchid=8441285>.
103. Cortes, J. 2004. Natural history and staging of chronic myelogenous leukemia. *Hematol Oncol Clin North Am* 18:569-584, viii.
104. Erikson, J., C. A. Griffin, A. ar-Rushdi, M. Valtieri, J. Hoxie, J. Finan, B. S. Emanuel, G. Rovera, P. C. Nowell, and C. M. Croce. 1986. Heterogeneity of chromosome 22 breakpoint in Philadelphia-positive (Ph+) acute lymphocytic leukemia. *Proc Natl Acad Sci U S A* 83:1807-1811.

105. Faderl, S., M. Talpaz, Z. Estrov, and H. M. Kantarjian. 1999. Chronic myelogenous leukemia: biology and therapy. *Ann Intern Med* 131:207-219.
106. Agrawal, M., R. J. Garg, H. Kantarjian, and J. Cortes. 2010. Chronic myeloid leukemia in the tyrosine kinase inhibitor era: what is the "best" therapy? *Curr Oncol Rep* 12:302-313.
107. Druker, B. J., M. Talpaz, D. J. Resta, B. Peng, E. Buchdunger, J. M. Ford, N. B. Lydon, H. Kantarjian, R. Capdeville, S. Ohno-Jones, and C. L. Sawyers. 2001. Efficacy and safety of a specific inhibitor of the BCR-ABL tyrosine kinase in chronic myeloid leukemia. *N Engl J Med* 344:1031-1037.
108. Sawyers, C. L., A. Hochhaus, E. Feldman, J. M. Goldman, C. B. Miller, O. G. Ottmann, C. A. Schiffer, M. Talpaz, F. Guilhot, M. W. Deininger, T. Fischer, S. G. O'Brien, R. M. Stone, C. B. Gambacorti-Passerini, N. H. Russell, J. J. Reiffers, T. C. Shea, B. Chapuis, S. Coutre, S. Tura, E. Morra, R. A. Larson, A. Saven, C. Peschel, A. Gratwohl, F. Mandelli, M. Ben-Am, I. Gathmann, R. Capdeville, R. L. Paquette, and B. J. Druker. 2002. Imatinib induces hematologic and cytogenetic responses in patients with chronic myelogenous leukemia in myeloid blast crisis: results of a phase II study. *Blood* 99:3530-3539.
109. Talpaz, M., R. T. Silver, B. J. Druker, J. M. Goldman, C. Gambacorti-Passerini, F. Guilhot, C. A. Schiffer, T. Fischer, M. W. Deininger, A. L. Lennard, A. Hochhaus, O. G. Ottmann, A. Gratwohl, M. Baccarani, R. Stone, S. Tura, F. X. Mahon, S. Fernandes-Reese, I. Gathmann, R. Capdeville, H. M. Kantarjian, and C. L. Sawyers. 2002. Imatinib induces durable

- hematologic and cytogenetic responses in patients with accelerated phase chronic myeloid leukemia: results of a phase 2 study. *Blood* 99:1928-1937.
110. Baccarani, M., J. Cortes, F. Pane, D. Niederwieser, G. Saglio, J. Apperley, F. Cervantes, M. Deininger, A. Gratwohl, F. Guilhot, A. Hochhaus, M. Horowitz, T. Hughes, H. Kantarjian, R. Larson, J. Radich, B. Simonsson, R. T. Silver, J. Goldman, and R. Hehlmann. 2009. Chronic myeloid leukemia: an update of concepts and management recommendations of European LeukemiaNet. *J Clin Oncol* 27:6041-6051.
  111. Cortes J, B. M., Guilhot F. 2008. A phase III, randomized, open-label study of 400mg versus 800mg of imatinib mesylate (IM) in patients (pts) with newly diagnosed, previously untreated chronic myeloid leukemia in chronic phase (CML-CP) using molecular endpoints: 1-year results of TOPS (tyrosine kinase inhibitor optimization and selectivity) study. *ASH Annual Meeting Abstracts* 112:335.
  112. Apperley, J. F. 2007. Part I: mechanisms of resistance to imatinib in chronic myeloid leukaemia. *Lancet Oncol* 8:1018-1029.
  113. O'Hare, T., D. K. Walters, E. P. Stoffregen, T. Jia, P. W. Manley, J. Mestan, S. W. Cowan-Jacob, F. Y. Lee, M. C. Heinrich, M. W. Deininger, and B. J. Druker. 2005. In vitro activity of Bcr-Abl inhibitors AMN107 and BMS-354825 against clinically relevant imatinib-resistant Abl kinase domain mutants. *Cancer Res* 65:4500-4505.
  114. Branford, S. 2007. Chronic myeloid leukemia: molecular monitoring in clinical practice. *Hematology Am Soc Hematol Educ Program*:376-383.



115. Willis, S. G., T. Lange, S. Demehri, S. Otto, L. Crossman, D. Niederwieser, E. P. Stoffregen, S. McWeeney, I. Kovacs, B. Park, B. J. Druker, and M. W. Deininger. 2005. High-sensitivity detection of BCR-ABL kinase domain mutations in imatinib-naive patients: correlation with clonal cytogenetic evolution but not response to therapy. *Blood* 106:2128-2137.
116. Press, R. D., C. Galderisi, R. Yang, C. Rempfer, S. G. Willis, M. J. Mauro, B. J. Druker, and M. W. Deininger. 2007. A half-log increase in BCR-ABL RNA predicts a higher risk of relapse in patients with chronic myeloid leukemia with an imatinib-induced complete cytogenetic response. *Clin Cancer Res* 13:6136-6143.
117. Shah, N. P., B. J. Skaggs, S. Branford, T. P. Hughes, J. M. Nicoll, R. L. Paquette, and C. L. Sawyers. 2007. Sequential ABL kinase inhibitor therapy selects for compound drug-resistant BCR-ABL mutations with altered oncogenic potency. *J Clin Invest* 117:2562-2569.
118. Quintás-Cardama A, G. D., Kantarjian HM. 2008. Mutational analysis of chronic phase chronic myeloid leukemia (CML-CP) clones reveals heightened BCR-ABL1 genetic instability in patients failing sequential imatinib and dasatinib therapy *Blood* (ASH Annual Meeting Abstracts) 112:Abstract 2114.
119. Joensuu, H., P. J. Roberts, M. Sarlomo-Rikala, L. C. Andersson, P. Tervahartiala, D. Tuveson, S. Silberman, R. Capdeville, S. Dimitrijevic, B. Druker, and G. D. Demetri. 2001. Effect of the tyrosine kinase inhibitor

- STI571 in a patient with a metastatic gastrointestinal stromal tumor. *New England Journal of Medicine* 344:1052-1056.
120. van Oosterom, A. T., I. Judson, J. Verweij, S. Stroobants, E. Donato di Paola, S. Dimitrijevic, M. Martens, A. Webb, R. Sciot, M. Van Glabbeke, S. Silberman, and O. S. Nielsen. 2001. Safety and efficacy of imatinib (STI571) in metastatic gastrointestinal stromal tumours: a phase I study. *Lancet* 358:1421-1423.
  121. von Mehren, M., C. Blanke, H. Joensuu, M. Heinrich, P. Roberts, B. Eisenberg, S. Silberman, S. Dimitrijevic, B. Kiese, J. Fletcher, C. Fletcher, and G. Demetri. 2002. High Incidence of durable responses induced by imatinib mesylate (Gleevec) in patients with unresectable and metastatic gastrointestinal stromal tumors (GISTs) (abstract # 1608). In *Proceedings of the American Society of Clinical Oncology*. American Society of Clinical Oncology, Orlando.
  122. Verweij, J., A. van Oosterom, J. Y. Blay, I. Judson, S. Rodenhuis, W. van der Graaf, J. Radford, A. Le Cesne, P. C. Hogendoorn, E. D. di Paola, M. Brown, and O. S. Nielsen. 2003. Imatinib mesylate (STI-571 Glivec, Gleevec) is an active agent for gastrointestinal stromal tumours, but does not yield responses in other soft-tissue sarcomas that are unselected for a molecular target. Results from an EORTC Soft Tissue and Bone Sarcoma Group phase II study. *Eur J Cancer* 39:2006-2011.
  123. Blanke, C. D., G. D. Demetri, M. von Mehren, M. C. Heinrich, B. Eisenberg, J. A. Fletcher, C. L. Corless, C. D. Fletcher, P. J. Roberts, D. Heinz, E.

- Wehre, Z. Nikolova, and H. Joensuu. 2008. Long-term results from a randomized phase II trial of standard- versus higher-dose imatinib mesylate for patients with unresectable or metastatic gastrointestinal stromal tumors expressing KIT. *Journal of Clinical Oncology* 26:620-625.
124. Rankin, C., M. von Mehren, C. D. Blanke, R. Benjamin, C. D. Fletcher, V. H. Bramwell, J. Crowley, E. Borden, and G. Demetri. 2004. Dose effect of imatinib (IM) in patients (pts) with metastatic GIST - Phase III Sarcoma Group Study S0033. *American Society of Clinical Oncology*. 23:815 (abstract 9005).
125. Verweij, J., P. G. Casali, J. Zalcberg, A. LeCesne, P. Reichardt, J. Y. Blay, R. Issels, A. van Oosterom, P. C. Hogendoorn, M. Van Glabbeke, R. Bertulli, and I. Judson. 2004. Progression-free survival in gastrointestinal stromal tumours with high-dose imatinib: randomised trial. *Lancet* 364:1127-1134.
126. Reynoso, D., and J. C. Trent. Neoadjuvant and adjuvant imatinib treatment in gastrointestinal stromal tumor: current status and recent developments. *Curr Opin Oncol* 22:330-335.
127. Debiec-Rychter, M., H. Dumez, I. Judson, B. Wasag, J. Verweij, M. Brown, S. Dimitrijevic, R. Sciot, M. Stul, H. Vranck, M. Scurr, A. Hagemeijer, M. van Glabbeke, and A. T. van Oosterom. 2004. Use of c-KIT/PDGFR $\alpha$  mutational analysis to predict the clinical response to imatinib in patients with advanced gastrointestinal stromal tumours entered on phase I and II studies of the EORTC Soft Tissue and Bone Sarcoma Group. *Eur J Cancer* 40:689-695.

128. Gronchi, A., J. Y. Blay, and J. C. Trent. 2010. The role of high-dose imatinib in the management of patients with gastrointestinal stromal tumor. *Cancer* 116:1847-1858.
129. McAuliffe, J., W.-L. Wang, G. Pavan, S. Pricl, D. Yang, S. Chen, A. Lazar, R. E. Pollock, and J. Trent. 2008. Unlucky 13? Differential sensitivity of exon 13 mutations to imatinib in GIST. *Molecular Oncology* 2:161-163.
130. Chen, H., K. Isozaki, K. Kinoshita, A. Ohashi, Y. Shinomura, Y. Matsuzawa, Y. Kitamura, and S. Hirota. 2003. Imatinib inhibits various types of activating mutant kit found in gastrointestinal stromal tumors. *Int J Cancer* 105:130-135.
131. Tamborini, E., S. Pricl, T. Negri, M. S. Lagonigro, F. Miselli, A. Greco, A. Gronchi, P. G. Casali, M. Ferrone, M. Fermeiglia, A. Carbone, M. A. Pierotti, and S. Pilotti. 2006. Functional analyses and molecular modeling of two c-Kit mutations responsible for imatinib secondary resistance in GIST patients. *Oncogene* 25:6140-6146.
132. Debiec-Rychter, M., J. Cools, H. Dumez, R. Sciot, M. Stul, N. Mentens, H. Vranckx, B. Wasag, H. Prenen, J. Roesel, A. Hagemeijer, A. Van Oosterom, and P. Marynen. 2005. Mechanisms of resistance to imatinib mesylate in gastrointestinal stromal tumors and activity of the PKC412 inhibitor against imatinib-resistant mutants. *Gastroenterology* 128:270-279.
133. Heinrich, M. C., C. L. Corless, C. D. Blanke, G. D. Demetri, H. Joensuu, P. J. Roberts, B. L. Eisenberg, M. von Mehren, C. D. Fletcher, K. Sandau, K. McDougall, W. B. Ou, C. J. Chen, and J. A. Fletcher. 2006. Molecular

- correlates of imatinib resistance in gastrointestinal stromal tumors. *Journal of Clinical Oncology* 24:4764-4774.
134. Rajasekaran, R., and R. Sethumadhavan. 2010. Exploring the cause of drug resistance by the detrimental missense mutations in KIT receptor: computational approach. *Amino Acids* 39:651-660.
  135. Conca, E., T. Negri, A. Gronchi, E. Fumagalli, E. Tamborini, G. M. Pavan, M. Fermeiglia, M. A. Pierotti, S. Pricl, and S. Pilotti. 2009. Activate and resist: L576P-KIT in GIST. *Mol Cancer Ther* 8:2491-2495.
  136. Alnaim, L. 2007. Therapeutic drug monitoring of cancer chemotherapy. *J Oncol Pharm Pract* 13:207-221.
  137. Hugen, P. W., D. M. Burger, R. E. Aarnoutse, P. A. Baede, P. T. Nieuwkerk, P. P. Koopmans, and Y. A. Hekster. 2002. Therapeutic drug monitoring of HIV-protease inhibitors to assess noncompliance. *Ther Drug Monit* 24:579-587.
  138. Peng, B., M. Hayes, D. Resta, A. Racine-Poon, B. J. Druker, M. Talpaz, C. L. Sawyers, M. Rosamilia, J. Ford, P. Lloyd, and R. Capdeville. 2004. Pharmacokinetics and pharmacodynamics of imatinib in a phase I trial with chronic myeloid leukemia patients. *J Clin Oncol* 22:935-942.
  139. Picard, S., K. Titier, G. Etienne, E. Teilhet, D. Ducint, M. A. Bernard, R. Lassalle, G. Marit, J. Reiffers, B. Begaud, N. Moore, M. Molimard, and F. X. Mahon. 2007. Trough imatinib plasma levels are associated with both cytogenetic and molecular responses to standard-dose imatinib in chronic myeloid leukemia. *Blood* 109:3496-3499.

140. Larson, R. A., B. J. Druker, F. Guilhot, S. G. O'Brien, G. J. Riviere, T. Krahne, I. Gathmann, and Y. Wang. 2008. Imatinib pharmacokinetics and its correlation with response and safety in chronic-phase chronic myeloid leukemia: a subanalysis of the IRIS study. *Blood* 111:4022-4028.
141. Demetri, G. D., A. T. van Oosterom, C. R. Garrett, M. E. Blackstein, M. H. Shah, J. Verweij, G. McArthur, I. R. Judson, M. C. Heinrich, J. A. Morgan, J. Desai, C. D. Fletcher, S. George, C. L. Bello, X. Huang, C. M. Baum, and P. G. Casali. 2006. Efficacy and safety of sunitinib in patients with advanced gastrointestinal stromal tumour after failure of imatinib: a randomised controlled trial.[see comment]. *Lancet* 368:1329-1338.
142. Demetri, G. D., Y. Wang, E. Wehrle, A. Racine, Z. Nikolova, C. D. Blanke, H. Joensuu, and M. von Mehren. 2009. Imatinib plasma levels are correlated with clinical benefit in patients with unresectable/metastatic gastrointestinal stromal tumors. *J Clin Oncol* 27:3141-3147.
143. Anderson, P. L. 2005. The ABC's of Pharmacokinetics. In *Positively Aware*. Test Positive Aware Network, Chicago, IL.
144. Widmer, N., L. A. Decosterd, S. Leyvraz, M. A. Duchosal, A. Rosselet, M. Debiec-Rychter, C. Csajka, J. Biollaz, and T. Buclin. 2008. Relationship of imatinib-free plasma levels and target genotype with efficacy and tolerability. *British journal of cancer* 98:1633-1640.
145. Widmer, N., L. A. Decosterd, C. Csajka, M. Montemurro, A. Haouala, S. Leyvraz, and T. Buclin. Imatinib plasma levels: correlation with clinical benefit in GIST patients. *Br J Cancer* 102:1198-1199.

146. Demetri, G. D., M. von Mehren, C. D. Blanke, A. D. Van den Abbeele, B. Eisenberg, P. J. Roberts, M. C. Heinrich, D. A. Tuveson, S. Singer, M. Janicek, J. A. Fletcher, S. G. Silverman, S. L. Silberman, R. Capdeville, B. Kiese, B. Peng, S. Dimitrijevic, B. J. Druker, C. Corless, C. D. Fletcher, and H. Joensuu. 2002. Efficacy and safety of imatinib mesylate in advanced gastrointestinal stromal tumors. *N Engl J Med* 347:472-480.
147. Peng, B., C. Dutreix, G. Mehring, M. J. Hayes, M. Ben-Am, M. Seiberling, R. Pokorny, R. Capdeville, and P. Lloyd. 2004. Absolute bioavailability of imatinib (Glivec) orally versus intravenous infusion. *J Clin Pharmacol* 44:158-162.
148. le Coutre, P., K. A. Kreuzer, S. Pursche, M. Bonin, T. Leopold, G. Baskaynak, B. Dèorken, G. Ehninger, O. Ottmann, A. Jenke, M. Bornhàuser, and E. Schleyer. 2004. Pharmacokinetics and cellular uptake of imatinib and its main metabolite CGP74588. *Cancer Chemother Pharmacol* 53:313-323.
149. Druker, B. J. 2003. Imatinib mesylate in the treatment of chronic myeloid leukaemia. *Expert Opin Pharmacother* 4:963-971.
150. Lynch, T., and A. Price. 2007. The effect of cytochrome P450 metabolism on drug response, interactions, and adverse effects. *Am Fam Physician* 76:391-396.
151. Wilkinson, G. R. 2005. Drug metabolism and variability among patients in drug response. *N Engl J Med* 352:2211-2221.

152. Slaughter, R. L., and D. J. Edwards. 1995. Recent advances: the cytochrome P450 enzymes. *Ann Pharmacother* 29:619-624.
153. Dresser, G. K., J. D. Spence, and D. G. Bailey. 2000. Pharmacokinetic-pharmacodynamic consequences and clinical relevance of cytochrome P450 3A4 inhibition. *Clin Pharmacokinet* 38:41-57.
154. Michalets, E. L. 1998. Update: clinically significant cytochrome P-450 drug interactions. *Pharmacotherapy* 18:84-112.
155. Poulsen, L., L. Arendt-Nielsen, K. Brosen, and S. H. Sindrup. 1996. The hypoalgesic effect of tramadol in relation to CYP2D6. *Clin Pharmacol Ther* 60:636-644.
156. Ray, W. A., K. T. Murray, S. Meredith, S. S. Narasimhulu, K. Hall, and C. M. Stein. 2004. Oral erythromycin and the risk of sudden death from cardiac causes. *N Engl J Med* 351:1089-1096.
157. Yasar, U., C. Forslund-Bergengren, G. Tybring, P. Dorado, A. Llerena, F. Sjoqvist, E. Eliasson, and M. L. Dahl. 2002. Pharmacokinetics of losartan and its metabolite E-3174 in relation to the CYP2C9 genotype. *Clin Pharmacol Ther* 71:89-98.
158. Cozza KL, A. S., Oesterheld JR. 2003. Drug interactions by medical specialty. In *Concise Guide to Drug Interaction Principles for Medical Practice: Cytochrome P450s, UGTs, P-Glycoproteins*. American Psychiatric Pub, Washington, D.C. 167–396.
159. Armstrong, S. C., K. L. Cozza, and N. B. Sandson. 2003. Six patterns of drug-drug interactions. *Psychosomatics* 44:255-258.



160. Marull, M., and B. Rochat. 2006. Fragmentation study of imatinib and characterization of new imatinib metabolites by liquid chromatography-triple-quadrupole and linear ion trap mass spectrometers. *J Mass Spectrom* 41:390-404.
161. Bolton, A. E., B. Peng, M. Hubert, A. Krebs-Brown, R. Capdeville, U. Keller, and M. Seiberling. 2004. Effect of rifampicin on the pharmacokinetics of imatinib mesylate (Gleevec, STI571) in healthy subjects. *Cancer Chemother Pharmacol* 53:102-106.
162. Frye, R. F., S. M. Fitzgerald, T. F. Lagattuta, M. W. Hruska, and M. J. Egorin. 2004. Effect of St John's wort on imatinib mesylate pharmacokinetics. *Clin Pharmacol Ther* 76:323-329.
163. O'Brien, S. G., P. Meinhardt, E. Bond, J. Beck, B. Peng, C. Dutreix, G. Mehring, S. Milosavljev, C. Huber, R. Capdeville, and T. Fischer. 2003. Effects of imatinib mesylate (STI571, Glivec) on the pharmacokinetics of simvastatin, a cytochrome p450 3A4 substrate, in patients with chronic myeloid leukaemia. *Br J Cancer* 89:1855-1859.
164. van Erp, N. P., H. Gelderblom, M. O. Karlsson, J. Li, M. Zhao, J. Ouwerkerk, J. W. Nortier, H. J. Guchelaar, S. D. Baker, and A. Sparreboom. 2007. Influence of CYP3A4 inhibition on the steady-state pharmacokinetics of imatinib. *Clin Cancer Res* 13:7394-7400.
165. Nassar, I., T. Pasupati, J. P. Judson, and I. Segarra. 2009. Reduced exposure of imatinib after coadministration with acetaminophen in mice. *Indian J Pharmacol* 41:167-172.

166. Nassar, I., T. Pasupati, J. P. Judson, and I. Segarra. 2010. Histopathological study of the hepatic and renal toxicity associated with the co-administration of imatinib and acetaminophen in a preclinical mouse model. *Malays J Pathol* 32:1-11.
167. Riechelmann, R. P., C. Zimmermann, S. N. Chin, L. Wang, A. O'Carroll, S. Zarinehbab, and M. K. Krzyzanowska. 2008. Potential drug interactions in cancer patients receiving supportive care exclusively. *J Pain Symptom Manage* 35:535-543.
168. Egorin, M. J., D. D. Shah, S. M. Christner, M. A. Yerk, K. A. Komazec, L. R. Appleman, R. L. Redner, B. M. Miller, and J. H. Beumer. 2009. Effect of a proton pump inhibitor on the pharmacokinetics of imatinib. *Br J Clin Pharmacol* 68:370-374.
169. Sparano, B. A., M. J. Egorin, R. A. Parise, J. Walters, K. A. Komazec, R. L. Redner, and J. H. Beumer. 2009. Effect of antacid on imatinib absorption. *Cancer Chemother Pharmacol* 63:525-528.
170. Therasse, P., S. G. Arbuck, E. A. Eisenhauer, J. Wanders, R. S. Kaplan, L. Rubinstein, J. Verweij, M. Van Glabbeke, A. T. van Oosterom, M. C. Christian, and S. G. Gwyther. 2000. New guidelines to evaluate the response to treatment in solid tumors. European Organization for Research and Treatment of Cancer, National Cancer Institute of the United States, National Cancer Institute of Canada. *J Natl Cancer Inst* 92:205-216.

171. Padhani, A. R., and L. Ollivier. 2001. The RECIST (Response Evaluation Criteria in Solid Tumors) criteria: implications for diagnostic radiologists. *Br J Radiol* 74:983-986.
172. Annick D Van den Abbeele, R. D. B., Jean-Pierre Cliche, Milos J Janicek, Richard Tetrault, Tricia Spangler, Amy Potter, Priscilla Merriam, Sandra Silberman, Sasa Dimitrijevic, George D Demetri, Dana-Farber Cancer Inst, Boston, MA; Novartis Oncology, Basel, Switzerland. 2002. 18F-FDG-PET predicts response to imatinib mesylate (Gleevec) in patients with advanced gastrointestinal stromal tumors (GIST) [Abstract]. *Proceedings of the American Society of Clinical Oncology* 21:abstr 1610.
173. Stroobants, S., J. Goeminne, M. Seegers, S. Dimitrijevic, P. Dupont, J. Nuyts, M. Martens, B. van den Borne, P. Cole, R. Sciot, H. Dumez, S. Silberman, L. Mortelmans, and A. van Oosterom. 2003. 18FDG-Positron emission tomography for the early prediction of response in advanced soft tissue sarcoma treated with imatinib mesylate (Glivec). *Eur J Cancer* 39:2012-2020.
174. Choi, H., C. Charnsangavej, S. de Castro Faria, E. P. Tamm, R. S. Benjamin, M. M. Johnson, H. A. Macapinlac, and D. A. Podoloff. 2004. CT evaluation of the response of gastrointestinal stromal tumors after imatinib mesylate treatment: a quantitative analysis correlated with FDG PET findings. *AJR Am J Roentgenol* 183:1619-1628.
175. Goerres, G. W., R. Stupp, G. Barghouth, T. F. Hany, B. Pestalozzi, E. Dizendorf, P. Schnyder, F. Luthi, G. K. von Schulthess, and S. Leyvraz.

2005. The value of PET, CT and in-line PET/CT in patients with gastrointestinal stromal tumours: long-term outcome of treatment with imatinib mesylate. *Eur J Nucl Med Mol Imaging* 32:153-162.
176. Choi, H. 2005. Critical issues in response evaluation on computed tomography: lessons from the gastrointestinal stromal tumor model. *Curr Oncol Rep* 7:307-311.
  177. Ng, E. H., R. E. Pollock, and M. M. Romsdahl. 1992. Prognostic implications of patterns of failure for gastrointestinal leiomyosarcomas. *Cancer* 69:1334-1341.
  178. Choi, H. 2008. Response evaluation of gastrointestinal stromal tumors. *Oncologist* 13 Suppl 2:4-7.
  179. Boonsirikamchai, P., D. A. Podoloff, and H. Choi. 2009. Imaging of gastrointestinal stromal tumors and assessment of benefit from systemic therapy. *Hematol Oncol Clin North Am* 23:35-48, vii.
  180. Chen, L. L., J. C. Trent, E. F. Wu, G. N. Fuller, L. Ramdas, W. Zhang, A. K. Raymond, V. G. Prieto, C. O. Oyedeleji, K. K. Hunt, R. E. Pollock, B. W. Feig, K. J. Hayes, H. Choi, H. A. Macapinlac, W. Hittelman, M. A. Velasco, S. Patel, M. A. Burgess, R. S. Benjamin, and M. L. Frazier. 2004. A missense mutation in KIT kinase domain 1 correlates with imatinib resistance in gastrointestinal stromal tumors. *Cancer Res* 64:5913-5919.
  181. Tamborini, E., L. Bonadiman, A. Greco, V. Albertini, T. Negri, A. Gronchi, R. Bertulli, M. Colecchia, P. G. Casali, M. A. Pierotti, and S. Pilotti. 2004. A new

- mutation in the KIT ATP pocket causes acquired resistance to imatinib in a gastrointestinal stromal tumor patient. *Gastroenterology* 127:294-299.
182. Wakai, T., T. Kanda, S. Hirota, A. Ohashi, Y. Shirai, and K. Hatakeyama. 2004. Late resistance to imatinib therapy in a metastatic gastrointestinal stromal tumour is associated with a second KIT mutation. *Br J Cancer* 90:2059-2061.
183. Van den Abbeele, A., R. Badawi, J.-P. Cliche, M. Janicek, T. Spangler, A. Paotter, P. Merriam, S. Silberman, S. Dimitrijevic, and G. Demitri. 2002. 18F-FDG PET predicts response to imatinib mesylate (Gleevec) in patients with advanced gastrointestinal stromal tumors (GIST) (abstract #1610). In *Proceedings of the American Society of Clinical Oncology*. American Society of Clinical Oncology, Orlando.
184. Benjamin, R. S., H. Choi, H. A. Macapinlac, M. A. Burgess, S. R. Patel, L. L. Chen, D. A. Podoloff, and C. Charnsangavej. 2007. We should desist using RECIST, at least in GIST. *J Clin Oncol* 25:1760-1764.
185. Antoch, G., J. Kanja, S. Bauer, H. Kuehl, K. Renzing-Koehler, J. Schuette, A. Bockisch, J. F. Debatin, and L. S. Freudenberg. 2004. Comparison of PET, CT, and dual-modality PET/CT imaging for monitoring of imatinib (STI571) therapy in patients with gastrointestinal stromal tumors. *J Nucl Med* 45:357-365.
186. Choi, H., C. Charnsangavej, S. C. Faria, H. A. Macapinlac, M. A. Burgess, S. R. Patel, L. L. Chen, D. A. Podoloff, and R. S. Benjamin. 2007. Correlation of computed tomography and positron emission tomography in patients with

- metastatic gastrointestinal stromal tumor treated at a single institution with imatinib mesylate: proposal of new computed tomography response criteria. *Journal of Clinical Oncology* 25:1753-1759.
187. Wang, Y., Y. L. Chia, J. Nedelman, H. Schran, F. X. Mahon, and M. Molimard. 2009. A therapeutic drug monitoring algorithm for refining the imatinib trough level obtained at different sampling times. *Ther Drug Monit* 31:579-584.
  188. Diggle, P., P. Heagerty, K.-Y. Liang, and S. Zeger. 2002. *Analysis of Longitudinal Data*. Oxford University Press, Oxford Oxfordshire.
  189. Kaplan, E., and P. Meier. 1958. Nonparametric estimation from incomplete observations. *J. American Statistical Association* 53:457-481.
  190. Cox, D. 1972. Regression models and life tables (with discussion). *Journal of the Royal Statistical Society* 34:187-220.

## **Vita**

Laura K Nolden is the daughter of Phillip and Sherrie Nolden of Sanibel, Florida. She received the degrees of Bachelor's of Science from Texas A&M University, College Station, Texas, and Master's of Science, Biomedical Science, from the University of Texas Graduate School of Biomedical Sciences, Houston, Texas. Laura worked as a Research Assistant in Cardiovascular Surgery Research at the Texas Heart Institute, Houston, Texas, and with the Department of Cardiothoracic Surgery in Oldenburg, Germany, prior to her acceptance in the PhD program at GSBS.

Permanent address:

P.O Box 541161

Houston, Texas 77254 - 1161